MECHANISTIC STUDY OF URACIL DNA GLYCOSYLASE

By

EVE LYNN HUNOVICE

A DISSERTATION PRESENTED TO THE GRADUATE SCHOOL
OF THE UNIVERSITY OF FLORIDA IN PARTIAL FULFILLMENT
OF THE REQUIREMENTS FOR THE DEGREE OF
DOCTOR OF PHILOSOPHY

UNIVERSITY OF FLORIDA
1999

This work is dedicated to my niece,
Lindsay Rae Epstein, and to the memory of
my grandfather, Irwin Klein.

ACKNOWLEDGMENTS

I would like to thank Dr. Benjamin Horenstein for the opportunity to work in his lab. His enthusiasm for science and his dedication to his job have been a source of motivation for me these past five years. I appreciate his advice and encouragement, without which I could not have completed this work.

I am grateful for the help I have received from faculty members in the chemistry department at UF, in particular Dr. Jon Stewart. Not only was he an excellent teacher, but also he was extremely instrumental in helping me plan for my future after graduate school. I am thankful for the help of Dr. Ion Ghiviriga with NMR. Additionally, I would like to thank Dr. Joanne Stubbe for supplying the plasmid for ribonucleotide triphosphate reductase and Dr. Katherine Joyce for supplying the plasmid for Klenow fragment.

Many thanks go to my friends in the Horenstein group both past and present: Mike, JingSong, John, Kim, Mirella, HongBin, and Natalie. Also, those in other research groups in the department with whom I have had the pleasure to interact: Jennifer, Sonia, Kavitha, Carlos, Missy, Brendan, Steve, Joe, and Craig. A special thank you to Tom for his editing.

I am especially indebted to the endless support I have received from my parents, Judy and Leslie Hunovice. They have

shared in all of my ups and downs helping me to see the big picture and keep my eyes on the prize. In addition to being loving parents, they are also my best friends. My sister and brother-in-law, Rachel and Rick Epstein, have also been a wonderful support system for me. In addition, my close bonds to Wendy and Jennifer have brought me much joy and I look forward to our lifelong friendships.

Finally, I am forever grateful to Ian, who has been my unceasing source of comfort. His genuine concern for my success and happiness will always strengthen me.

TABLE OF CONTENTS

Abstract of Dissertation Presented to the Graduate School of the University of Florida in Partial Fulfillment of the Requirements for the Degree of Doctor of Philosophy

MECHANISTIC STUDY OF
URACIL DNA GLYCOSYLASE

By

Eve Lynn Hunovice

December 1999

Chairman: Dr. Benjamin A. Horenstein
Major Department: Chemistry

Uracil DNA glycosylase specifically cleaves uracil from DNA by hydrolysis of the C-N glycosidic bond. Uracil appears in DNA as a result of deamination of cytosine or misincorporation of dUTP during replication. This dissertation describes a mechanistic study of UDG, featuring kinetic isotope effects.

The first portion of this work details the synthesis of the uracil-containing UDG substrates used to perform the kinetic investigations. UDG's natural substrate is uracil-containing single- and double-stranded DNA. One of the molecules synthesized is a 781 base pair, uracil-containing, double stranded DNA substrate (HCAII-U). The other synthesized molecules are the catalytically challenged molecules 2'-deoxyuridine-3',5'-diphosphate (pdUp), pd(UTT), and pd(UCC).

In the next part, kinetic experiments are described for the reaction of UDG with HCAII-U and pdUp. A UDG mutant, C200S, was synthesized to determine the role of a lone cysteine residue in *Escherichia coli* UDG. The kinetic behavior for the C200S UDG versus the wild type UDG with HCAII-U was observed. In addition, it is demonstrated that pdUp is a substrate for UDG. The smallest known substrate for UDG prior to this study was pd(UT)p. These results demonstrate that UDG does not require binding of an oligonucleotide for activity.

The dissertation concludes with a description of method development, and application, of a technique to measure kinetic isotope effects for the reaction of UDG with pdUp and pd(UTT). Measured effects include primary ^{13}C, secondary α tritium, secondary α deuterium, and secondary β deuterium. The results from these experiments allow for determination of transition state characteristics for the reaction and demonstrate the validity of the method developed for measuring kinetic isotope effects.

CHAPTER 1
INTRODUCTION

The chemical component of essentially all genetic material is deoxyribonucleic acid (DNA). Although once believed to be a very stable molecule, DNA's chemical lability makes it vulnerable to both natural endogenous threats as well as damaging environmental agents. If chemical modification of DNA remains uncorrected, possible outcomes of these damaging agents are mutations and cell death. Fortunately, organisms are equipped with elaborate mechanisms to combat and repair DNA damage. One DNA repair enzyme that is of interest is uracil DNA glycosylase (UDG), which cleaves the base uracil, normally found in RNA, from DNA. Over the past 25 years much has been learned about this DNA repair enzyme, however, the mechanism by which it works remains unknown. The goal of this project is to investigate the mechanism of UDG.

DNA Damage

There are two major categories of DNA damage: environmental and spontaneous. Environmental damage accumulates due to environmental factors such as chemical agents or radiation. Spontaneous damage, on the other hand, occurs naturally in a living organism as a result of normal cellular

processes. The damage can occur at the bases, sugars, or phosphodiester linkages of DNA.

Environmental Damage to DNA

Two sources of environmental damage are radiation and chemical agents. When DNA is irradiated at wavelengths approaching 260 nm (its absorption maximum), cyclobutane pyrimidine dimers are formed. A covalent linkage forms between adjacent pyrimidines resulting in a four-membered ring structure due to saturation of their respective 5,6 double bonds (Lober, 1977; McLaren, 1964; Setlow, J., 1966; Setlow, R.,1966; Setlow, 1969; Varghese, 1972; Wacker, 1964; Wang, 1965; Wang, 1976). There are theoretically 16 possible isomeric forms because of the 4 chiral centers, however, the *cis-syn* form (see figure 1-1) predominates in double-stranded B-form DNA (Wacker, 1964). It

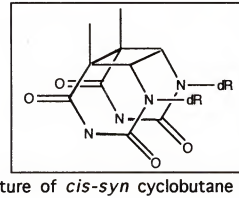

Figure 1-1: Structure of *cis-syn* cyclobutane thymine dimer (from Friedberg 1995).

was previously thought that cyclobutane dimers cause distortion of the helix and the halt of replication, because no base can be inserted which can form stable hydrogen bonds (Chan, 1985; Hayes,

1971; Witkin, 1976). More recent studies, however, indicate that B-DNA can accommodate the *cis-syn* lesion without much distortion (Taylor, 1990). UV radiation can also cause pyrimidine hydrates and thymine glycols which involve saturation of the 5,6 double bond. In addition, ultraviolet radiation results in DNA-DNA and DNA-protein crosslinks which lead to many problems in the cell.

There are many chemical agents that can cause DNA damage. Some of these chemical agents have been used as warfare agents while others have been used as cancer chemotherapeutic agents (Friedberg, 1995). The DNA bases possess nucleophilic centers which can react with electrophilic compounds (alkylating agents). The N^7 position of guanine and the N^3 position of adenine are the most reactive sites, however, the oxygens and nitrogens in all of the bases are reactive as well (see figure 1-2) (Roberts, 1978; Singer, 1986; Singer 1983; Singer, 1982). If two sites of alkylation are on opposite strands of the DNA, an interstrand cross-link is formed which prevents DNA strand separation. Interstrand cross-links halt replication and transcription which leads to the demise of rapidly dividing cell populations such as cancer cells. Some examples of cancer chemotherapeutic agents are nitrogen and sulfur mustard (Chun, 1969; Fox, 1980; Kohn, 1966), mitomycin (Borowy-Borowski, 1990; Iyer, 1963), and *cis*-platinum (Chu, 1994; Eastman, 1987; Fram, 1992; Roberts, 1972).

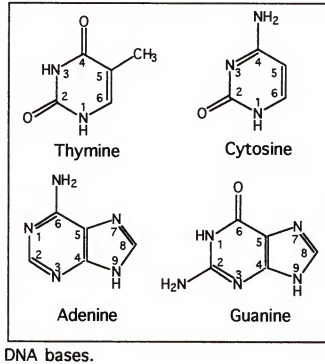

Figure 1- 2: DNA bases.

Spontaneous Damage to DNA

The major types of spontaneous damage effecting DNA are hydrolysis, hydrolytic deamination, oxidation, and nonenzymatic methylation (Lindahl, 1993). Hydrolysis of the N-glycosyl bond leads to depurination and depyrimidination. The instability of the N-glycosyl bonds in DNA containing ^{14}C-labeled purines or pyrimidines has been measured as a function of pH, temperature, ionic strength, and nucleic acid secondary structure (Lindahl, 1972; Lindahl, 1973; Loeb, 1986). Thymine and adenine are liberated from DNA at 5% the rate of guanine and cytosine (Lindahl, 1972). At physiological conditions, the reaction is mainly acid catalyzed, i.e., protonation of the base followed by direct cleavage of the glycosyl bond (Lindahl 1972; Zoltewicz, 1970). In each human cell, it is estimated that 2,000 - 10,000 DNA purine bases are lost per day

due to hydrolytic depurination/pyrimidination (Lindahl, 1972). The product of hydrolytic depurination/depyrimidination is an apurinic/apyrimidinic site (see figure 1- 3).

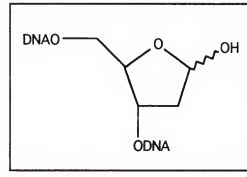

Figure 1-3: Apurinic/apyrimidinic site in DNA.

In addition to the N-glycosidic bonds, the DNA bases are also sensitive to hydrolysis. The result of this type of damage is deamination. The main targets of deamination are cytosine and its homologue 5-methylcytosine (Lindahl, 1993). The half life at 37 °C, pH 7.4 of an individual cytosine residue located in single- and double-stranded DNA in solution is 200 years and 30,000 years, respectively (Frederico, 1990). Deamination of 5-methylcytosine occurs 3-4 times faster than deamination of cytosine (Lindahl, 1974; Ehrlich, 1990). In a genome of 10^{10} base pairs, approximately 200 deaminations occur per day (Mosbaugh, 1988). Upon deamination, cystosine becomes uracil which is pro-mutagenic. During the next round of DNA replication a G-C to A-T transition mutation will occur.

The DNA in aerobically growing cells can also be damaged by reactive oxygen species to which the cell is exposed during normal metabolism. The volume of a typical human cell is approximately

10 μm^3 and the weight is 1 ng. A cell such as this metabolizes about 10^{12} molecules of molecular oxygen per day and produces 3 x 10^9 molecules of hydrogen peroxide per hour (Newcomb, 1998). The resulting reactive oxygen species cause approximately 2 x 10^4 oxidative DNA lesions per day to the human genome (Ames, 1992). Some of the lesions caused by oxidative damage are 5,6-dihydroxyuracil, 5-hydroxyuracil, 5-hydroxycytosine, 8-hydroxyguanine, and 8-hydroxyadenosine, which are generated by hydroxide radicals (Aruoma, 1989) (see figure 1-4). The lesion 8-hydroxyguanine is the major mutagenic

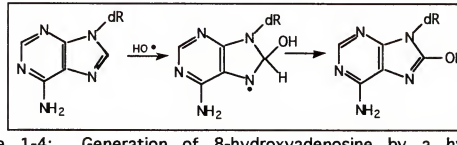

Figure 1-4: Generation of 8-hydroxyadenosine by a hydroxide radical (from Blackburn, 1990).

oxidatively induced lesion. When guanine is converted to 8-hydroxyguanine its base pairing behavior is altered and instead of pairing with cytosine it now pairs with adenine. This alteration leads to a G-C to T-A transition mutation during the next round of DNA replication.

The final type of spontaneous damage to be discussed is non-enzymatic methylation. In addition to reactive oxygen species, living cells contain other small reactive molecules that can cause DNA damage (Lutz, 1990). One of these reactive molecules, S-adenosylmethionine, is normally used as a cofactor in most cellular

transmethylation reactions. It also targets, however, nitrogens in purines causing the formation of 7-methylguanine and 3-methyladenine. The second molecule, 3-methyladenine, blocks replication and therefore is much more dangerous to the cell than 7-methylguanine which has the same base-pairing behavior as guanine. In a human cell, approximately 600 3-methyladenines are generated per day (Rydberg, 1982).

DNA Repair Pathways

The DNA in living cells is continually exposed to environmental and natural endogenous factors which, if left unfixed, could cause the demise of the cell. In order to combat the damage cells have elaborate mechanisms involving many enzymes. Two important cellular responses to DNA damage which will not be discussed are reversal and tolerance of DNA damage (Friedberg, 1995). The third cellular response to DNA damage is excision repair. DNA's two complementary strand duplex structure enables recovery of information by this mechanism. The two main pathways for excision repair are nucleotide excision repair, and base excision repair. Mismatch repair is another excision repair mechanism which corrects DNA-replication errors.

Nucleotide Excision Repair

The nucleotide excision repair pathway corrects DNA lesions that cause large distortions in the helical structure of DNA (Lehninger, 1993). The mechanism is a five step pathway: 1) damage recognition, 2) incision, 3) excision, 4) repair synthesis,

and 5) ligation (Grossman, 1998). DNA containing pyrimidine dimers is one example of a lesion repaired by NER. In *E. coli* a group of enzymes called UvrABC endonuclease perform the first 3 steps using a series of ATP-dependent reactions. Unlike other endonucleases, UvrABC incises the DNA both 5' and 3' to the lesion in a "dual incision" reaction (Yeung, 1986; Sancar, 1983)). The adducted base is excised as part of an oligonucleotide fragment and the intact DNA strand serves as a template in the synthesis of new DNA. The broad range of specificity of UvrABC endonuclease has lead to the proposal that the enzyme recognizes conformational changes resulting from damage in the DNA rather than the chemically modified bases (Grossman, 1988; Sancar, 1983; Sancar, 1993; Van Houten, 1990; Weiss, 1987).

Nucleotide excision repair in eukaryotes is much more involved than that of prokaryotes like *E. coli.* The structural complexity of eukaryotic genomes limits the accessibility of DNA repair enzymes and it is believed that repair occurs during other aspects of DNA metabolism when the chromatin is in more open conformations. Many enzymes form a large multiprotein complex referred to as a repairosome which is responsible for the repair of the damaged DNA (Friedberg, 1995).

Base Excision Repair

Individual damaged DNA bases are repaired by the base excision repair pathway (BER) (Friedberg, 1995; Krokan, 1997). The BER in a human cell repairs more than 10,000 damaged bases each day (Ames, 1993). By reconstituting BER *in vitro* using cell free

extracts or purified enzymes, the minimal requirements for repair have been determined (Dianov, 1994; Dianov,1992; Wiebauer,1990). The first step in a five step process (see Figure 1-5) utilizes a specific DNA glycosylase which catalyzes the cleavage of the N-glycosidic bond between the inappropriate base and the deoxyribose. The products of this reaction are the

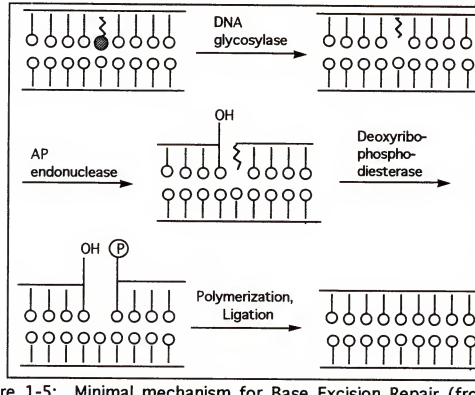

Figure 1-5: Minimal mechanism for Base Excision Repair (from Nickoloff, 1998).

free base and an apurinic/apyrimidinc site (Barnes, 1993) which is both mutagenic and cytotoxic and must be repaired further (Gentil, 1992). The next step involves the action of an apurinic/apyrimidinic endonuclease which incises the sugar phosphate backbone at the 5'-side of the AP-site (Lindahl, 1979) leaving a 3'-OH terminus and 5'-abasic residue. Some DNA-

glycosylases also possess a β-lyase activity which produces a strand scission after base removal (Krokan, 1997) without the use of a separate AP-endonuclease. The third step is degradation of the 5'-abasic residue by a DNA-deoxyribophosphodiesterease which creates a single nucleotide gap. Step four and five are addition of the correct nucleotide by DNA polymerase and ligation of the single-stranded DNA gap by DNA ligase (Singhal, 1995). This is a minimal mechanism because it was determined from *in vitro* reconstitution whereas BER *in vivo* might involve more enzymes.

As in nucleotide excision repair, base excision repair in eukaryotes is more complex than in prokaryotes. In mammalian cells, for example, after the base is removed, either short-patch or long-patch removal can occur. The short-patch method requires DNA polymerase β to enact single-nucleotide gap replacement (Wood, 1997; Nealon, 1996). The long-patch pathway depends on DNA polymerase β or δ to remove and replace patches of 2-10 nucleotides (Wood, 1997; Frosina, 1996).

Origins of Uracil DNA Glycosylase Research

Many DNA glycosylases, the enzymes responsible for initiating BER, have been well characterized (David, 1998; Krokan, 1997). The first DNA glycosylase to be discovered was *E. coli* uracil DNA glycosylase. It is this enzyme that is the focus of this dissertation. Thomas Lindahl used a [^{3}H]-dU substrate oligonucleotide to find an enzymatic activity that would recognize uracil in DNA resulting from deamination of cytosine (Lindahl,

1974). The enzyme was named uracil DNA glycosylase because it excised the base uracil from DNA.

Uracil in DNA

Deamination of cytosine is one of two ways uracil can appear in DNA (see above). The other method whereby uracil can appear in DNA is by misincorporation of dUMP rather than TMP during replication (Tomilin, 1989; Mosbaugh, 1988; Frederico, 1993). The amount of misincorporation of dUMP is related directly to the size of the intracellular dUTP pool relative to the TTP pool (Friedberg, 1995) because DNA polymerase is indiscriminate. The dUTP pool size is maintained by the enzyme dUTPase which degrades dUTP to dUMP. Both the dUTP and TTP pool sizes are maintained by the enzyme thymidylate synthetase. During the synthesis of TMP from dUMP, thymidylate synthetase transfers a methyl group from methylenetetrahydrofolate to dUMP to form dUTP and dihydrofolate. If the enzyme dihyrofolate reductase (the enzyme that regenerates tetrahydrofolate from dihydrofolate) is inhibited, the dUMP pool size increases and the TTP pool size decreases (Jackson, 1978; Myers, 1975). In a genome of 10^{10} base pairs, it is estimated that over 10,000 deoxyuri
dine incorporation events occur per DNA replicative cycle (Mosbaugh, 1988). Since U and T share the same Watson-Crick base-pairing pattern, misincorporated U is not mutagenic per se. There is evidence that protein DNA interactions are sensitive to this substitution (Focher, 1992). Uracil which arises via the deamination route is potentially mutagenic, since semi-

conservative replication would lead to a CG to TA transition. The enzyme is (and must be) highly selective for uracil residues in DNA, such that uridine ribonucleosides in RNA or A,T,G, and C deoxyribonucleoside residues in DNA are not substrates.

UDG General Background

UDG has been identified in a variety of sources including *E. coli* (Lindahl, 1974), humans (Olsen et al, 1989), Herpes virus (McGeoch, 1988), rat liver (Domena, 1985) and *Saccharomyces cervisiae* (Crosby, 1981). Endopterygota insects (insects that undergo pupal and larval stages of development) (Dudley, 1992) and the *Bacillus subtilis* bacteriophages PBS1 and PBS2 (organisms that naturally use uracil in place of thymine in their DNA) (Takahashi, 1963; Mosbaugh, 1994) appear to be among the few living organisms that may lack UDG activity. The molecular weights of UDGs from different organisms range from 18,000 - 50,000 Daltons (Domena, 1985), and have been found to contain 199 - 359 amino acids (Savva, 1995). UDG's from *E. coli*, herpes virus, and humans have been found to share a 40-55% sequence identity, and as a pair, the *E. coli* and human enzymes are 73% homologous (Olsen, 1989). X-ray crystallographic structures for *E. coli*, herpes virus, and human UDG (Xiao, 1999; Putnam, 1999; Savva, 1995; Mol, 1995; Parikh, 1998; Slupphaug, 1996) demonstrate that the enzymes have substantial structural similarities as anticipated from the high level of sequence conservation.

Characteristics and Structure of *E. coli* UDG

E. coli UDG has a deduced molecular weight of 25,694 and comprises 228 amino acid residues (Varshney, 1988; Bennett, 1994). It's maximal activity is reached at pH 8.0 (Lindahl, 1977). UDG cleaves uracil from single stranded DNA two times faster than from double stranded DNA containing U/G mispairs. It recognizes both U/G mispairs and U/A base pairs in double stranded DNA, however, it recognizes the first approximately 2.4 times more efficiently than the latter (Bennet, 1995). Uracil inhibits the enzyme in a noncompetitive manner, while apyrimidinic sites in DNA inhibit the enzyme in a competitive manner (Mosbaugh, 1994; Lindahl, 1977; Domena, 1988). *E. coli* UDG is a single domain enzyme which possesses a classic α/β structure consisting of a four-stranded all parallel β-sheet surrounded by α helices (see figure 1-6). There is a ~15 Å wide narrow groove formed between $\beta 1$ and $\beta 3$ which is lined with positively charged amino acids which are functionally conserved among all UDGs (Putnam, 1999). A distinct pocket, the UDG active site (see figure 1-7), is located at the end of this narrow channel and contains the absolutely conserved residues glutamine 63, aspartate 64, tyrosine 66, phenylalanine 77, asparagine 123, and histidine 187 (Xiao, 1999, Putnam, 1999). The five major structural motifs which confer UDG functionality found in the human UDG and herpes UDG are also conserved in *E. coli* UDG. These include the uracil specificity region (120-LLLN-123), the catalytic water-activating loop (63-QDPYH-67), the Leu intercalation loop (187-HPSPLSAHR-195), the

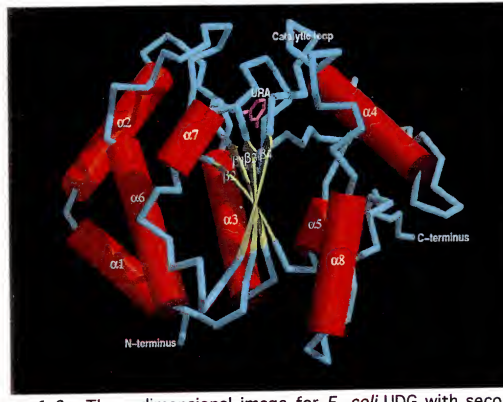

Figure 1-6: Three dimensional image for *E. coli* UDG with secondary structure labeled (from Xiao, 1999).

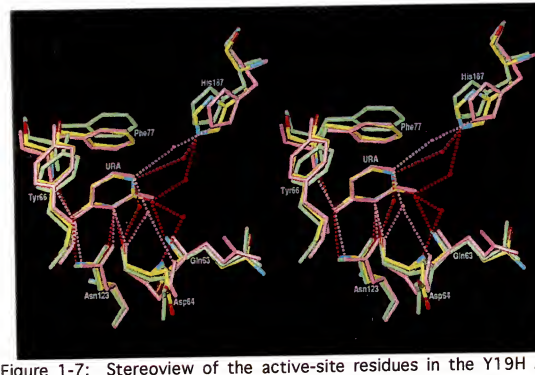

Figure 1-7: Stereoview of the active-site residues in the Y19H *E. coli* UDG-uracil complex (colored by atom type), aligned with Herpes UDG (pink), and human UDG (green) (from Xiao, 1999).

Pro-rich loop (84-AIPPS-88), and the Gly-Ser loop (165-GS166) (Putnam, 1999).

Substrate Specificity

UDG is able to specifically bind uracil and avoid binding to normal DNA and RNA bases. As demonstrated by the crystal structure for Herpes UDG (Savva, 1995) the side chain of the highly conserved active site tyrosine 90 (tyrosine 66 in *E. coli*) residue prevents adenine, guanine, and thymine from entering the active site pocket by a steric clash with the imidizole rings of the purine bases and the 5-methyl group of the pyrimidine. In addition, unfavorable interactions between the purine bases and polar residues in the active site also prevent binding of these molecules (Savva, 1995). Cytosine is small enough to enter the binding pocket, however, polar residues lining the active site cause highly unfavorable repulsive interactions (Savva, 1995). A human UDG mutant in which aspartate replaced the highly conserved active site residue, asparagine 204 (asparagine 123 in *E. coli*), possessed CDG activity (it excised cytosine from DNA) in addition to UDG activity (Kavli, 1996). These results suggest that the unfavorable interactions between cytosine and asparagine 204 prevent UDG from accepting cytosine as a substrate. Ribonucleotides are excluded because of a steric clash between the hydroxyl group at C2 and phenylalanine 101 (phenylalanine 77 in *E. coli*). The uracil base specificity is not absolute, however, as shown by the observation that 5-fluorouracil, 5-hydroxyuracil, alloxan and

isodialuric acid analogs are substrates (Mauro, 1993; Hatahet, 1994; Dizdaroglu, 1996).

Substrate Recognition

UDG's mechanism of substrate recognition has been studied extensively. One important question yet to be answered is: does UDG scan the DNA in a one-dimensional diffusion process, or is the mechanism of substrate recognition a distributive process? Some studies suggest that UDG utilizes a processive method. Partial-processivity of UDG was indicated in an experiment involving a kinetic analysis of uracil hydrolysis by a combination of UDG and T4 endonuclease V from uracil-containing circular DNA at various concentrations of NaCl (Higley, 1993). Since a mixture of both T4 endonuclease V (an enzyme that behaves by a known processive mechanism) and UDG was used in the experiment the question of UDG processivity remains unclear. The T4 endonuclease V present in the reaction mixture might have altered the behavior of UDG. Structural and kinetic results from mutant and wild type human UDG-DNA reactions also pointed toward a processive mechanism (Parikh, 1998). In addition, the ionic dependence of UDG suggests a scanning mechanism (Bennett, 1995; Higley, 1993).

Other studies, however, indicate a distributive mechanism for UDG. When UDG was reacted with ^{32}P labeled deoxyuridine-containing decanucleotides, followed by heating, observation of the distribution of ^{32}P DNA fragments on denaturing polyacrylamide DNA sequencing gel indicated a distributive mechanism (Purmal, 1994). Experiments using surface plasmon resonance showed that

UDG resides on uracil-free DNA for a very short time. In addition, the rates of association and dissociation from uracil-containing DNA fit to a model for a single process much better than to a biphasic model required if scanning were in operation (Panayotou, 1998). Structural data also suggest that after C-N glycosidic bond cleavage, UDG must dissociate from DNA in order for the bound uracil to escape the active site (Slupphaug, 1996).

An oriented "hopping" process (von Hippel, 1989; Berg, 1981) has been suggested for UDG which integrates the apparently conflicting data. This type of mechanism has both processive and distributive characteristics and rationalizes the data suggesting that UDG interacts with DNA in a distributive fashion, yet still has a scan length of 1.5-2 kilobases before dissociation from the DNA (Panayotou, 1998). Location of uracils during bimolecular collisions is made more efficient by electrostatic steering of UDG's positively charged DNA binding groove (Mol, 1995; Slupphaug, 1996) toward the negatively charged DNA.

Base Flipping

An interesting feature of the UDG mechanistic pathway is base flipping. Base flipping means that a base in normal B-DNA is swung out of the helix and into an extrahelical position (Roberts, 1998). The first example of base flipping was the crystal structure of the cytosine-5 DNA methyltransferase M.*Hha* I, its DNA substrate, and S-adenosyl-L-homocystine (the reaction product) (Klimasauskas, 1994). In this structure, the base was swung out of the helix 180°. Since this discovery, base flipping has been

implicated or directly observed in 3 other systems: the cytosine-5 DNA methyltransferase M.*Hha* III (Reinisch, 1995), a catalytically compromised form of T4 endonuclease V (Vassylyev, 1995), and human uracil DNA glycosylase (Slupphaug, 1996).

The key crystal structure for base flipping in the UDG system was the complex of a human UDG L272R/D145N double mutant with a double stranded 20-mer oligonucleotide substrate containing a central U-G mismatch (see Figure 1-8). Earlier site directed mutagenesis work by Mol. et al suggested that leucine 272, located above the uracil recognition site, was involved in uracil recognition and base flipping (Mol, 1995). DNA-binding and kinetic data for wild type human UDG and three leucine 272 mutants (leucine 191 in *E. coli*) showed that k_{cat}/K_m for the leucine mutants was reduced. The mutation to aspartate 145 (aspartate 64 in *E. coli*) helped to further reduce k_{cat}/K_m to about 10,000 times less than wild type UDG. With this catalytically compromised UDG the authors hoped to obtain crystallographic data for an enzyme-substrate complex, however, an enzyme-product complex was obtained instead (Slupphaug, 1996). Additionally, it is important to note that a mutant enzyme was used in this crystallography study and there is no structure available for leucine-containing wild-type UDG bound to DNA.

The X-ray crystallography data combined with modeling (Slupphaug, 1996) demonstrated that Arg 272 was inserted into the DNA, the N-glycosidic bond had been cleaved, and free uracil and a deoxyribose C1' OH were bound in the specificity pocket. The UDG

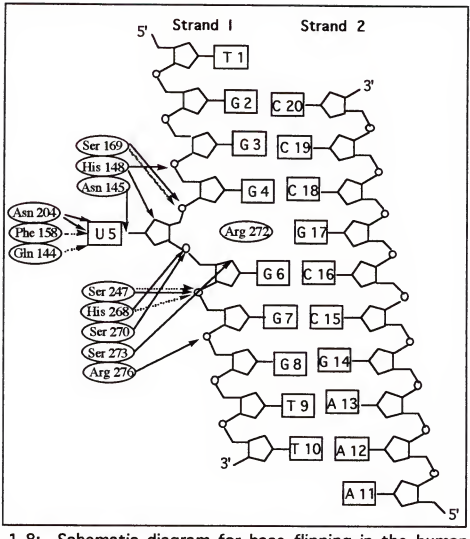

Figure 1-8: Schematic diagram for base flipping in the human UDG L272R/D145N double mutant-DNA complex. Hydrogen-bond interactions with amino-acid side chains are indicated by solid arrows while hydrogen-bond interactions with backbone atoms are indicated by dotted arrows (from Slupphaug,1996).

mainly contacts the minor groove, while the uracil flips out of the major groove. The uracil, deoxyribose and 5' phosphate are all rotated 180° out of the helix. In addition, the distance between the two phosphates flanking the extrahelical uracil is 8.3 Å while for strand 2 the distance is 11.5 Å (Slupphaug, 1996).

Proposed Mechanisms for Base Flipping

One area of controversy and much study is the question of whether base flipping is actively produced by UDG or if the base is spontaneously extruded from the helix and UDG recognizes this configuration (Panayotou, 1998). Some evidence that suggests that UDG recognizes flipped out bases is the fact that it would be highly difficult for UDG to distinguish between very different base pairs (G:C and A:T base pairs, A:U and G:U pairs, and unpaired uracil in ssDNA) which makes the passive mechanism more likely (Panayotou, 1998). In addition, the association rates for the UDG-DNA complex differ in the order of ssU-DNA>dsU/G-DNA>>dsU/A-DNA which suggests that the formation of the complex is dependent on the relative strength of base pairing (Panayotou, 1998).

The proposed process by which UDG may actively flip uracil out of the DNA helix is often referred to as a 'push' and 'pull' mechanism (Slupphaug, 1996; Kunkel, 1996). A leucine residue in the highly conserved motif, the leu intercalation loop, inserts into the minor groove of the double stranded DNA substrate and 'pushes' the dUMP residue into the major groove. Selective amino acids on the surface of UDG interact with phosphate groups on the DNA to help stabilize the leucine insertion. Next, side chains of highly conserved residues in the UDG active site 'pull' the uracil into major groove, thus flipping the base 180° out of the helix (Kumar, 1997). In addition to structural support for the 'push' and 'pull' mechanism for uracil flipping (Slupphaug, 1996; Parikh, 1998), there is also kinetic evidence that supports the theory. Stivers tracked the kinetics of uracil flipping by studying tryptophan

fluorescence changes during the reaction. He suggested a two step mechanism whereby UDG destabilizes the DNA before base flipping which renders the base flipping step independent of base-pair stability (Stivers, 1999). These conflicting results in addition to the unanswered question of whether base flipping confers catalysis, highlight the need for more study of the base flipping behavior apparent in UDG.

Proposed Mechanisms for Glycosidic Bond Cleavage

Before undertaking a mechanistic study of UDG it is important first to consider the mechanism for non-enzymatic cleavage. A mechanistic scheme for acid catalyzed hydrolysis of the C-N glycosidic bond is shown in Figure 1-9. In this mechanism, protonation of the uracil O4 triggers cleavage of the glycosidic bond, and renders uracil a neutral leaving group.

It is estimated that UDG increases the spontaneous rate of glycosidic bond cleavage between uracil and the deoxyribose sugar by a factor of approximately 10^{12} (Xiao, 1999). Several different mechanisms have been proposed to account for this considerable gain in rate, however, the true mechanism of uracil DNA glycosylase remains unknown.

Mechanistic Proposal by Prior and Santi (1984)

One of the earliest proposed mechanisms for hydrolysis of the C-N glycosidic bond by UDG was proposed by Prior and Santi in 1984 (Prior, 1984; Prior, 1984; Ivanetich, 1992). A nucleophilic

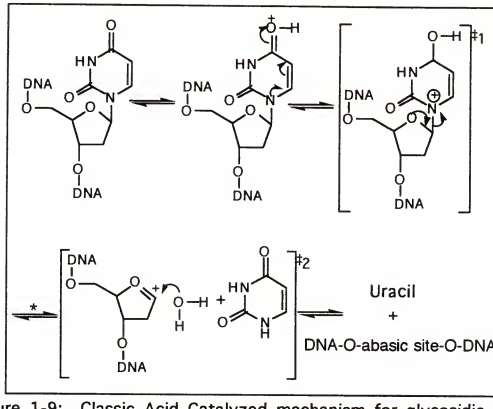

Figure 1-9: Classic Acid Catalyzed mechanism for glycosidic bond cleavage of uracil in DNA. *Two discrete transition states are shown, but a single oxocarbenium ion-like transition state involving simultaneous loss of the base and water attack is also possible.

residue in the enzyme attacks C-6 of the uracil ring in a Michael addition mechanism (see Figure 1-10). One of the tools used while formulating this mechanism was kinetic isotope effects of the acid catalyzed cleavage of uracil from uridine. There were two critical KIE experiments. The first was a secondary ^{3}H isotope effect for the hydrolysis of [6-^{3}H] uridine with a value of 0.87. This inverse value suggests a change in hybridization from sp^2 to sp^3 at C6 during hydrolysis. The second key KIE, an α-secondary deuterium isotope effect for the hydrolysis of uridine [1'-^{2}H], was measured

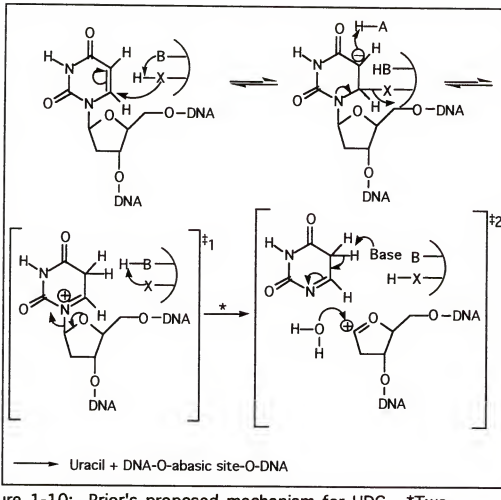

Figure 1-10: Prior's proposed mechanism for UDG. *Two discrete transition states are shown. Attack of H_2O at C1' may be more or less concerted with N-glycosidic bond cleavage. (from Prior, 1984).

to be 1.11. This value suggests oxocarbenium-like character at C1' during hydrolysis (Prior, 1984). Prior and Santi also studied the kinetics of the acid catalyzed reaction of uridine. They observed the formation of 6-hydroxy-5,6-dihydrouridine (Urd-H_2O) and found that Urd-H_2O (or an intermediate in the reaction for the formation of Urd-H_2O from uridine) is kinetically competent to account for C-N glycosidic bond cleavage of uridine (Prior, 1984). Also, the acid catalyzed hydrolysis of the C-N glycosidic bond of 5,6-

dihydrouridine occurrs about 2 x 10^3 times faster than glycosidic bond hydrolysis of uridine (Ivanetich, 1992). Additional support for this Michael addition mechanism came from the observation of nucleophilic attack at the 6-position of pyrimidine heterocycles in other enzymatic reactions of pyrimidine nucleosides and nucleotides such as thymidylate synthetase (Pogolotti, 1979) and aminoacyl tRNA synthetase (Starzyk, 1982). Work presented in this dissertation will address the mechanism proposed by Prior and Santi.

Mechanistic Proposal by Savva et al. (1995)

The next mechanistic proposals for UDG came in 1995 along with the publication of X-ray crystal structures for Herpes and human UDG (Savva, 1995; Mol, 1995). The mechanism proposed by Savva was determined through analysis of X-ray crystal structure data of HSV-1 UDG crystallized alone and with a thymine-trinucleotide. In addition, the proposed catalytic residues aspartate 88 (aspartate 64 in *E. coli*) and histidine 210 (histidine 187 in *E. coli*) were identified by site directed mutagenesis of human UDG (Mol, 1995). In the mechanism proposed by Savva et al., aspartate 88 behaves as a general base by abstracting a proton from a water molecule that is simultaneously hydrogen-bonded to the peptide carbonyl and side chain carboxyl of aspartate 88. The aspartate 88 activated water molecule is in van der Waals contact with C1' of the deoxyribose ring and performs a nucleophilic attack at C1' of the glycosidic bond (see Figure 1-11). Cleavage of the N-glycosidic bond is achieved by either physical or electronic

distortion, or by protonation of the uracil O2 by histidine 210 to make it a better leaving group. One caveat to this proposal is that histidine 210 is located 5.1Å away from the uracil O-2 which is too far for a direct proton transfer. As a result, a conformational change must be invoked (Savva, 1995). Since the crystal structure is an enzyme-product complex, the suggestion of a required conformational change is reasonable.

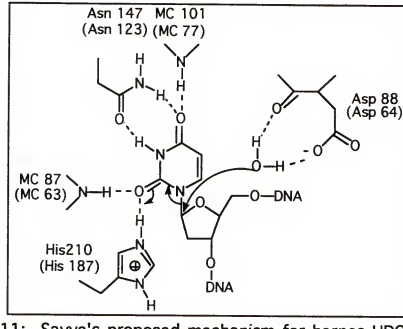

Figure 1-11: Savva's proposed mechanism for herpes UDG (from Savva, 1995). Corresponding *E. coli* residues are shown in parentheses.

Mechanistic Proposal by Mol et al. (1995)

Two mechanisms for glycosidic bond hydrolysis by UDG were proposed by Mol. To determine this mechanism the authors utilized kinetic data from human UDG mutants and crystallographic data from human UDG crystallized alone and with the inhibitor 6-aminouracil. In these proposed mechanisms histidine 268

(histidine 187 in *E. coli*) behaves as a catalytic residue. The first mechanism involves nucleophilic substitution in which histidine 268 attacks C1' directly causing cleavage of the glycosidic bond (see Figure 1-12). In the second mechanism histidine abstracts a proton from a water molecule in a general base mechanism. A hydroxide nucleophile is created which then attacks at C1' of uracil. In both of these mechanisms a critical step is polarization

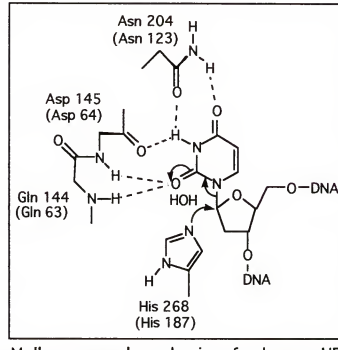

Figure 1-12: Mol's proposed mechanism for human UDG (from Mol, 1995). Corresponding *E. coli* residues are shown in parentheses.

of the glycosidic bond by hydrogen bonds formed between N3 and O4 of uracil and the aspartate 145 backbone carbonyl and asparagine 204 side chain. The backbone amides of aspartate 145 and glutamine 144 form an oxyanion hole for the uracil O2 (Mol, 1995). This is a novel suggestion for a glycosylase mechanism since

there is no acid catalysis. More recent crystallographic studies of UDG help to disprove these hypothetical mechanisms proposed by Mol by demonstrating that histidine 268 is not on the α-face of the deoxyribose so neither of the mechanisms are reasonable (Slupphaug, 1996; Parikh, 1998).

Recent pH versus rate studies (Xiao, 1999) helped to better elucidate the mechanism of UDG. The pH dependence of k_{cat} for wild type *E. coli* UDG demonstrated that a deprotonated residue with a pK_a in the range of 6.2 - 6.6 is required. The catalytically compromised mutant H187Q enzyme showed the same pH dependence of k_{cat}, however, there was no pH dependence of k_{cat} for the catalytically compromised mutant D64N. These results suggest that general base catalysis is accomplished by aspartate 64 (in humans aspartate 145, in herpes aspartate 88) and not by histidine 187 (in humans histidine 268, in herpes histidine 210) as previously proposed by Mol et. al. in 1995 (Xiao, 1999). Since both mutants demonstrate a significant reduction in rate, these results also show that aspartate 64 and histidine 187 are critical residues for catalysis as proposed in 1995 by Mol (1995).

These pH studies also shed some light on Savva's hypothesis that histidine 210 of the herpes enzyme protonates uracil O2 rendering uracil a good leaving group. The results show no evidence for general-acid catalysis (there is no descending limb at high pH values on the pH versus rate plots). It is possible, however, that the pH dependence is out of the range studied (i.e. higher than pH 9.5) (Xiao, 1999). Furthermore, the pH dependence of kinetic

parameters is likely to be complex in a steady-state mechanism. These results shed some doubt on the Savva hypothesis concerning protonation of O2 by a highly conserved active site histidine during catalysis and suggest that further pH versus rate studies are required.

Mechanistic Proposal by Shroyer et al. (1999)

The role of the highly conserved active site histidine residue was recently probed by studying the characteristics of a H187D *E. coli* UDG mutant (Shroyer, 1999). Both biochemical and structural data were used to propose a new twist on Savva's previously proposed mechanistic scheme for UDG (see Figure 1-13). This mechanism differs from the Savva mechanism in that protonation of uracil O2 is not necessary for making uracil a better leaving group. Instead, the leaving group quality of uracil is improved by distribution of the negative charge that is created at the transition state to the N1, O2, and O4 of uracil by resonance and hydrogen bonding (Shroyer, 1999) and not solely at O2 as previously hypothesized (Savva, 1995).

The work discussed in this dissertation furthers the analysis of the mechanistic pathway of UDG. The mechanistic proposal by Prior and Santi is tested through the study of an *E. coli* UDG mutant. Site directed mutagenesis of a lone cysteine residue in the *E. coli* UDG enzyme tested for its possible role in the Michael addition pathway. Kinetic isotope effect experiments are another powerful tool utilized in this work to probe the mechanism of UDG. Much of

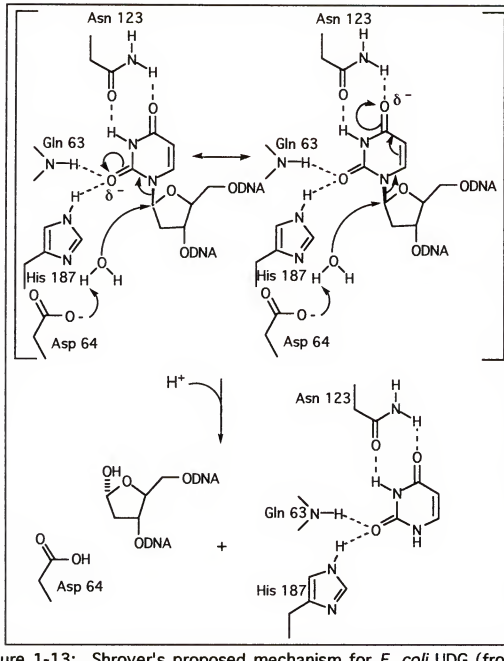

Figure 1-13: Shroyer's proposed mechanism for *E. coli* UDG (from Shroyer, 1999).

the current literature is based on data obtained from X-ray crystal structures. A caveat to X-ray crystallography is that it reports on only a snap-shot of time over the course of an entire reaction, typically the product state and never a transition state. The benefit to kinetic isotope effects is that they report on a reaction

in process, by providing information about transition state structure. Background information on the theory and measurement of kinetic isotope effects will be discussed in chapter 4.

CHAPTER 2
SYNTHESIS OF URACIL-CONTAINING SUBSTRATES

Introduction

This chapter includes a discussion of the synthetic routes for formation of the various UDG substrates studied in this project. A comprehensive study of an enzyme's mechanistic pathway necessitates several different substrates. The UDG substrates synthesized for this project include: HCAII-U (a uracil-containing 781 base pair double stranded piece of DNA), pd(UTT) (a 5'-phosphorylated trinucleotide), pd(UCC), and 2'-deoxyuridine-3',5'-diphosphate (pdUp) (a 3',5'-nucleotide diphosphate).

The HCAII-U substrate was prepared by PCR and contains dU in place of thymidine. It was utilized to measure the specific activity of WT UDG purified in the lab. In addition, the kinetic behavior of C200S UDG with HCAII-U was studied versus the wild type.

Another substrate that was synthesized was pd(UTT). This substrate was utilized to measure a secondary α KIE. In a 1979 dissertation by Charles Garrett, an attempt to measure a secondary α KIE using a DNA substrate was describe, however a unity KIE was reported. It is possible, however, that chemistry was not the rate determining step and therefore the value of unity did not reflect

reflect the true KIE. With these results in mind, our goal was to synthesize a non-sticky and "slow" substrate for UDG and to study the KIEs. A trend for UDG is that as the substrate decreases in size the K_m increases and the V_{max} decreases. The smallest known substrate for UDG (previous to our study) was pd(UT)p, however, the extremely slow rate prevented the authors from determining kinetic parameters. The smallest substrate with measured kinetic parameters was pd(UTT) (Varshney, 1991). This molecule (see figure 2-1) was synthesized by Dr. Benjamin Horenstein using organic chemistry techniques.

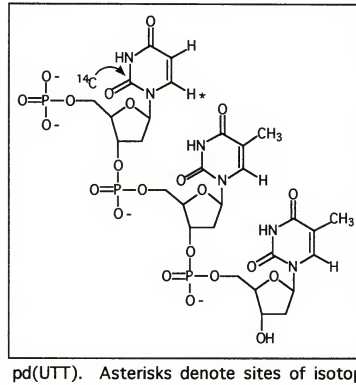

Figure 2-1: pd(UTT). Asterisks denote sites of isotopic labeling.

The substrate pd(UCC) was synthesized enzymatically. The enzymatic route can be completed more quickly and with less manipulation of radioactivity than the organic synthesis route. The

method utilizes a hairpin loop oligomer template and Klenow fragment which elongates the 3' end of the oligomer by inserting a dUTP and two dCTPs. Since Klenow fragment cannot distinguish between dUTP and dTTP, pd(UCC) was synthesized instead of pd(UTT). A long term goal of this project is to measure kinetic isotope effects for uracil-containing oligomers with increasing size. The enzymatic route that was used to synthesize pd(UCC) can be modified to allow for facile synthesis of larger oligomers by changing the sequence of the hairpin-loop template.

The final substrate that was synthesized for this study was pdUp (See figure 2-2). Although Varshney determined pd(UT)p to be

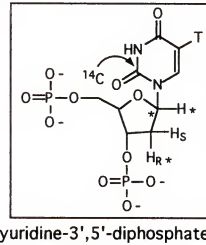

Figure 2-2: 2'-deoxyuridine-3',5'-diphosphate. Asterisks denote sites of stable-isotopic labeling.

the smallest substrate for UDG (Varshney, 1991), we reasoned that pdUp might be a substrate because the phosphate groups on the 3' and 5' sides of the uridine mimic the phosphate backbone of DNA. The trends which correlated an oligonucleotide substrate's length with K_m and k_{cat} (Varshney, 1991) suggested that pdUp would have an elevated K_m and reduced k_{cat} relative to longer substrates.

These kinetic features are necessary to measure intrinsic kinetic isotope effects, and the shortened length of pdUp may be informative in its own right by providing information on the role of sugar-phosphate backbone binding interactions on catalysis.

Results

Synthesis of[5-^{3}H] dU DNA (HCAII-U)

PCR (Saiki, 1985) amplification of the gene coding human carbonic anhydrase II (Montgomery, 1987) afforded 7.1 μg of the 781 bp double stranded DNA substrate at a concentration of 0.032 μg/μL (7.6×10^{-4} μmole uracil/μg DNA) with a specific activity of 480 μCi/μmole uracil. The overall purified yield was approximately 13% based on the amount of radiolabeled [5-^{3}H] dUTP employed.

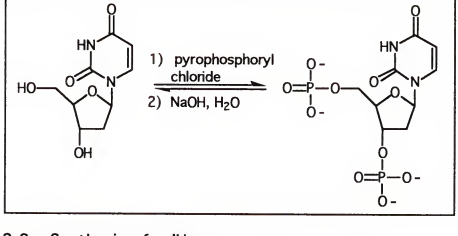

Figure 2-3: Synthesis of pdUp.

Synthesis of pdUp

The potential UDG substrate, pdUp, was obtained in 37% yield (unoptimized) by bis-phosphorylation of 2'-deoxyuridine with pyrophosphoryl chloride as shown in figure 2-3 (Barrio, 1978). Proton (see figure 2-4) and phosphorus (see figure 2-5) NMR were used to confirm that the desired compound had been obtained. The two definitive NMR experiments involved phosphorus NMR with proton decoupling of the H3' and H5' hydrogens which allowed assignment of the two phosphate resonances and demonstrated that O3' and O5' had been monophosphorylated (see figure 2-5). By the same methodology, [2-^{14}C] pdUp was prepared in 35% yield. The yield was estimated by UV absorbance at 260 nm (ε_{260} = 9900) (Dawson, 1987). The other pdUp isotopomers, [5-^{3}H]-pdUp, [5-^{3}H; 1'-^{2}H] pdUp, [5-^{3}H, 1'-^{13}C] pdUp, and [5-^{3}H; 2'R-2'-^{2}H] pdUp (the appropriate dUTP (see below for synthesis of dUTPs) was first treated with calf intestinal alkaline phosphatase and phosphodiesterase to form 2'-deoxyuridine, and then converted to pdUp with pyrophosphorylchloride) were prepared in 40%, 44%, 31%, and 64% yield, respectively (see table 2-1).

Synthesis of UMP, UTP, dUTP radioisotopomers

The syntheses for these radioisotopomers involved a multienzyme method illustrated in figures 2-6 through 2-8. The first step in the synthesis of UMP as shown in figure 2-6, performed by hexokinase, is the phosphorylation of glucose to form glucose-6-phosphate. The following steps convert glucose-6-phosphate to ribose-5-phosphate utilizing the oxidative reactions

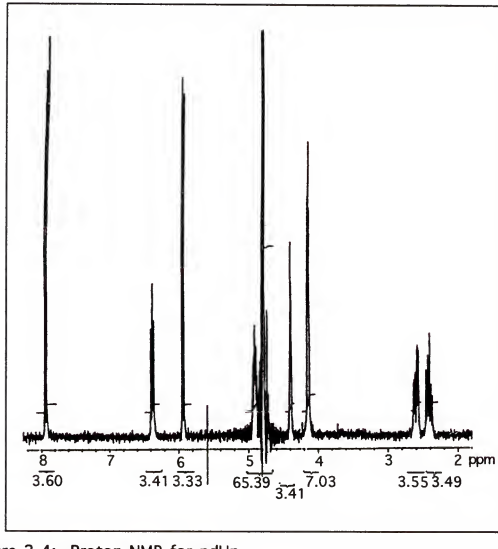

Figure 2-4: Proton NMR for pdUp.

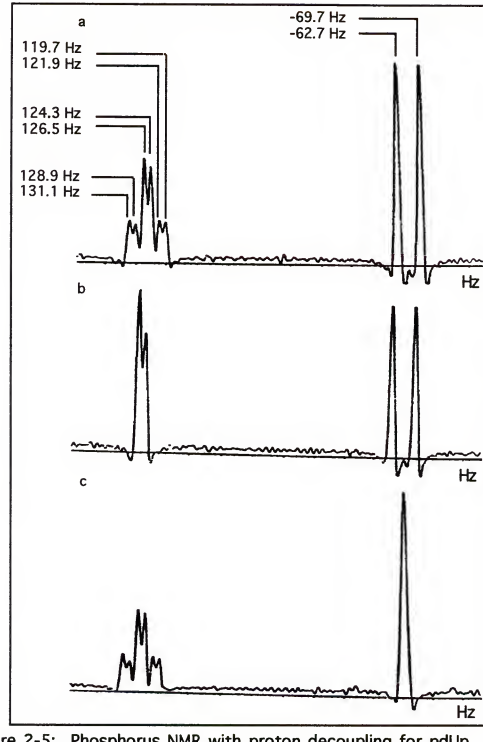

Figure 2-5: Phosphorus NMR with proton decoupling for pdUp. a) proton coupled, b) decoupling at H-5, c) decoupling at H-3.

Table 2-1: Isolated yields of pdUp isotopomers.

pdUp Isotopomer	Isolated % Yield
[5-^{3}H]	40
[2-^{14}C]	35
[5-^{3}H; 1'-^{2}H]	44
[5-^{3}H; 1'-^{13}C]	31
[5-^{3}H; 2'R-2'-^{2}H]	64

of the pentose phosphate pathway. The first step of this pathway is dehydrogenation of glucose-6-phosphate by glucose-6-phosphate dehydrogenase to form 6-phosphogluconate. Next, the action of 6-phosphogluconate dehydrogenase causes the decarboxylation of 6-phosphogluconate to form the ketopentose, ribulose -5-phosphate. Finally, phosphopentose isomerase converts ribulose-5-phosphate to its aldose isomer, ribose-5-phosphate (Lehninger,1993). Once ribose-5-phosphate has been made, 5-phosphoribosyl-1-pyrophosphate synthase (PRPP synthase) utilizes ATP to achieve conversion to 5-phosphorybosyl-1-pyrophosphate (PRPP). Next, orotate phosphoribosyl transferase transfers an orotate to the PRPP to form orotidylate while orotidylate decarboxylase removes the carboxylate at position six to yield the desired product, uridine-5'-monophosphate.

The enzymatic synthesis of uridine-5'-triphosphate from UMP is shown in figure 2-7. Uridine-5'-monophosphate (synthesized in the above reaction) is first phosphorylated by nucleoside monophosphate kinase (NMPK) to form uridine-5'-diphosphate. In the next step, nucleoside diphosphate kinase

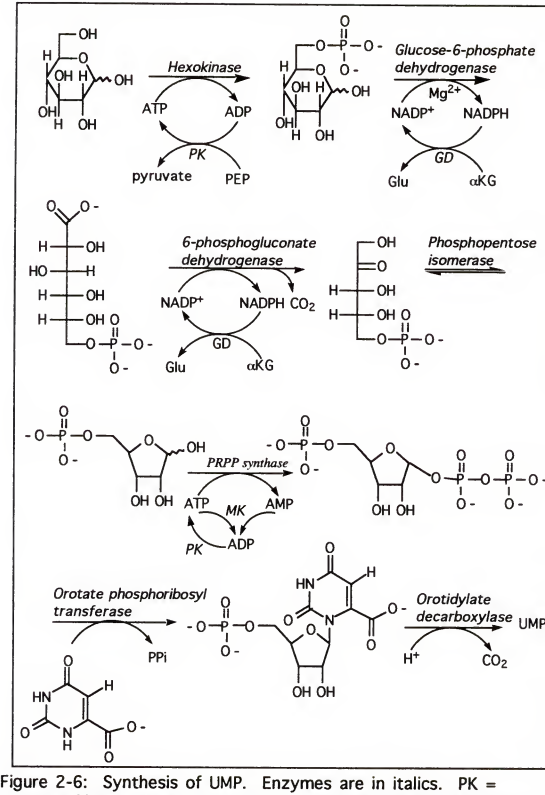

Figure 2-6: Synthesis of UMP. Enzymes are in italics. PK = pyruvate kinase, MK = myokinase, GD = glutamate dehydrogenase. Reagents are in normal font. PEP = phosphoenol pyruvate, αKG = α-ketoglutarate.

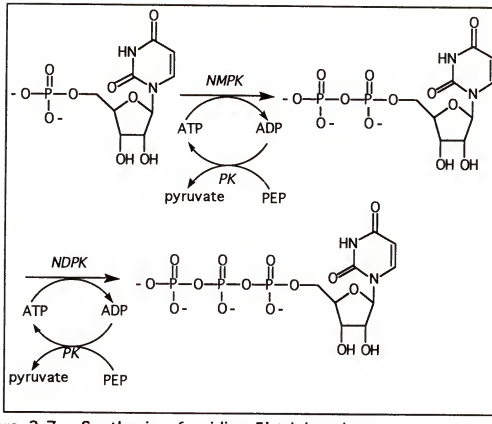

Figure 2-7: Synthesis of uridine-5'-triphosphate.

(NDPK) phosphorylates the urdine-5'-diphosphate to uridine-5'-triphosphate.

The enzymatic synthesis of 2'-deoxyuridine'-5'-triphosphate from UTP is shown in figure 2-8. In this reaction, *Lactobacillus leichmannii* ribonucleotide triphosphate reductase stereospecifically reduces the uridine-5'-triphosphate. The new product hydrogen is derived from solvent, while the original reactant hydrogen remains with retention of its configuration (Blakley, 1966; Gottesman, 1966; Batterham, 1967; Griffin, 1966).

The synthesis of the dUTPs was monitored by HPLC analysis on a Mono-Q column. Figure 2-9 illustrates typical chromatograms

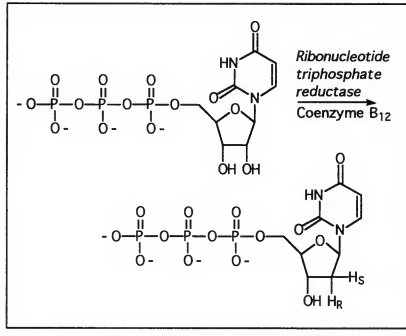

Figure 2-8: Synthesis of 2'-deoxyuridine-5'-triphosphate.

for the synthesis. The % conversion for each of the 3 steps in the synthesis of dUTP were determined by quantifying the radioactivity which eluted from the MonoQ column when the molecule of interest eluted. This amount was compared to the total amount of radioactivity applied to the column. The % conversion for each step ranged from 48 - 75 % for the synthesis of UMP and > 95% for the synthesis of UTP. For the synthesis of [5-^{3}H; 2'R-2'-^{2}H] dUTP the % conversion was 60% while for the other dUTPs the % conversion was > 95 %. The overall purified yields of the dUTP isotopomers are presented in table 2-2.

Proton NMR spectroscopy confirmed the presence of [5-^{3}H; 2'R-2'-^{2}H] dUTP (see figure 2-10a). The proton resonance for the proton at the anomeric carbon (~6.3 ppm) collapsed from a triplet in the undeuterated material (see figure 2-10b) to a doublet in the

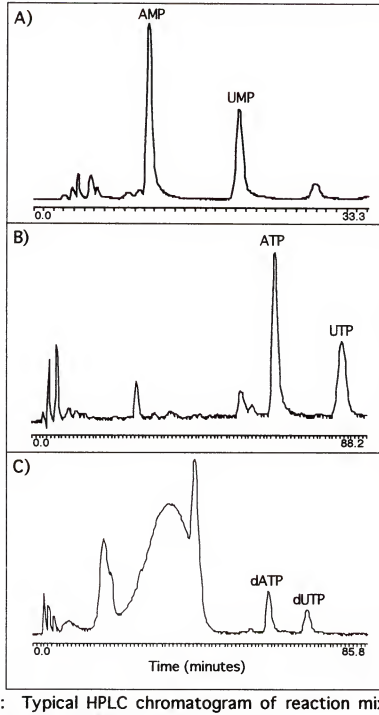

Figure 2-9: Typical HPLC chromatogram of reaction mixtures for the synthesis of: A) UMP, B) UTP, and C) dUTP.

Table 2-2: Isolated % yields of dUTP isotopomers.

dUTP Isotopomer	Isolated % Yield
[5-^{3}H]	13
[2-^{14}C]	36
[5-^{3}H; 1'-^{2}H]	53
[5-^{3}H; 1'-^{13}C]	18
[5-^{3}H; 2'R-2'-^{2}H]	38

deuterated material. This result indicates that [5-^{3}H; 2'R-2'-^{2}H] dUTP was made (Batterham, 1967).

Attempted Synthesis of [5-^{3}H; 2'S-2'-^{2}H dUTP

Several attempts to synthesize [5-^{3}H; 2'S-2'-^{2}H] dUTP were made. In each attempt slight modifications to the method were made such as the omission of a heat shock quench, careful adjustment of pH, and shorter reaction time. Proton NMR demonstrated that only partial deuteration was achieved. The key feature in the NMR is the peak at 6.3 ppm representing the 1'-H. In the NMR for authentic dUTP, this peak is a triplet. If deuteration at C-2 occurred, this peak should collapse to a doublet (Batterham, 1967) as seen in the NMR for [5-^{3}H; 2'R-2'-^{2}H] dUTP (figure 2-10a). In a typical NMR spectrum for [5-^{3}H; 2'S-2'-^{2}H] dUTP synthesized in the lab, however, a multiplet was observed at 6.3 ppm (figure 2-10c).

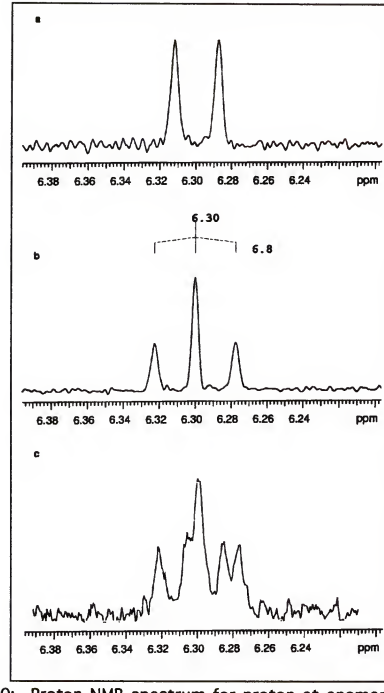

Figure 2-10: Proton NMR spectrum for proton at anomeric carbon for a) [5-^{3}H; 2'R-2'-^{2}H] dUTP, b) dUTP, c) typical attempted synthesis of [5-^{3}H; 2'S-2'-^{2}H] dUTP.

Synthesis of [2-^{2}H] Ribose-5-phosphate

The synthesis of [5-^{3}H; 2'S-2'-^{2}H] dUTP utilized [2-^{2}H] ribose-5-phosphate (see figure 2-11) as a starting material.

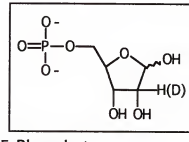

Figure 2-11: Ribose-5-Phosphate.

Two different synthetic methods were employed. One method involved conversion of ribose-5-phosphate to [2-^{2}H] ribose-5-phosphate by phosphoriboisomerase in the presence of D_2O. The equilibrium established in this reaction is shown in figure 2-12. The reaction lies more toward the formation of [2-^{2}H] ribose-5-phosphate which is the only material of the two that is active for

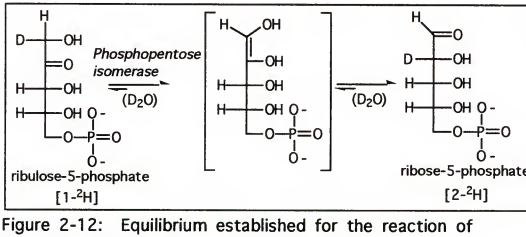

Figure 2-12: Equilibrium established for the reaction of phosphopentose isomerase with ribose-5-phosphate.

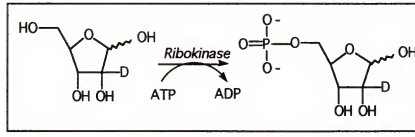

Figure 2-13: Synthesis of ribose-5-phosphate [2-^{2}H] with ribokinase.

the proceeding syntheses (Rising, 1994). The other method involved conversion of [2-^{2}H] ribose to [2-^{2}H] ribose-5-phosphate by ribokinase as shown in figure 2-13. The ribokinase used in this synthesis was cloned, overexpressed, and partially purified in the lab.

Proton NMR demonstrated that position 2 was monodeuterated in the [2-^{2}H] ribose-5-phosphate synthesized by either method. The key feature in the NMR of undeuterated ribose-5-phosphate is a doublet at 5.2 ppm representing the anomeric hydrogen (see figure 2-14b). A proton NMR of [2-^{2}H] ribose-5-phosphate synthesized by either method shows that this doublet has collapsed to a singlet (see figure 2-14a). These results are in accord with deuteration at C-2 (Feather, 1969).

Synthesis of pd(UCC)

The enzymatic route to produce pd(UCC) (Zimmer, 1995) utilized the hairpin-loop template depicted in figure 2-15 and is shown in figure 2-16. All of the bases in the template were deoxyribonucleotides except for the ribouracil located at the 3' terminus. There was a three base overhang on the 5' end which

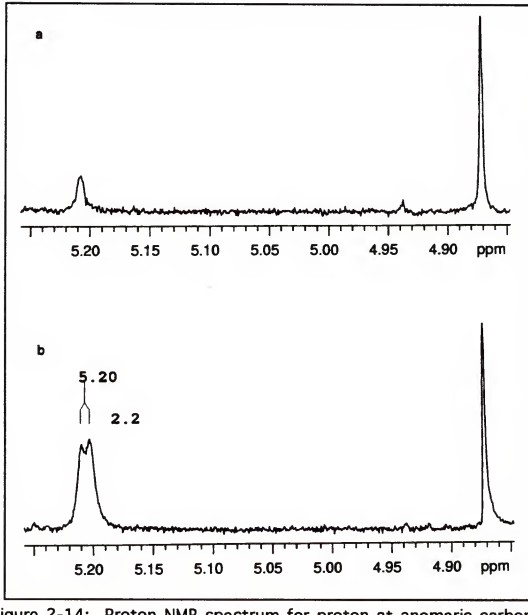

Figure 2-14: Proton NMR spectrum for proton at anomeric carbon for a) [2-^{2}H] ribose-5-phosphate, b) ribose-5-phosphate.

Figure 2-15: Hairpin loop template (19 bp) used in the synthesis of pd(UCC).

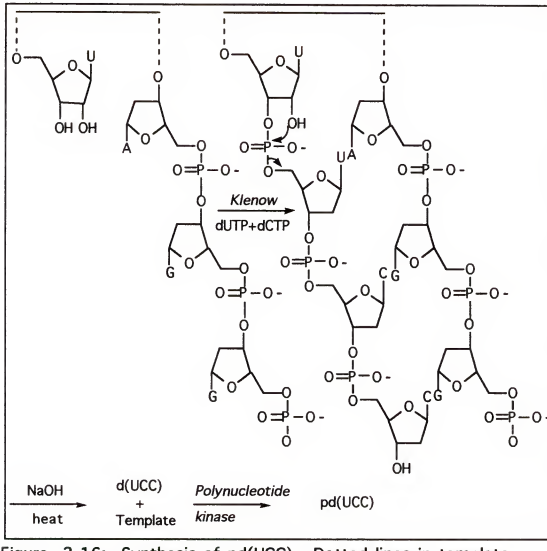

Figure 2-16: Synthesis of pd(UCC). Dotted lines in template represent the 15 other bases of the hairpin loop.

served as the template for formation of d(UCC). In this reaction, first, Klenow fragment inserts the proper bases on the 3' side of the template. Next, the reaction is treated with sodium hydroxide and heat which causes cleavage of the d(UCC) from the template (Zimmer, 1995). Finally, the action of polynucleotide kinase 5'-phosphorylates the 5' side of the d(UCC) to form pd(UCC).

To determine if d(UCC) was synthesized, the reaction mixture was analyzed using MonoQ HPLC with a UV detector. An authentic sample of d(UCC) chemically synthesized by the University of Florida Interdisciplinary Center for Biotechnology Research (ICBR) allowed for coinjection with a d(UCC) reaction mixture. The d(UCC) eluted at 16.7 minutes and the percent conversion, determined by integration of HPLC peaks, was 10% (see figure 2-17). A possible reason for the low yield is incomplete cleavage of the d(UTT) by treatment with NaOH and heat. Optimization of the yield is an area for future work.

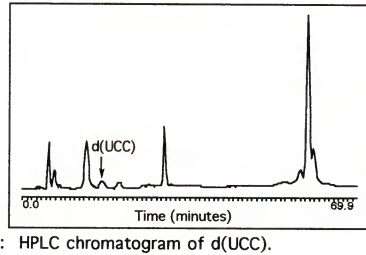

Figure 2-17: HPLC chromatogram of d(UCC).

The next step was to 5'-phosphorylate the d(UCC). Since authentic samples of both d(UTT) and pd(UTT) (synthesized by ICBR) were readily available in the lab but authentic samples of both d(UCC) and pd(UCC) were not, the d(UTT) was 5'-phosphorylated instead to test the reaction on a trinucleotide substrate. The success of this reaction suggests that 5'-phosphorylation of d(UCC) by the same method should yield pd(UCC). An authentic sample of d(UTT) was treated with polynucleotide kinase and analyzed by reversed phased C18 HPLC. An aliquot of the reaction mixture before addition of T4 polynucleotide kinase showed a peak that co-eluted with an authentic sample of d(UTT). An aliquot of the reaction mixture after treatment with T4 polynucleotide kinase showed a peak that co-eluted with an authentic sample of pd(UTT). In this aliquot there was no peak corresponding to d(UTT) which suggests the phosphorylation reaction was quantitative.

Overexpression of *E. coli* Ribokinase

E. coli ribokinase was used to convert [2-^{2}H] ribose to [2-^{2}H] ribose-5-phosphate. PCR was used to amplify the *E. coli* ribokinase gene from genomic DNA. The PCR product was cloned directly into the pET22b+ expression vector to form p10EH43.2, and BL21(DE3) *E. coli* were transformed with this expression construct. Overexpression was induced with IPTG and the cells were harvested, then lysed. The ribokinase activity assay (see figure 2-18) was used to confirm that overexpression had occurred. The ribokinase activity assay is a coupled enzyme assay which

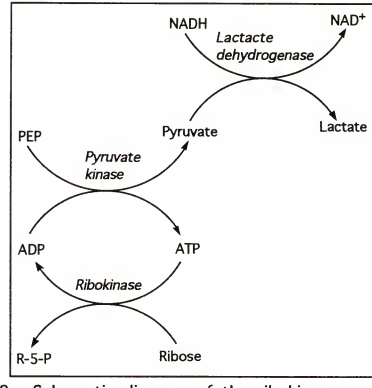

Figure 2-18: Schematic diagram of the ribokinase purification assay.

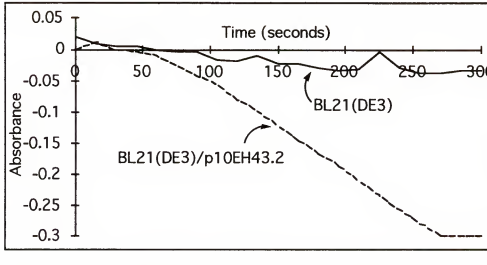

Figure 2-19: Overexpression of *E. coli* ribokinase as indicated by the ribokinase activity assay. The solid line represents the control while the dotted line represents the test material.

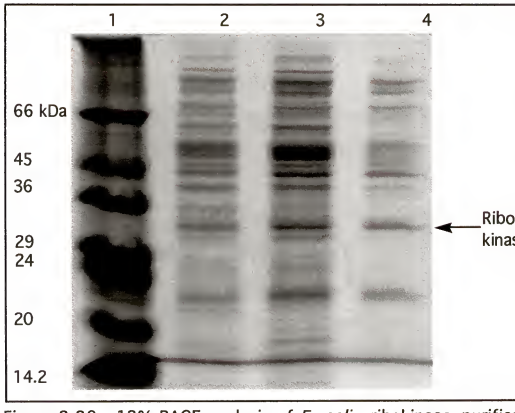

Figure 2-20: 12% PAGE analysis of *E. coli* ribokinase purification. Lane 1: SDS-7 molecular weight markers, Lane 2: lysate, Lane 3: dialyzate, Lane 4: partially purified ribokinase by DEAE Sephadex (2 μg).

involved UV analysis at 340 nm of the oxidation of NADH to NAD^+ (Parkin, 1984). The overxpression is depicted in figure 2-19, where the solid squares represent the control (soluble protein from BL21(DE3) *E. coli* that had not been transformed with p10EH43.2), and the open squares represent the test material (soluble protein from BL21(DE3) *E. coli* that had been transformed with p10EH43.2 and induced with IPTG). There is little or no oxidation for the control reaction, whereas, oxidation of NADH to NAD^+ for the test material is indicated by the decrease in absorbance at 340 nm.

Conclusively, overexpression of ribokinase occurred in the test material.

The overexpression and partial purification by DEAE-Sephadex of *E. coli* ribokinase from a 500 ml liquid culture (Parkin, 1984; Sigrell, 1997; Anderson, 1969) afforded 62 mg (570 units) of active enzyme. The enzyme's specific activity was 9.12 μmole/min/mg. The purified *E. coli* ribokinase (32.3 KDa) was analyzed by PAGE (see figure 2-20).

Discussion

Synthesis of[5-^{3}H]-dU DNA (HCAII-U)

The synthesis of [5-^{3}H]-dU DNA (HCAII-U) utilized the polymerase chain reaction. There was no TTP present in the reaction mixture; instead dUTP was present. This forced taq polymerase to insert dUTP whenever TTP was supposed to be inserted. In this way, a uracil-containing DNA substrate was produced (Schmidt, 1996). The synthesis and subsequent purification afforded 7.1 μg of HCAII-U at a concentration of 0.032 μg/μL (7.6×10^{-4} μmole uracil/μg DNA) with a specific activity of 6.88×10^8 cpm/μmole uracil.

A classic method not utilized in this project, is to prepare radiolabeled uracil-containing DNA by growing bacteria in radioactive culture (Lindahl, 1977). The bacteriophage PBS1 is used because it incorporates uracil instead of thymine in its DNA. A liquid culture of *Bacillus subtilis* is infected with PBS1 phage in the presence of 1 mCi of [^{3}H] uridine. After a few hours, the cells

are lysed and the DNA is recovered and purified. This method, as compared to the PCR/gel purification method used in this project, is not very practical for several reasons. Firstly, the PCR/gel purification method can yield pure radiolabeled uracil-containing DNA in a day, whereas the method involving the growth of bacteria in radioactive culture takes at least 5 days. Secondly, the PCR/gel purification uses 1/20 of the radioactivity. Lastly, the PCR/gel purification method is much less tedious and involves less manipulation of radioactivity.

Synthesis of Radiolabeled dUTP Isotopomers

In order to measure kinetic isotope effects for the UDG hydrolysis of pdUp it was necessary to develop a method for synthesizing radiolabeled pdUps. The molecule dUTP can easily be converted to 2'-deoxyuridine (the starting material for the synthesis of pdUp) by dephosphorylation. A multi-enzymatic synthetic route was employed to synthesize the dUTP isotopomers which involved a combination of previously established enzymatic syntheses. The method is superior to chemical synthesis as indicated by the high yields and the ease by which the enzymatic synthesis can be performed.

The enzymatic synthesis of uridine-5'-monophosphate is shown in figure 2-6 and is based on literature procedures (Tao, 1996; Rising, 1994). Early attempts to synthesize UMP using the method described by Parkin and Schramm (1987) were unsuccessful. The main differences between this method and the method that was used in this work is that phosphate buffer was

used instead of triethanolamine and larger amounts of enzyme were used.

The enzymatic synthesis of uridine-5'-triphosphate from UMP is shown in figure 2-7 and is a straightforward process that proceeded in good yields. The enzyme, nucleoside monophosphate kinase, is expensive, however an overexpression construct for the *E. coli* enzyme has recently been prepared in the lab by Natalie Ramezani.

The enzymatic synthesis of 2'-deoxyuridine-5'-triphosphate from UTP is shown in figure 2-8 and when performed in H_2O proceeded in good yields. The synthesis of [5-^{3}H; 2'R-2'-^{2}H] dUTP required D_2O as the solvent and the yield was lower. Great care was taken to fully exchange the ribonucleotide triphosphate reductase into deuterated buffer. Chemical means exist to replace a ribose hydroxyl with a hydrogen, but not with the high stereospecificity of this enzymatic transformation.

Synthesis of [2-^{2}H] Ribose-5-phosphate

The starting material for the synthesis of [5-^{3}H; 2'S-2'-^{2}H] dUTP was [2-^{2}H] ribose-5-phosphate which was synthesized in the lab. The starting material, [3-^{2}H] glucose, could not be used because loss of the deuterium would occur during oxidative decarboxylation.

Since ribose-5-phosphate is one of the intermediates in the multienzyme synthesis of UMP, it can also serve as a starting material. Two different methods were used. The first method used phosphoriboisomerase to convert ribose-5-phosphate to [2-^{2}H]

ribose-5-phosphate and was based on the procedure described by Rising (1994). Although the proton NMR spectrum demonstrated that position 2 of the [2-^{2}H] ribose-5-phosphate was fully deuterated, when this same material was used as a starting material for the synthesis of dUTP, the proton NMR spectrum demonstrated that the 2' position had experienced deuterium washout. A second method for synthesis of [2-^{2}H] ribose-5-phosphate was developed.

The second method utilized to synthesize [2-^{2}H] ribose-5-phosphate involved the conversion of [2-^{2}H] ribose to [2-^{2}H] ribose-5-phosphate by ribokinase. As observed with the first method for synthesis of [2-^{2}H] ribose-5-phosphate, the NMR spectrum of the [2-^{2}H] ribose-5-phosphate demonstrated that position 2 was fully deuterated. The proton NMR spectrum of the [5-^{3}H; 2'S-2'-^{2}H] dUTP made from this starting material, however, demonstrated that the 2' position was not fully deuterated. This issue is discussed further in the proceeding section.

Attempted Synthesis of [5-^{3}H; 2'S-2'-^{2}H] dUTP

The synthesis of [5-^{3}H; 2'S-2'-^{2}H] dUTP was attempted several times, however, the material was never successfully synthesized with high ^{2}H incorporation. The first attempts utilized phosphoriboisomerase to deuterate ribose-5-phosphate at carbon 2 in a separate reaction (see figure 2-12). These attempts differed in quenching and concentrating procedures. One of the reactions was heat inactivated while another was not. In addition, one was concentrated to dryness while another was lyophilized to

dryness. Proton NMR spectroscopy of the resulting [2-^{2}H] ribose-5-phosphate demonstrated that full deuteration at C2 had occurred because the H1 signal was a singlet in the [2-^{2}H] ribose-5-phosphate proton NMR spectrum as opposed to the doublet observed in the proton NMR spectrum of undeuterated ribose-5-phosphate. The NMR spectrum for [5-^{3}H; 2'S-2'-^{2}H] dUTP synthesized from the [2-^{2}H] ribose-5-phosphate made by the above procedure, however, was not fully deuterated at the 2' position. These results suggest that the deuterium was washed out during the synthetic pathway from [2-^{2}H] ribose-5-phosphate to [5-^{3}H; 2'S-2'-^{2}H] dUTP. A logical solution was to perform the synthesis of [2'-^{2}H] UMP from [2-^{2}H] ribose-5-phosphate in D_2O instead of H_2O. The proton NMR spectrum of the final dUTP product, however, indicated that the ribose C2 was deuterated as well as the uracil C6. There was no signal for the uracil C6 in the spectrum. This probably occurred during the decarboxylation of orotic acid.

The other trial syntheses utilized *E. coli* ribokinase to convert [2-^{2}H] ribose to [2-^{2}H] ribose-5-phosphate (see figure 2-13). As mentioned for the above synthesis, the NMR for [2-^{2}H] ribose-5-phosphate demonstrated that the molecule had been made (see figure 2-14 (a)), however, the [5-^{3}H; 2'S-2'-^{2}H] dUTP that was made from this [2-^{2}H] ribose-5-phosphate was not fully deuterated at the 2' position (see figure 2-10c). One possibility was that an increase in pH during preparation of the 2X UMP synthesis buffer caused loss of the deuterium at position 2. To test this theory, a trial synthesis of [5-^{3}H; 2'S-2'-^{2}H] dUTP was completed in which the pH of the 2X reaction buffer was adjusted to pH 7.8 prior to

addition of [2-^{2}H] ribose-5-phosphate. Proton NMR of the resulting material showed only partial deuteration at position 2'. Another theory was that loss of the deuterium at position 2' might be avoided if formation of UMP occurred immediately after the deuteration step. To test this theory, a synthesis of [5-^{3}H; 2'S-2'-^{2}H] dUTP in which the synthesis of ribose-5-phosphate was included with the synthesis of UMP was performed. The product also showed only partial deuteration at the 2' position.

A possible explanation for the loss of deuterium at position 2' is a contaminating enzyme. If phosphoriboisomerase, for example, is present during the synthesis which takes place in H_2O, then the deuterium at position 2 could be exchanged for hydrogen. To determine at which step in the synthesis of dUTP the loss was occurring, NMR was performed on the [2-^{2}H] ribose-5-phosphate starting material and on the purified UMP made in the UMP synthesis reaction. Full deuteration at position 2 was observed in the [2-^{2}H] ribose-5-phosphate, however, loss of deuterium was seen for the UMP. This suggests that the deuterium was washed out during the synthesis of UMP from [2-^{2}H] ribose-5-phosphate. In the future, addition of a phosphoriboisomerase inhibitor, further purification of the ribokinase, or purchase of highly pure UMP synthesis enzymes might help halt deuterium exchange. The best next experiment would be to first add only PRPP synthase to the [2-^{2}H] ribose-5-phosphate. If the "contaminant" is not present in the PRPP synthase solution then the problem will be solved because once the PRPP is made ^{2}H/^{1}H exchange will not occur at the 2' position. In the worst case, syntheses could be conducted entirely

in D_2O, which would provide double labeled UMPs having deuterium at C-6 of the uracil and C2' of the ribose. Any KIEs measured with these substrates would require correction with a control substrate labeled with deuterium at C6 of the uracil.

Synthesis of pdUp

The dUTP isotopomers were easily converted to 2'-deoxyuridine using calf intestinal alkaline phosphatase and phosphodiesterase. This reaction proceeded in high yield. Though 3',5' deoxynucleoside diphosphates are known (Barrio, 1978), the radiolabeled pdUps reported in this work are new compounds.

Synthesis of pd(UCC)

The enzymatic synthesis of pd(UCC) involved the 19-mer hairpin-loop template shown in figure 2-15 and the method is illustrated in figure 2-16 (Zimmer, 1995). The results presented in this dissertation for the synthesis of pd(UCC) represents the preliminary results of the synthesis. The percent yield of d(UCC) was 10 %, which is low. Some of the difficulties which might have contributed to the low yield are the impurities in the hairpin-loop template stock and incomplete cleavage of d(UTT) after treatment with NaOH and heat. Once optimized, it is anticipated that this method will be well suited for synthesis of small oligonucleotides that incorporate radiolabels at specific positions.

Overexpression and Purification of Ribokinase

Overexpression of *E. coli* ribokinase was necessary to provide an enzymatic route to convert [2-^{2}H] ribose to [2-^{2}H] ribose-5-phosphate. This second method for synthesizing [2-^{2}H] ribose-5-phosphate was developed because the [2-^{2}H] ribose-5-phosphate synthesized by the original method (conversion of ribose-5-phosphate to [2-^{2}H] ribose-5-phosphate by treatment of ribose-5-phosphate with phosphoriboisomerase in the presence of D_2O) did not ultimately yield [5-^{3}H; 2'S-2'-^{2}H] dUTP. Though as yet unproven, we considered that traces of the heat stable isomerase could have been contributing to deuterium washout. Use of deuterated ribose as a starting material allowed us to avoid use of the isomerase and enter the multi-enzyme synthetic pathway by the action of ribokinase.

Experimental

Materials

Buffers, reagents, and enzymes were purchased from Sigma, Aldrich, Fisher Scientific, New England Biolabs, Biorad, and Boehringer Mannheim Biochemicals. D_2O was obtained from Aldrich or Cambridge Isotope Laboratories, Inc. and was 99.9% deuterium. D-[2-^{13}C] glucose and D-[2'-^{2}H] glucose were purchased from Omicron Biochemicals Inc. Orotic acid isotopomers ([5-^{3}H] and [2-^{14}C]) and [2-^{14}C] deoxyuridine were purchased from Moravek Biochemicals. Liquid scintillation fluid (ScintiSafe 30%) was purchased from Fisher. Oligodeoxynucleotide primers were purchased from the Interdisciplinary Center for Biotechnology

Research (ICBR) core facilities at the University of Florida and from Integrated DNA Technologies, Incorporated (IDT). HCAII-U DNA was gel purified using DNA Purification Kit by Biorad. Cells were lysed using a French pressure cell with a Carver hydraulic press.

Instrumental

HPLC was performed on a Rainin HPXL gradient unit interfaced to a Macintosh personal computer. Separations were performed on a MonoQ HR10/10 anion exchange column (Pharmacia). A Rainin Dynamax UV-1 detector was utilized to monitor separations at 260 nm. A Rainin-Dynamax fraction collector (Model FC-1) was used to collect eluent samples from the HPLC. Liquid scintillation counting utilized a Packard 1600 TR instrument which transferred data to a floppy disk for subsequent analysis on a personal computer. An Orion Sure-Flow pH probe was used in conjunction with an Accumet model 15 pH meter for all pH measurements. FAB-MS, with nitrobenzyl alcohol as matrix, were obtained at the University of Florida Chemistry Department on a Finnigan MAT95Q Hybrid Sector mass spectrometer. ^{1}H and ^{31}P NMR spectra were obtained in D_2O on Unity 500 MHz, Gemini 300 MHz, and VXR 300 MHz spectrometers. Chemical shifts were referenced to the residual HDO line (4.80 ppm). Centrifugation was performed using a Sorvall RC 5B centrifuge or a Sorvall MC 12V centrifuge.

Synthesis of [5-^{3}H]-dU DNA (HCAII-U)

PCR was used to prepare a radioactive dU containing substrate. The PCR template was the coding sequence for human carbonic anhydrase II (hCAII) (Montgomery, 1987) which had previously been cloned into a pET22b expression vector (B. Horenstein, unpublished results). The resulting PCR product contains 376 mole dU/mol oligonucleotide. The primer sequences were: 5'-GGG GGG GCA TAT GTC ACA TCA CTG GGG GT-3', and 5'-TTT GAA TTC TTA TTT GAA GGA GGC TTT GAT-3'. PCR reaction mixtures (25 x 100 mL) consisted of 2.5 mM $MgCl_2$, PCR buffer, 2 mM each dATP, dCTP, dGTP, [5-^{3}H]-dUTP (s.a. 483 mCi/mmol), and 0.5 units Taq polymerase (Schmidt, 1996). The PCR cycle consisted of a hot start at 94°, followed by (94°,1 min; 55°, 1 min.; 72° 1 min.) x 25 cycles. The DNA was purified from the reaction mixtures with the Prep-A-Gene DNA Purification System (Biorad).

Synthesis of 2'-deoxyuridine-3',5'-diphosphate (pdUp)

The following procedure is based on the method of Barrio, et al. (Barrio, 1978). A conical flask containing 2'-deoxyuridine (0.154 mmole, 35 mg) was cooled to 0 °C on ice with stirring. Tetrachloropyrophosphate (Crofts, 1960) (213 mL, 1.53 mmole) was added dropwise. After 4 hours of stirring at 0 °C, the mixture was maintained at -20 °C for 12 hours. The reaction was quenched by addition of 10 g of ice and 1M NaOH until the pH stabilized at pH 7. The percent isolated yield was 37. ^{1}H NMR (D_2O) d: 2.40 [ddd, 1H, CH_2(2'a), J=14.3, 7.9, 6.2 Hz]; 2.59 [ddd, 1H, CH_2(2'b), J=14.3, 6.2, 2.7 Hz]; 4.14 [m, 2H, CH_2(5'), J= 3.4, 4.8 Hz]; 4.38 [m, 1H, CH(4')];

4.89-4.93 [m, 1H, CH(3')]; 5.93 [d, 1H, CH(5), J=8.2 Hz]; 6.35 [dd, 1H, CH(1'), J=7.9, 6.2 Hz]; 7.91 [d, 1H, CH(6), J=8.2 Hz]. ^{31}P NMR (D_2O) d: -0.24 [d, 1P, PO_4^{2-}(3'), J=7.8 Hz]; 0.46 [td, 1P, PO_4^{2-}(5'), J=5.0, 2.0 Hz]. FAB(-) MS: M(-H) 387.1.

Purification and Desalting of pdUps

The crude pdUp reaction mixture was applied to a 1 x 25 cm Dowex 1x8 -200 anion exchange column equilibrated with 200 mM NH_4HCO_3, ~pH 7.3, and eluted with the same buffer until all of the inorganic phosphate was eluted from the column (tested by malachite green assay) (Baykov, 1988) After all of the inorganic phosphate was eluted, the pdUp was eluted with a 200-800 mM NH_4HCO_3 gradient. The tubes containing pdUp (assayed by HPLC) were pooled, and desalted with Amberlite IR-120 (H^+) ion-exchange resin. To prepare the resin approximately 100g of the resin were washed with 2 L deionized water followed by 500 mL 95% ethanol and 2L deionized water. Next, the resin was washed with 1 L 4N HCl. The resin was finally washed with water until the pH was neutral by pH paper. The resin was stored at 4°C and washed with water prior to use. Amberlite and product containing fractions were combined in a 250 mL flask. The mixture was swirled for about 30-60 seconds. The liquid was poured into a second 250 mL flask containing Amberlite. The Amberlite in the original 250 mL flask was washed three times with water and the washings were added to the second 250 mL flask. The material in the second 250 mL flask was swirled for 30-60 seconds and the liquid was filtered through a glass pipette containing glass wool directly into

a round bottom flask. The remaining Amberlite resin was washed 3 times with water and the washings were filtered through a glass pipette into the round bottom. The desalted solutions were carefully concentrated to dryness *in vacuo* without heating and redissolved in water. The pH was carefully adjusted to 7 with 1N NH_4OH and the solution was again concentrated to dryness *in vacuo*. The purified pdUp was dissolved in H_2O and stored at -20° C.

Synthesis of [2-^{14}C] pdUp

The radioisotopomer was synthesized as described above. Thus 20 mCi [2-^{14}C] 2'-deoxyuridine (s.a. 50 mCi/mmol) was bis-phosphorylated to afford 7 mCi [2-^{14}C] pdUp (35%) after chromatography. [2-^{14}C] pdUp was found to co-elute with unlabeled pdUp upon co-injection in anion-exchange HPLC (MonoQ HR10/10, 300 mM NH_4HCO_3, pH 7.8, 10% MeOH, 2 mL/min, A_{260} retention time = 25.7 min.) The isolated yield was 35 %.

Synthesis of pdUp [5-^{3}H]

First, [5-^{3}H] dUTP was dephosphorylated to form [5-^{3}H] dU. Approximately 0.08 mg [5-^{3}H] dUTP (~10 μCi) were concentrated to dryness and converted to dU by mixing with 885 μl H_2O, 100 μl 10X calf intestinal alkaline phosphatase (CIAP) buffer (0.5M Tris-HCl(pH 9.3), 10 mM $MgCl_2$, 1mM $ZnCl_2$), phosphodiesterase from Crotalus durissus (0.03U) (Boehringer Mannheim 108 260), and alkaline phosphatase from calf intestine (5U) (Promega M 1821). The reaction was incubated at room temperature for 1 hour and 20 minutes. To quench the reaction, 20μl 0.5M EDTA, pH 8 was added

and the reaction was concentrated 3X to dryness from pyridine. Next, the dU was converted to pdUp. The dU [5-^{3}H] was cooled on ice and 125µl tetrachloropyrophosphate was added. The reaction was stirred on ice for 4 hours and quenched by adding ice cold 2N NaOH until the pH remained constant at 7. The crude mixture was purified using the same procedure mentioned above for the synthesis of 2'-deoxyuridine-3',5'-diphosphate. [5-^{3}H]-pdUp was found to co-elute with unlabeled pdUp upon co-injection in anion-exchange HPLC (MonoQ HR10/10, 300 mM NH_4HCO_3, pH 7.8, 10% MeOH, 2 mL/min, A_{260} retention time = 25.7 min). The isolated yield was 40 %.

Synthesis of [5-^{3}H;1'-^{13}C], [5-^{3}H;1'-^{2}H], and [5-^{3}H; 2'R-2'-^{2}H] pdUp

These materials were synthesized the same as [5-^{3}H] pdUp. The respective % isolated yields were 31, 44, and 64 %.

Synthesis of [uracil-2-^{14}C], [uracil-6-^{3}H], and [uracil-2'-^{3}H] pd(UTT)

These molecules were synthesized by Dr. Benjamin Horenstein.

Synthesis of [5-^{3}H] Uridine-5'-monophosphate

A 2X UMP synthesis buffer was prepared containing 100 mM triethanolamine, pH 7.8, 10 mM $MgCl_2$, 4 mM glucose, 2 mM ATP, 0.3 mM $NADP^+$, 10 mM NH_4OAc, 2 mM cold orotic acid, 20 mM

phosphoenolpyruvate, 20 mM $Mg(OAc)_2$, and 20 mM α-ketoglutarate. [5-^{3}H] orotic acid (13.5 Ci/mmol), 180 μCi, was concentrated to dryness in a 10 ml pear shaped flask. One and a half milliliters 2X UMP synthesis buffer plus 1.3 mL of water was added to the concentrated radiolabeled orotic acid. The following enzymes were then added to the mixture with hexokinase added last: pyruvate kinase from rabbit muscle (12U) (Boehringer Mannheim 127 418), phosphoriboisomerase from Tortula yeast (12U) (Sigma P7434), myokinase from rabbit muscle (6U) (Boehringer Mannheim 107 506), glutamic dehydrogenase from bovine liver (1.5U) (Sigma G 2501), phosphoribosyl-pyrophosphate synthetase from *E. coli* (0.6U) (Sigma P 0287), orotidine-5'-phosphate pyrophosphorylase and orotidine-5'-phosphate decarboxylase from yeast (12U) (Sigma O 6250), 6-phosphogluconic dehydrogenase from Tortula yeast (0.3U) (Sigma P 0507), glucose-6-phosphate dehydrogenase from baker's yeast (0.3U) (Sigma G 7877), and hexokinase from baker's yeast (0.3U) (Sigma H 5625). The reaction mixture (total volume = 3 mL) was incubated at 37° C for 8 hours. The reaction was heat inactivated at 95 °C for 5 minutes. The quenched reaction was centrifuged at 12,000 rpm and the pellet was discarded. The supernatant was used in the synthesis of [5-^{3}H] UTP. To confirm that UMP had been made, an aliquot was analyzed by MonoQ HPLC (see experimental section titled "Analytical HPLC Method for Monitoring the Synthesis of dUTPs").

Synthesis of [5-^{3}H; 1'-^{2}H] and [5-^{3}H; 1'-^{13}C] UMP

These materials were synthesized the same as [5-^{3}H] uridine-5'-monophosphate with the exception that 4 mM D-[2-^{2}H] glucose and 4 mM D-[2-^{13}C] glucose, respectively, were used instead of 4 mM glucose.

Synthesis of [2-^{14}C] UMP

This material was synthesized the same as [5-^{3}H] uridine-5'-monophosphate except no unlabeled orotic acid was present in the 2X buffer and 180 μCi [2-^{14}C] orotic acid (55 mCi/mmole) was used instead of [5-^{3}H] orotic acid.

Synthesis of [5-^{3}H] Uridine-5'-triphosphate

Solid phosphoenolpyruvate and potassium chloride were added to the quenched UMP reaction to final concentrations of 25 mM and 50 mM, respectively. Pyruvate kinase from rabbit muscle (48 U), nucleoside-5'-diphosphate kinase from baker's yeast (3U) (Sigma N 0379), and nucleoside monophosphate kinase from bovine liver (0.75U) (Boehringer Mannheim 107 948) were added. The reaction was incubated at 37 °C for 1.5 hours then heat inactivated at 95 °C for 5 minutes. The reaction was centrifuged at 12,000 rpm and the pellet was discarded. The supernatant was extracted with 2 ml chloroform then used in the synthesis of dUTP. To assure that UTP had been made, an aliquot was analyzed by MonoQ HPLC (see experimental section titled "Analytical HPLC Method for Monitoring the Synthesis of dUTPs").

Synthesis of [5-^{3}H; 1'-^{2}H], [5-^{3}H; 1'-^{13}C], and [2-^{14}C] Uridine-5'-triphosphate

These materials were synthesized the same as [5-^{3}H] uridine-5'-triphosphate.

Synthesis of [5-^{3}H] 2'-deoxyuridine-5'-triphosphate

To the chloroform-extracted UTP reaction mixture, solid DTT, EDTA, NaOAc, and HEPES were added to final concentrations of 33 mM, 77 mM, 500 mM, and 28 mM, respectively. The pH was adjusted to 7.5 with 1M HCl. The reaction mixture was wrapped in aluminum foil (coenzyme B_{12} is light sensitive) and coenzyme B_{12} was added to a final concentration of 80 μM. Finally, ribonucleotide triphosphate reductase (300 μg) was added and the reaction was incubated at 37 °C for 1 hour. The mixture was heat inactivated at 95 °C for 5 minutes and centrifuged at 12,000 rpm. The pellet was discarded and the supernatant was extracted from 2 ml chloroform. The specific activity was approximately 55 mCi/mmole. To assure that dUTP had been made, an aliquot was analyzed by MonoQ HPLC (see experimental section titled "Analytical HPLC Method for Monitoring the Synthesis of dUTPs"). The isolated yield was 13 % from the orotic acid starting material.

Synthesis of [5-^{3}H; 1'-^{2}H], [5-^{3}H; 1'-^{13}C], and [2-^{14}C] 2'-deoxyuridine-5'-triphosphate

These materials were synthesized the same as [5-^{3}H] 2'-deoxyuridine-5'-triphosphate. The respective isolated yields were

53, 18, and 36 % from the corresponding orotic acid starting material.

Synthesis of [5-^{3}H, 2'R-2'-^{2}H] 2'-deoxyuridine-5'-triphosphate

The chloroform-extracted [5-^{3}H] UTP reaction mixture was concentrated to dryness and 4.5 ml deuterated RTPR buffer (33 mM DTT, 77 mM EDTA, 500 mM NaOAc, and 28 mM HEPES, pH 7.1) was added. The reaction was then concentrated 3X to dryness from D_2O and dissolved in 4.5 ml D_2O. The reaction mixture was wrapped in aluminum foil and coenzyme B_{12} was added to a final concentration of 80 μM. Finally, ribonucleotide triphosphate reductase (350 μg) in deuterated buffer (see experimental section titled "Purification of Ribonucleotide Triphosphate Reductase (RTPR)") was added and the reaction was incubated at 37 °C for 1 hour. The mixture was heat inactivated at 95 °C for 5 minutes and centrifuged at 12,000 rpm. The pellet was discarded and the supernatant was extracted with 2 ml chloroform. To assure that UTP had been made, an aliquot was analyzed by MonoQ HPLC (see experimental section titled "Analytical HPLC Method for Monitoring the Synthesis of dUTPs"). The isolated % yield was 38 % from the orotic acid starting material. In the proton NMR spectrum, the H2 signal integrated to one proton and the H1 was a doublet at 6.3 ppm.

Attempted Synthesis [5-^{3}H; 2'S-2'-^{2}H] of Uridine-5'-monophosphate

For the synthesis of [5-^{3}H; 2'S-2'-^{2}H] UMP, [2-^{2}H] ribose-5-phosphate was used instead of glucose. The 2X reaction buffer was

composed of: 100 mM triethanolamine, pH 7.8, 4 mM [2-^{2}H] ribose-5-phosphate, 10 mM $MgCl_2$, 2 mM ATP, 10 mM NH_4OAc, 2 mM cold orotic acid, 20 mM phosphoenolpyruvate, and 20 mM $Mg(OAc)_2$. [5-^{3}H] orotic acid (13.5 Ci/mmol), 180 μCi, was concentrated to dryness in a 10 mL pear shaped flask. One and a half milliliters of 2X reaction buffer plus 1.3 mL of water was added to the concentrated radiolabeled orotic acid. The following enzymes were then added to the reaction mixture: 12 units pyruvate kinase, 6 units myokinase, 0.6 units PRPP synthase, 15 units inorganic pyrophosphatase, 12 units orotidine-5'-phosphate pyrophosphorylase and 12 units orotidine-5'-phosphate decarboxylase from yeast. The reaction was incubated for 12 hours at 37 °C then heat inactivated at 95 °C for 5 minutes. The quenched reaction was centrifuged at 12,000 rpm and the pellet was discarded. To assure that UMP had been made, an aliquot was analyzed by MonoQ HPLC (see experimental section titled "Analytical HPLC Method for Monitoring the Synthesis of dUTPs"). The supernatant was used in the synthesis of [5-^{3}H; 2'S-2'-^{2}H] UTP.

Attempted Synthesis of [5-^{3}H; 2'S-2'-^{2}H] Uridine-5'-triphosphate and 2'-deoxyuridine-5'-triphosphate

The attempted synthesis of these materials utilized the same methods used for the synthesis of [5-^{3}H] uridine-5'-triphosphate and [5-^{3}H] 2'-deoxyuridine-5'-triphosphate. Proton NMR demonstrated that a multiplet was present at δ 6.3 ppm and not a doublet as would be expected if complete deuteration had occurred at the 2' position of ribose (see figure 2-6).

Synthesis of [2-^{2}H] Ribose-5-phosphate

Two different methods for the synthesis of[2-^{2}H] ribose-5-phosphate were tried. The first involved converting ribose-5-phosphate to[2-^{2}H] ribose-5-phosphate by treatment with phosphoriboisomerase in D_2O (Rising, 1994). Ten milligrams of ribose-5-phosphate was concentrated to dryness three times from D_2O. Deuterium oxide and ~230 units phosphoriboisomerase were added. The final composition of the reaction mixture was 20 mM ribose-5-phosphate, pH 7.0. The mixture was incubated at room temperature for three hours then heat inactivated at 105 °C for 5 minutes (Rising, 1994; Feather, 1969). Finally, the reaction was exchanged into H_2O. The proton NMR spectrum showed that H1 was a singlet at δ 5.2 ppm.

The second method involved converting [2-^{2}H] ribose to [2-^{2}H] ribose-5-phosphate by treatment with ribokinase. The final composition of the reaction mixture (2 mL) was 10 mM Tris-HCl, pH 7.8, 1 mM ribose, 1 mM ATP, and 10 mM phosphoenolpyruvate. Eight units pyruvate kinase and 4.6 units ribokinase (s.a. = 9.12 μmole/min/mg) were added and the reaction was incubated for 1 hour at 37 °C. The proton NMR spectrum showed that H1 was a singlet at δ 5.2 ppm.

A final and unsuccessful attempt to synthesize [5-^{3}H; 2'S-2'-^{2}H] dUTP included the synthesis of[2-^{2}H] ribose-5-phosphate in the reaction mixture for UMP synthesis. The 2X buffer contained 4 mM [2-^{2}H] ribose instead of 4 mM [2-^{2}H] ribose-5-phosphate. Ribokinase, 1.5 units, was added to the reaction mixture along with the other enzymes. The proton NMR spectrum for the resulting

dUTP showed a multiplet for H1 at δ 6.3 ppm and the H2 signal did not integrate to one proton.

Analytical HPLC Method for Monitoring the Synthesis of dUTPs

A 5 μL aliquot was removed from the reaction mixture and placed directly into an LSC vial containing 2 mL HPLC buffer (250 mM NH_4HCO_3, pH 8.65/15% MeOH). Twelve milliliters of LSC fluid was added to the tube and the tube was counted by liquid scintillation counting. Another 5 μL aliquot was removed from the reaction mixture and applied to a Mono Q HR 10/10 anion exchange column (flow rate = 2 mL/min). The column was equilibrated with 125 mM NH_4HCO_3, pH 8.65/15% MeOH. After application of the 5 μL aliquot, a 55 minute linear gradient was run from 125 mM NH_4HCO_3 pH 8.65/15% MeOH to 310 mM NH_4HCO_3 pH 8.65/15% MeOH (absorbance at 260 nm was monitored) (see figure 2-4). Co-injection of standards for UMP, UTP, and dUTP confirmed the identities of the synthesized materials.

Preparative HPLC Method for Purification of dUTPs

The 2'-deoxyuridine-5'-triphosphates were purified by HPLC on a Mono Q HR 10/10 anion exchange column (flow rate = 2 mL/min). The column was equilibrated with 25 mM NH_4HCO_3, pH 8.65/15% MeOH. After applying the crude reaction mixture to the column the material was eluted with 25 mM NH_4HCO_3, pH 8.65/15% MeOH for 25 minutes. Then the gradient was changed from 25 mM to 125 mM NH_4HCO_3, pH 8.65/15% MeOH over 5 minutes. Next, the gradient was changed from 125 mM to 310 mM NH_4HCO_3, pH

8.65/15% MeOH over 80 minutes. The absorbance at 260 nm was monitored. The dUTP peak was collected from 98-108 minutes and was detected by UV/VIS at 260 nm. The material was subsequently desalted with Amberlite IR120-H^+ cation exchange resin using the same procedure employed for pdUp.

Synthesis of pd(UCC)

A hairpin loop (19 bp) comprising of 18 deoxynucleotides and one ribonucleotide on the 3' end (5'-GGA AGA TCC GAA AGG ATC U-3') was used as a template for the synthesis of d(UCC). The 750 μL reaction mixture contained 19 μM hairpin loop template, 50 mM Tris-HCl, pH 7.2, 10 mM $MgCl_2$, 5 mM DTT, 20 μg/ml BSA, 0.1 mM dCTP, 0.1 mM dUTP, and approximately 2400 units Klenow fragment. It was incubated at 20 °C for 14 hours then heat inactivated at 70 °C for 10 minutes. The cleavage between the 3' ribonucleotide and the d(UCC) was achieved by addition of NaOH to the quenched reaction mixture to a final concentration of 0.3 M. The reaction was incubated for 2 hours at 55 °C. The HPLC conditions for visualizing the d(UCC) product were as follows: the reaction was applied to MonoQ HPLC column equilibrated with 0.1 M NaCl/50 mM NaOH, 2 mL/min. The column was washed with this buffer for 15 minutes at which time a linear gradient from 0.1 M NaCl/50 mM NaOH to 0.65 M NaCl/50 mM NaOH was started which ran for 40 minutes. The wavelength for detection was 260 nm. The d(UCC) eluted at 16.6 minutes as detected by UV/VIS.

The next step was to 5'-phosphorylate the d(UCC). Since an authentic sample of d(UTT) was readily available in the lab but an

authentic sample of d(UCC) was not, the d(UTT) was 5'-phosphorylated instead. The success of this reaction suggests that 5'-phosphorylation of d(UCC) by the same method should yield pd(UCC). The reaction mixture consisted of 2.5 μM d(UTT), 70 mM Tris-HCl, pH 7.6, 10 mM $MgCl_2$, 5 mM DTT, 1 mM ATP, and 40 units of T4 polynucleotide kinase. It was incubated at 37 °C for 1 hour and 35 minutes at which time 0.5 M EDTA was added to a final concentration of 25 mM in order to quench the reaction. The reaction was analyzed by C18 HPLC. The flow rate was 1 mL/min and a 40 minute gradient from 1.2% CH_3CN/100 mM NH_4HCO_3 to 10.4 % CH_3CN/100 mM NH_4HCO_3 was run. The absorbance at 260 nm was monitored.

Purification of Ribonucleotide Triphosphate Reductase (RTPR)

Lactobacillus leichmannii ribonucleotide triphosphate reductase was purified from *E. coli* pSquire/HB101 (provided by Dr. Joanne Stubbe) as previously described (Booker, 1993). Dialysis of the RTPR enzyme against deuterated buffer yielded RTPR that was used for the synthesis of [5-^{3}H; 2'R-2'-^{2}H] dUTP from [5-^{3}H] UTP.

Purification of Klenow Fragment

E. coli Klenow fragment (D355A, E357A) was purified from *E. coli* CJ375 (provided by Dr. Catherine Joyce) as previously described (Joyce, 1995).

Preparation of *E. coli* Ribokinase Expression Construct

The gene for *E. coli* ribokinase (EC 2.7.1.15) (Burland, 1993) was amplified from *E. coli* genomic DNA by PCR using the following 5' and 3' primers: (5'-CAT CCC GCA TAT GCA AAA CGC AGG C-3') and (5'-CGA ATT CTT ACC TCT GCC TGT CTA AAA ATG-3'). The 5' primer contained a restriction site for *Nde* I, and the 3' primer contained a restriction site for *EcoR* I to be utilized for cloning directly into the pET22b expression vector. PCR utilized the following scheme: 55°, 1 min; 72°, 1 min; 94°, 1 min (30 cycles). The PCR product (947 bp) was purified on a 1.6% agarose gel, then digested sequentially with *Nde* I and *EcoR* I. The UDG insert was ligated into pET22b which had previously been double digested with *Nde* I and *EcoR* I, and dephosphorylated with shrimp alkaline phosphatase. The resulting pET22b/ribokinase construct was labeled p10EH42.3. Restriction mapping with *Pvu* II and with *EcoR* I/*Nde* I demonstrated that an insert of the correct size had been ligated into pET22b.

Overexpression and Purification of *E. coli* Ribokinase

A 500 mL culture of BL21(DE3) *E. coli* transformed with p10EH43.2 was grown at 37 °C in LB/ampicillin to an OD_{600} of 1.4, induced with 1 mM IPTG, then grown for an additional 4 hours at 30 °C before the cells were harvested. The enzyme was purified with slight modifications of previously reported work (Sigrell, 1997; Parkin, 1984; Anderson,1969). The harvested cells were resuspended in 20 ml of ribokinase resuspension buffer (10 mM Tris-HCl, pH 7.8, 3 μM PMSF, 10 mM EDTA) and lysed using a French

pressure cell (2 runs) and Carver hydraulic press. The lysed cells were centrifuged at 17,000 rpm at 4 °C for 20 minutes and the resulting pellet was discarded. An equal volume of 2% streptomycin sulfate dissolved in ribokinase resuspension buffer was added to the supernatant and the mixture was stirred for 20 minutes at 4 °C. The mixture was centrifuged at 7,000 rpm at 4 °C for 20 minutes and the resulting pellet was discarded. Ammonium sulfate (5.98 g) was added to the supernatant to 30% saturation. The mixture was centrifuged at 4 °C at 7,000 rpm for 20 minutes and the resulting pellet was discarded. Ammonium sulfate (9.23 g) was added to the supernatant to 70% saturation. The mixture was centrifuged at 4 °C at 7,000 rpm for 20 minutes and the supernatant was discarded. The protein rich ammonium sulfate pellet was resuspended in 4 mL ribokinase purification buffer (25 mM Tris-HCl, pH 8, 1 mM EDTA, 1 mM DTT, 3 μM PMSF) and dialyzed for 18 hours against 2 changes of ribokinase purification buffer. The dialyzate was applied to a column (1.5 x 22 cm) of DEAE Sephadex equilibrated with ribokinase purification buffer. The column was washed with one column volume of ribokinase purification buffer. A linear salt gradient of 0 - 0.3 M KCl in the same buffer (150 ml each) was applied. The ribokinase eluted toward the end of the gradient and one column volume of 0.3 M KCl in ribokinase purification buffer was applied to the column to elute the remaining ribokinase activity. The ribokinase activity was measured using a previously reported assay (Parkin, 1984). The fractions containing ribokinase activity were pooled and concentrated using an Amicon filtration apparatus. The specific

activity of the enzyme was 9.1 μmole/min/mg and the total yield was 570 units.

CHAPTER 3
KINETIC STUDIES WITH URACIL DNA GLYCOSYLASE

Introduction

The study of UDG began in 1974 when Thomas Lindahl isolated a partially purified solution of the enzyme from *E. coli*. Over the years many studies of UDG have been performed. Much of the current knowledge about the enzyme is based on X-ray crystallography data. Since X-ray crystallography reports on only a moment in time during the reaction (in the case of UDG, all of the crystal structures are enzyme-product complexes) it is important to combine this information with other studies such as kinetics (presented in this chapter) and kinetic isotope effects (KIEs) (presented in chapter 4).

The kinetic studies performed in this project required large amounts of enzyme. Consequently, an overexpression system was developed which afforded large quantities of wild type UDG. The overexpression construct that produced wild type UDG was also modified in order to obtain histidine-tagged wild type UDG and a C200S mutant UDG. This C200S mutant was used to determine the role of the highly conserved, lone cysteine residue in *E. coli* UDG.

The proposed Michael addition mechanism for UDG was also tested through the use of the C200S mutant. Other groups have tried to determine what purpose cysteine 200 serves; however, its

role remained elusive. A study involving photochemical cross-linking of *E. coli* UDG to oligonucleotide dT_{20} revealed that cysteine 200 is located in a DNA-binding region of the enzyme (Bennet, 1994), suggesting that the residue could be involved in catalysis. Assuming that cysteine 200 is in (or near) the active site, the question becomes, is *E. coli* UDG cysteine 200 a catalytic residue?

Studies were conducted to determine if the cysteine at position 200 was involved in catalysis, however, the results were inconclusive. One group measured the enzyme activity in the presence of sulfhydryl blocking agents. *E. coli* UDG has only one cysteine residue, therefore if activity were decreased or eliminated in the presence of these agents one could argue that cysteine 200 is a catalytic residue or near the active site. The enzyme was not inhibited by N-ethylmaleimide or iodoacetate (hydrophilic reagents), indicating that cysteine 200 is not a catalytic residue. However, p-mercuribenzoate (a hydrophobic reagent) caused a 70% inhibition of enzyme activity (Lindahl, 1977), indicating that cysteine 200 *is* important for catalysis. The author rationalized these confusing results by hypothesizing that cysteine 200 is located in a hydrophobic region of the enzyme making it accessible to organomercurials, but inaccessible to hydrophilic reagents. In addition to being ambiguous, these results do not demonstrate that cysteine 200 was modified, and therefore, drawing conclusions about a possible catalytic function for cysteine 200 from this study is difficult.

The Michael addition hypothesis for the mechanism of UDG (Prior, 1984; Prior, 1984) can be tested by studying the kinetic behavior of the C200S UDG mutant. In this hypothetical mechanism, a nucleophilic residue in the enzyme attacks C-6 of the uracil ring (see figure 1-10). The lone cysteine residue in *E. coli* UDG is a good candidate for serving as this nucleophilic residue. Support for the Michael addition hypothesis comes from the kinetic competence of 6-hydroxy-5,6-dihydrouridine (Prior, 1984) and an inverse secondary α kinetic isotope effect for the hydrolysis reaction of [6-^{3}H] uridine (Prior, 1984) (see chapter 4 for background on kinetic isotope effects). Additional support comes from observation of nucleophilic attack at the 6-position of pyrimidine heterocycles in other enzymatic reactions of pyrimidine nucleosides and nucleotides (Pogolotti, 1979; Starzyk, 1982) (see Chapter 1 for more details).

In addition to kinetic studies of C200S UDG, the kinetic behavior for the reaction of wild type UDG with pdUp (See figure 3-1) was also studied. The purpose of this work was to determine if oligonucleotide binding is an absolute requirement for catalysis by UDG, and to perhaps identify a "slow" substrate for kinetic isotope effect analysis. Substrate specificity studies of *E. coli* UDG are in accord with the importance of backbone phosphate/active site interactions (Varshney, 1991). In a study of single stranded oligonucleotide substrates it was reported that the minimum substrate requirement is pd(UT)p, though kinetic parameters were not described for this substrate. Addition of a 3'-T to pd(UTT)

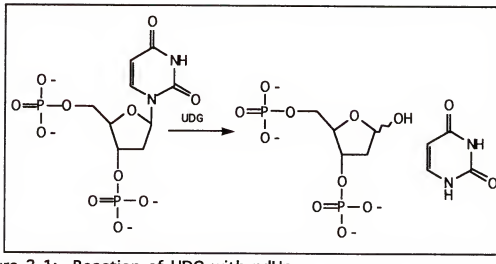

Figure 3-1: Reaction of UDG with pdUp.

yields pd(UTTT) which afforded a 10-fold decrease in K_m. The k_{cat} increased by a factor of 6 relative to pd(UTTT) when the U was moved internal to form pd(TUTT), and k_{cat} increased by another factor of 14 for the substrate pd(T_5UT_5). A picture of UDG catalysis thus emerges which suggests that oligonucleotide substrates or larger are required for cleavage of the glycosidic bond. The kinetic analysis of the hydrolysis of pdUp by UDG presented in this chapter tests to see if binding of an oligonucleotide substrate is truly required for UDG catalysis.

Results

Overexpression and Purification of UDGs

UDG was cloned from *E. coli* genomic DNA by Ben Horenstein (1993, Horenstein, unpublished work) using PCR and primers designed from the reported sequence (Varshney, 1988). Overexpression of *E. coli* UDG was efficiently achieved from the pET22b expression vector, which uses the T7 RNA polymerase

promoter. A typical purification of wild type UDG afforded approximately 30 - 37 mg of purified enzyme from a 500 mL culture. Purification of C200S and His-tagged UDG yielded 29 mg and 33 mg, respectively, from a 500 mL culture. The His-tagged material was engineered to enable elimination of background WT UDG from mutants. Preliminary studies indicated that the enzyme could be further purified on a nickel column.

Table 3-1: Purification Table for a Typical UDG Purification.

	Volume	Protein	Specific Activity	Total Activity
Fraction	*mL*	*mg*	*units/mg*	*units*
I. Crude Extract	50	425	9.5	4040
II. $(NH_4)_2SO_4$	13	211	11	2400
III. Sephadex G-75	11	99	19	1900
IV. Hydroxyapatite	10	37	43	1600

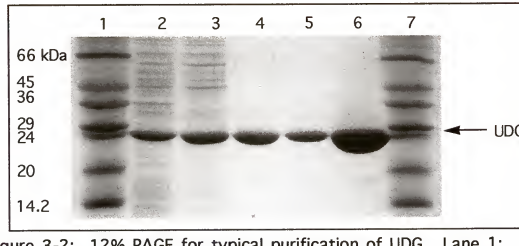

Figure 3-2: 12% PAGE for typical purification of UDG. Lane 1: SDS-7 molecular weight markers, Lane 2: fraction I, Lane 3: fraction II, Lane 4: fraction III, Lane 5: fraction IV (5 μg), Lane 6: fraction IV (50 μg), Lane 7: SDS-7 molecular weight markers.

protein purification was based on Lindahl's method (Lindahl, 1977) with the exception that a final chromatographic step on DNA agarose was not required. Fraction IV was found to be homogeneous by SDS-PAGE (see figure 3-2), and the purified enzyme had a specific activity of 43 μmol/min/mg, in good agreement with the reported value of 38 μmol/min/mg (Lindahl, 1977). No phosphatase activity was detected in the purified UDG. N-terminal sequencing of the purified UDG provided a sequence of ANELTW in agreement with previous reports that UDG has the N-terminal Met residue cleaved in the mature protein (Varshney, 1988). In addition, mass spectrometry (see table 3-2) revealed that the molecular weights of all three UDGs are correct within experimental error.

Table 3-2: MALDI-MS H^+ Data for UDG Enzymes.

	Mass Spec (KDa)	Theoretical (KDa)
WT	25.613	25.546
C200S	25.566	25.661
His-tagged	26.500	26.467

Kinetic Studies for UDG vs. HCAII-U

The kinetic data for WT, C200S, and His-tagged UDG were fit to Lineweaver-Burke plots (see figure 3-3) and to the Michaelis-Menten equation shown in equation 3-1. The calculated values for K_m, V_{max}, and k_{cat} are shown in table 3-3.

$$V_0 = V_{max} \times [S]/(K_m + [S]) \qquad \text{eq. 3-1}$$

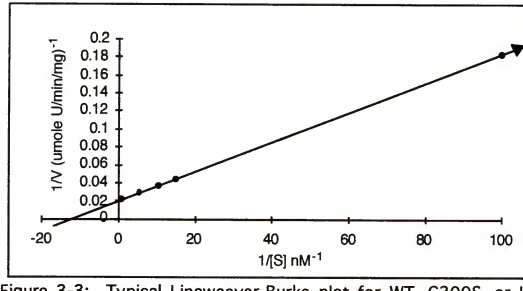

Figure 3-3: Typical Lineweaver-Burke plot for WT, C200S, or His-tagged UDG vs. HCAII-U.

Table 3-3. Kinetic parameters for WT, C200S, and His-tagged UDG.

	K_m *10-5 (μM)	V_{max} (μmole/min/mg)	k_{cat} (sec^{-1})
WT	8.4 ± 1.6	59 ±14	25 ± 6
C200S	10 ± 1.5	43 ± 11	17 ±3
His-tagged	5.6 *	39 *	16 *

* Only one experiment performed for this reaction.

The K_m, V_{max}, and k_{cat} values measured for the wild type and mutant enzymes were determined to be very similar. In order to test for the possibility of a salt effect, the kinetic reactions were repeated in the presence of 0.06 M NaCl. The modest NaCl concentration severely inhibited binding of UDG to the substrate and as a result, only an accurate measure for k_{cat}/K_m was obtained. This value was similar for both the WT and C200S UDGs (see table 3-4).

Table 3-4. Kinetic Parameters for WT and C200S UDG in the Presence and Absence of 0.06M NaCl.

	WT k_{cat}/K_m ($M^{-1}s^{-1}$)	C200S k_{cat}/K_m ($M^{-1}s^{-1}$)
no NaCl	29	17
0.06 M NaCl	1.1	1.4

Kinetic Studies of UDG Catalyzed Hydrolysis of pdUp

The HPLC chromatogram for the reaction of UDG with pdUp is shown in figure 3-4. Uracil eluted at 3.5 minutes and pdUp eluted at 12.5 minutes. The amount of uracil produced (in μmoles) was determined by the expression in equation 1, where A_u represents the area under the uracil peak (normalized for the change in extinction coefficient that arises on glycosidic bond cleavage) (Dawson, 1987), A_{pdUp} represents the integrated area under the unreacted pdUp peak, and V is the aliquot volume and $[pdUp]_0$ represents the initial concentration of pdUp in the reaction mixture. Initial velocity data were fit to equation 3-2 with MacCurveFit (Kevin Raner Software) to obtain kinetic constants.

amount of uracil produced = $(A_u/(A_u + A_{pdUp}))*V*[pdUp]_0$ eq. 3-2

$v = V_{max}*[pdUp]/(K_m + [pdUp])$ eq. 3-3

The results of steady state kinetic studies of pdUp are presented in Figure 3-5. Saturation kinetics were observed for UDG vs. pdUp. The respective apparent values for K_m, V_{max}, and k_{cat}, were 200 ± 17 μM, (1.1 ± 0.4) x 10^{-3} μmole/min/mg, and 0.027 min^{-1}. Hydrolysis of pdUp by UDG could be completely inhibited in the presence of added DNA.

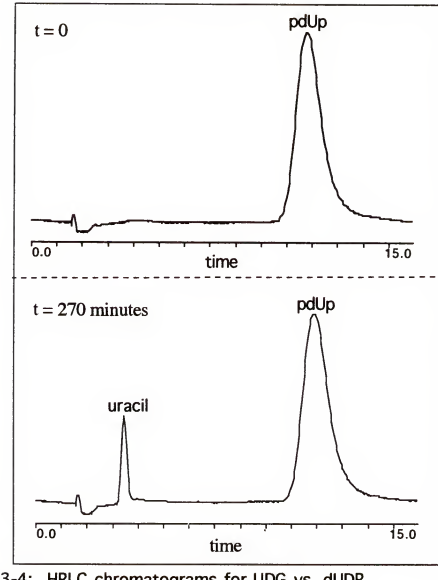

Figure 3-4: HPLC chromatograms for UDG vs. dUDP

Discussion

Overexpression and Purification of UDGs

We suspected that the detection limit for a slow reaction might be an issue, and so we sought a system which would afford sufficient enzyme to observe slow turnover rates. Based on comparison of initial specific activity from crude cell lysate, the T7 promoter expression system used here affords a 2700-fold

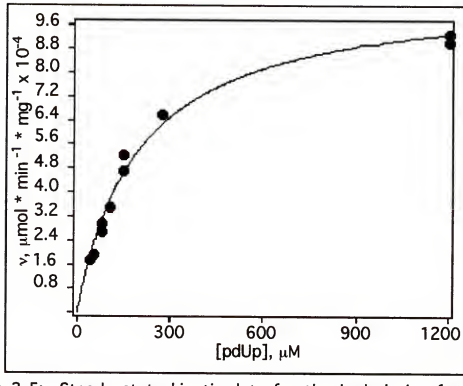

Figure 3-5: Steady state kinetic data for the hydrolysis of pdUp by UDG.

overexpression of UDG relative to WT *E. coli* and is about 6-fold more efficient than expression driven by the λP_L promoter (Lindahl, 1977; Duncan, 1984) The expression system employed in this work appears to be a useful one for kinetic studies and other applications that require large quantities of UDG.

The C200S mutant demonstrated that cysteine 200 is not an essential residue for catalysis by UDG. In addition, His-tagged mutants can be synthesized by following the outlined procedure contained in this chapter. Since the overexpression host is *E.coli*, background wild type UDG might interfere with correct measurement of mutant behavior. Therefore, the His-tagged system might prove to be a very useful tool to help eliminate the wild type UDG.

Kinetic Studies for the Reaction of UDG with HCAII-U

Site directed mutagenesis studies have been conducted for human UDG to determine residues that are important for catalysis (Mol, 1995; Slupphaug, 1996). The theory behind the experiment is if a residue is mutated and the rate of uracil hydrolysis for the resultant mutant enzyme is significantly decreased, then that residue may be important for catalysis. The site directed mutagenesis studies indicated that the following residues in human UDG are critical for UDG activity (the corresponding *E. coli* residues are in parentheses): asparagine 204 (123), glutamine 144 (63), aspartate 145 (64), and histidine 268 (187). This same type of analysis was applied to the work presented in this chapter.

The kinetic constants for WT and C200S UDG are nearly identical. These results suggest that cysteine 200 is not a critical residue for UDG catalysis. Further evidence that C200 is not involved in catalysis comes from crystallographic data of UDG (Mol, 1995; Xiao, 1999; Savva, 1995; Parikh, 1998; Putnam, 1999; Slupphaug) which unfortunately was released after this project was well underway. In an overlay model of the sequence of *E. coli* UDG with the crystal structure for Herpes UDG, Herpes cysteine 222 and *E. coli* cysteine 200 are located ~15 Å away from the active site pocket and are not located near the DNA binding channel. In order for cysteine 200 to directly participate in catalysis, a large conformational change would have to be induced. These results suggest that cysteine 200 does not interact with C6 of uracil in a Michael addition mechanism.

The above results do not completely rule out the hypothesized Michael addition mechanism. It is important to note that since the X-ray crystallography data is derived from an enzyme-product complex, a conformational change is possible. If cysteine 200, however, truly is not involved in catalysis, there are other nucleophilic residues near the active site of the enzyme that could serve as the catalytic nucleophile that attacks C-6 of the uracil ring. Kinetic isotope effect studies presented in chapter 4 for the reaction of UDG with pd(UTT) further address the plausibility of the Michael addition mechanism.

Kinetic Studies for the Hydrolysis of pdUp by UDG

A key question we wished to answer in this study was if oligonucleotide binding was an absolute requirement for catalysis by UDG. As presented in Figure 3-5, pdUp is indeed a substrate for UDG, which shows that binding of an oligonucleotide substrate is not an absolute requirement for catalysis. On the other hand, pdUp is a poor substrate, both in its high K_m and low V_{max}. Compared to the single stranded oligonucleotide pd(T_5UT_5), K_m is increased by a factor of 1.5×10^3, and V_{max} is reduced by a factor of 7×10^2 (Varshney, 1991). The obvious difference between the two substrates is that pdUp lacks flanking 5' and 3' nucleotides, and therefore has two extra charges.

The crystal structures for UDG have established that the active site features a long groove for binding of DNA (Mol, 1995; Xiao, 1999; Savva, 1995; Parikh, 1998; Putnam, 1999). The mononucleotide pdUp lacks the number of possible active site

interactions enjoyed by oligonucleotides. Oligonucleotide binding may be a cooperative process, where initial extended binding interactions facilitate development of the competent Michaelis complex.

Another possibility for the catalytic inefficiency of pdUp is that it presents insufficient contacts with the enzyme for it to be oriented optimally for catalysis. In the "base-flipping" scheme, this would imply that the conformational changes that arise in the dU unit when it is extrahelical may have catalytic consequences. The crystal structure of HhaI cytosine 5-methyltransferase with a bound extrahelical cytidine-containing oligonucleotide provides a basis for this suggestion (Klimassauskas, 1994). The dihedral angle about C4'-O4'-C1'-C2' of the extrahelical cytidylate deoxyribosyl ring is almost planar, at about -11°. If similar distortion occurs in the UDG Michaelis complex, this may productively lead to an oxocarbenium ion-like transition state, in which the deoxyribosyl dihedral would be very close to planarity.

A third reason for possible catalytic inefficiency of pdUp may relate to electrostatics. The terminal 5' and 3' phosphates of pdUp are multiply charged, whereas an internal dU located in an oligonucleotide is flanked by unit-charged phosphate residues. Thus productive binding of pdUp would presumably result in a higher negative charge density in the active site than would occur for productive binding of a dU internally located in an oligonucleotide. Purmal et al. recently found that severe penalties for *E. coli* UDG binding and catalysis are realized when either the 5' or 3' phosphodiester bond to the dU in oligonucleotides is replaced by a

pyrophosphate linkage (Purmal, 1996). Little penalty was observed if the pyrophosphate link was located at nucleotides far from the dU. Monoesters of phosphate and pyrophosphate share a higher charge density than that found for a typical internucleotide phosphodiester link. This leads us to suggest that the poor binding and catalysis of pdUp may be in part due to an electrostatic penalty, in addition to a lack of favorable active-site contacts enjoyed by oligonucleotides and DNA. Analogs of pdUp with altered charge at the 5' and 3' phosphates will be prepared to test this hypothesis.

The observation that pdUp is a UDG substrate presents a number of opportunities to probe the reaction mechanism that are not likely to be available with better substrates. The kinetics for UDG are dominated by physical steps when good substrates are employed. For example, surface plasmon resonance analysis of mutant Herpes simplex I (HSV-1) UDG binding kinetics (Panayotou, 1998) showed that off-rates for uracil containing oligonucleotides(35-mers) were in the range of 0.018 - 0.055 s^{-1}, but k_{cat}'s for substrates of this size are certainly faster. This demonstrates that "good" substrates will have kinetic complexity associated with catalytic turnover. Challenged substrates like pdUp with $k_{cat} = 4.5 \times 10^{-4}$ s^{-1}, and with weak binding, are likely to be suitable for kinetic experiments which seek to probe the chemical steps of the UDG reaction mechanism. Kinetic isotope effect analysis for pdUp is presented in chapter 4.

Conclusions

A C200S mutant was constructed to investigate the role of cysteine 200 in *E. coli* UDG. The kinetic constants measured for the C200S mutant and WT UDG reaction with HCAII-U were very similar. These results, in addition to structural data obtained from x-ray crystal structures, demonstrate that cysteine 200 is not a catalytic nucleophile in the proposed Michael addition mechanism for UDG.

The nucleoside diphosphate, pdUp, was also synthesized and kinetic parameters for its reaction with UDG were determined. These parameters were as follows: $K_m = 200 \pm 17$ μM, $V_{max} = (1.1 \pm 0.4) \times 10^{-3}$ μmole/min/mg, and $k_{cat} = 0.027$ min^{-1}. These results showed that oligonucleotide binding was not an absolute requirement for catalysis by UDG. In addition, these experiments help to identify a "slow" substrate that will be useful for studying kinetic isotope effects.

Experimental

Materials

Buffers, reagents, and enzymes were purchased from Sigma, Fisher Scientific, New England Biolabs, Biorad, Boehringer Mannheim Biochemicals, Promega, and Novagen. Oligodeoxynucleotide primers were purchased from the Interdisciplinary Center for Biotechnology Research (ICBR) core facilities at the University of Florida. DNA was gel purified in conjunction with the DNA Purification Kit by Biorad and the QUIAquick Gel Extraction kit from Quiagen. YM-10 Centripreps

were purchased from Millipore. Liquid scintillation fluid (ScintiSafe 30%) was purchased from Fisher. Plasmid minipreps were performed using the Wizard Mini-preps kit from Promega.

Instrumental

Liquid scintillation counting utilized a Packard 1600 TR instrument which dumped data to a floppy disk for subsequent analysis on a personal computer. An Orion Sure-Flow pH probe was used in conjunction with an Accumet model 15 pH meter for all pH measurements. FAB-MS used nitrobenzyl alcohol as matrix and were obtained at the University of Florida Chemistry Department. MALDI-MS was performed by the Department of Chemistry and the ICBR (Nancy Denslow). N-terminal sequencing was performed by the ICBR (Nancy Denslow). Centrifugation was performed using a Sorvall RC 5B centrifuge or a Sorvall MC 12V centrifuge. Cells were lysed using a French pressure cell with a Carver hydraulic press.

Preparation of the Wild Type *E. coli* UDG expression construct

Dr. Benjamin Horenstein performed the synthesis of this construct. The gene for *E. coli* UDG (ung) (Varshney, 1988) was amplified from *E. coli* genomic DNA by PCR using the following 5' and 3' primers: (5'-CCG AAT TCC ATA TGG CTA ACG AAT TAA CCT-3') and (5'-GCG AAT TCT ATT ACT CAC TCT CTG CCG GTA-3'). The 5' primer contained a restriction site for *Nde* I, and the 3' primer contained a restriction site for *EcoR* I to be utilized for cloning into the pET22b expression vector. PCR utilized 0.5 units Taq

polymerase and the following scheme: 55 °C, 1 min; 72 °C, 1 min; 94 °C, 1 min (30 cycles). The PCR product (710 bp) was purified on an 1% low melt agarose gel, then digested sequentially with *Nde* I and *EcoR* I. The UDG insert was ligated into pET22b which had previously been double digested with N*de* I and *EcoR* I, and dephosphorylated with shrimp alkaline phosphatase. The resulting pET22b/UDG construct, pBH190.25, was sequenced to confirm that the correct in-frame UDG sequence had been obtained.

Preparation of the C200S *E. coli* UDG expression construct

Overlap extension PCR was used to create the C200S mutant (Hornton, 1989). The N-terminal and C-terminal fragments were amplified from pBH190.25 in two separate PCR reactions. For the synthesis of the N-terminal piece the following 5' and 3' primers were used: (5'-CCG AAT TCC ATA TGG CTA ACG AAT TAA CCT-3') and (5'-GGA TTC TTT GGC TCC AAC CAT TTT GTG CTG-3'). The 3' primer contains a site mutation (underlined) for the C200S mutant. For the synthesis of the C-terminal piece the following 5' and 3' primers were used: (5'-CAG CAC AAA ATG GTT GGA GCC AAA GAA TCC-3') and (5'-GCG AAT TCT ATT ACT CAC TCT CTG CCG GTA-3'). The 5' primer contains a site mutation (underlined) for the C200S mutant. PCR utilized 0.5 units Taq polymerase and the following scheme: 55 °C, 1 min; 72 °C, 1 min; 94 °C, 1 min (30 cycles). The PCR products (N-terminal: 623 bp; C-terminal: 115 bp) were purified on a 1.6% agarose gel with a QUIAquick Gel Extraction kit. The gel purified N-terminal and C-terminal pieces were combined with the following 5' and 3' primers: (5'-CCG AAT TCC ATA TGG CTA

ACG AAT TAA CCT-3') and (5'-GCG AAT TCT ATT ACT CAC TCT CTG CCG GTA-3'). PCR utilized the following scheme: 55 °C, 1 min; 72 °C, 1 min; 94 °C, 1 min (30 cycles). The PCR product (711 bp) was purified with a Wizard PCR Preps kit and then ligated into a Novagen pT7 Blue T-vector. The resulting pT7 Blue/UDG construct, pEH199.1, was sequenced to confirm that the correct in-frame C200S sequence had been obtained. The construct, pEH199.1, was digested sequentially with EcoR I and Nde I and the C200S insert (711 bp) was obtained by gel purification. The C200S insert was ligated into pET22b which had previously been double digested with *Nde* I and *EcoR* I, and dephosphorylated with shrimp alkaline phosphatase. The resulting pET22b construct was labeled pEH231.1.

Preparation of the His-tagged *E. coli* UDG expression construct

The following procedure (see figure 3-4) was performed by Dr. Benjamin Horenstein. The construct, pBH190.25, was reengineered to have a His-6 tail. The pBH190.25 construct contained the his-tail, however, there was a stop codon at the end of the UDG gene. The following procedure splices the two making the new C-terminal sequence 5'-GTA TTA CCG GCC GCA-3' (underlined). pBH190.25 was digested with *Cfr* 10I and the desired band was gel purified. The material was treated with Klenow fragment DNA polymerase in a reaction mixture containing dCTP and no other dNTPs. Next, the material was digested with *Nde* I and gel purified. The pET22b expression vector was digested with *Xma*

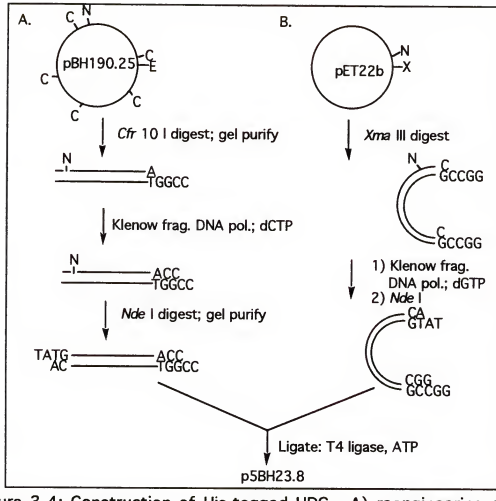

Figure 3-4: Construction of His-tagged UDG. A) reengineering of pBH190.25, B) preparation of pET22b for ligation.

III following treatment with Klenow fragment DNA polymerase in a reaction mixture containing dGTP and no other dNTPs. Next, the vector was treated with *Nde* I. The vector was then ligated with the reengineered pBH190.25 and the resulting construct was labeled p5BH23.8.

Overexpression and purification of UDG

A 500 mL culture of BL21(DE3) *E. coli* transformed with pBH190.25, pEH231.1, or p5BH23.8 was grown at 37 °C in LB/ampicillin to an OD_{600} of 1.6, induced with 1 mM IPTG, then grown for an additional 5 hours at 30 °C before the cells were harvested. The method of Lindahl (Lindahl, 1977) was used for the purification of UDG with the exception that the final DNA-agarose column was not required. The harvested cells were pH 7.4, 1 mM DTT, 1 mM EDTA, 5 % glycerol) and lysed by French press. The lysate was centrifuged at 4 °C for 20 minutes in a GS3 rotor at 7,000 rpm. One volume of 1.6% streptomycin sulfate in UDG purification buffer was added to the supernatant and the mixture stirred at 4 °C for one hour. The mixture was centrifuged at 4 °C for 20 minutes in a GS3 rotor at 7,000 rpm. Ammonium sulfate was added to the supernatant until 45 % saturation was achieved. This mixture was centrifuged at 4 °C for 20 minutes in a GS3 rotor at 7,000 rpm. Ammonium sulfate was added to the supernatant until 65% saturation was achieved. This mixture was centrifuged at 4 °C for 20 minutes in a GS3 rotor at 7,000 rpm. The pellet was resuspended in 3 ml of UDG purification buffer and dialyzed for 14 hours against 1 change of 1 L UDG purification buffer. The dialyzate was applied to a column (45 x 3 cm) of Sephadex G-75 equilibrated with UDG purification buffer. UDG eluted later than most of the protein and fractions containing UDG (analyzed by Bradford assay) were pooled and concentrated to approximately 10 ml in a YM-10 Centriprep. The protein was then dialyzed for 20 hours against 2 changes of 1 L hydroxyapatite

buffer (0.01 M K_2PO_4, pH 7.4, 0.2 M KCl, 1 mM DTT). The dialyzate was applied to a column (23 x 1.5 cm) of hydroxyapatite equilibrated with hydroxyapatite buffer. The fractions containing UDG (analyzed by Bradford Assay) were pooled and concentrated to approximately 10 ml. The protein was dialyzed for 20 hours against 2 changes of UDG storage buffer (0.03 M Tris-HCl, pH 7.4, 1 mM DTT, 0.1 mM EDTA, 5% glycerol). The enzyme was stored at 4 °C.

Enzyme kinetic assay with HCAII-U DNA

Assays (Lindahl, 1977) were conducted in a total volume of 100 μL at 37 °C in 1.5 mL microfuge tubes. Reactions were initiated by addition of 10 μL WT, C200S, or His-tagged UDG (approximately $4\text{-}15 \times 10^{-6}$ μg/μL UDG) to reaction mixtures containing various amounts of HCAII-U (0.1 - 100 nM) (s.a. 480 μCi/μmole uracil) in 25 mM Tris-HCl pH 8 and 0.1 mg/ml BSA. Three time point aliquots were withdrawn, and added to 60 μL ice cold 0.8 N $HClO_4$ followed by addition of 10 μL of 1 mg/mL heat-denatured calf thymus carrier DNA. The mixture was cooled on ice for 10 minutes then centrifuged for 10 minutes at 12,000 rpm. The supernatant (105 μL) was assayed by liquid scintillation counting. Linear initial velocity behavior was observed. The background controls (UDG was replaced with buffer) were treated in an identical fashion. Uracil cleavage was not detected in the background controls.

Salt effect assay with HCAII-U

The enzyme kinetic assay was repeated with 0.06 M NaCl present in the reaction mixture (Lindahl, 1977). Linear initial velocity behavior was observed.

Kinetic Assay for UDG vs. pdUp

Assays (Lindahl, 1977) were conducted in a total volume of 100 μL at 37 °C in 1.5 mL microfuge tubes. The presence of relatively high levels of BSA was required to stabilize the enzyme over the relatively long time course of the kinetic assays. Reactions were initiated by addition of 10 μL of UDG (37 μg) to reaction mixtures (90 μL) containing 0.04 - 1.2 mM pdUp in 25 mM Tris-HCl pH 8.0 and 1.0 mg/ml BSA. Time point aliquots at time 90, 180, and 270 minutes were removed and analyzed by anion exchange HPLC (BioRad Q5; 50 mM Tris HCl, 60 mM NaCl, pH 8.5; 2 mL/min; A_{260}).

Inhibition of UDG activity with DNA

Two reaction tubes (A and B) containing 26 μg of UDG and 1 mM [2-^{14}C]-pdUp (s.a. 50 μCi/μmole) in 25 mM Tris-HCl pH 8.0, 0.5 mg/ml BSA (60 μL final volume) were used in this experiment. Tube A contained 39 μg of heat-denatured calf thymus DNA, while no DNA was present in tube B. The reactions were incubated at 37 °C. At time intervals of 100, 180, and 260 minutes aliquots were removed and applied to a 2.5 cm Dowex 1x8-200 phosphate-form mini-column in a disposable Pasteur pipet (Duncan, 1984). DNA and pdUp were retained on the column but uracil was not. The uracil was

eluted with 4 ml de-ionized water into liquid scintillation vials to which 18 ml liquid scintillation fluid were added. The tubes were counted by liquid scintillation counting and the amount of uracil produced at each time point was determined.

Phosphatase Assay with p-nitrophenylphosphate

The assay was conducted in a total volume of 1 mL in a 1 mL quartz cuvette with a 1 cm pathlength. The reaction mixture contained 50 mM Tris-HCl pH 8.6, 1 mM $MgCl_2$, 1 mM p-nitrophenylphosphate, and 37 μg UDG. The mixture was incubated at room temperature for 3 hours over which time the optical absorption at 410 nm was monitored.

CHAPTER 4
KINETIC ISOTOPE EFFECTS ON URACIL DNA GLYCOSYLASE

Introduction

Kinetic isotope effects were used to probe the mechanism of uracil DNA glycosylase (UDG). Much of the current knowledge concerning the mechanism of UDG is based on X-ray crystallographic studies. A limitation to X-ray crystallography is that it only reports on stable species (i.e. ground states) or very long-lived intermediates. Kinetic isotope effect (KIE) studies, on the other hand, report on a reaction in progress. They allow transition state information about the reaction mechanism to be learned and are the only direct experimental method currently available for determination of enzyme transition state structure (Schramm, 1994). By studying a family of isotope effects around the reaction center, information about the catalytic mechanism of an enzyme can deduced.

In this chapter KIEs are discussed for the reaction of UDG with pdUp (see figure 3-1) and with pd(UTT) (see figure 4-1). In a 1979 dissertation by Charles Garrett, a unity secondary α KIE was measured for the reaction of UDG with uracil-containing DNA in which position 6 of the uracil base was labeled with tritium. It is possible that this value does not represent the intrinsic KIE because of a commitment to catalysis. Since uracil-containing

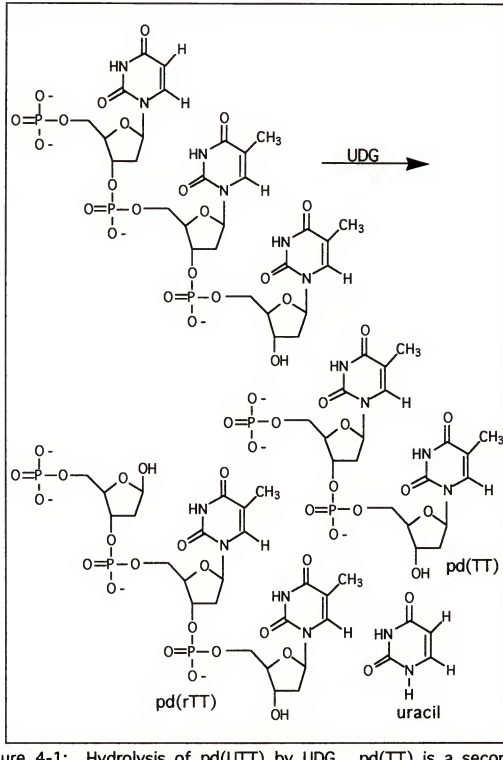

Figure 4-1: Hydrolysis of pd(UTT) by UDG. pd(TT) is a secondary product formed by spontaneous β-elimination of pd(rTT).

DNA is UDG's natural substrate, it is likely to be a "sticky" substrate (see proceeding "Commitment to Catalysis" section below). A reduction in substrate length yields slower substrates that are also bound less tightly (Varshney, 1991) and the commitment to catalysis for these molecules is likely to be reduced. Accordingly, the substrates pd(UTT) and pdUp were synthesized and studied by kinetic isotope effect analysis.

Kinetic Isotope Effect Background

One of the earliest reports in the field of isotope effects dates back to a 1947 paper by Bigeleisen and Mayer (Bigeleisen, 1947). This work provided a theoretical framework to interpret isotope effects on a structural basis based on statistical thermodynamics. The Bigeleisen equation for equilibrium isotope effects can be represented in two ways as shown in equations 4-1 and 4-2. The terms K_L and K_H refer to the equilibrium

$$K_L/K_H = MMI \times EXC \times ZPE \qquad \text{eq. 4-1}$$

$$K_L/K_H = VP \times EXC \times ZPE \qquad \text{eq. 4-2}$$

constants for the two isotopically labeled molecules (L = light and H = heavy) while ZPE is the difference in zero-point energy for the initial and final state between the two isotopic species. The term EXC accounts for the effect if the energy levels above the zero point level are populated and MMI represents a combination of the molecular-mass and moments of inertia of the two isotopic molecules (Buddenbaum, 1977). The MMI term can also be

represented as VP and is the ratio of the ratios of all vibrational frequencies separating the two isotopic species in the initial state and the final state.

A slight modification of the Bigeleisen equation renders it applicable to rate effects. A transition state theory requirement is that one normal mode have a zero or imaginary frequency, ν_L (see equation 4-3). Motion along this coordinate is the geometric change in going forward from transition state to products, or

$$k_L/k_H = \nu_{LL}/\nu_{HL} \times VP/VP^{\ddagger} \times EXC/EXC^{\ddagger} \times ZPE/ZPE^{\ddagger} \qquad \text{eq. 4-3}$$

backward from the transition state to reactants. Consequently, transition states possess 3N-7 frequencies plus one imaginary frequency while ground states contain 3N-6 frequencies (Bigeleisen, 1947; Buddenbaum, 1977).

The value of an isotope effect is generally dominated by the ZPE term. This is because contributions from mass, moment of inertia, and higher vibrational excited states tend to be small relative to the zero-point energy factor and often tend to cancel. For an isotope effect on rate, the size of the ZPE term depends on the change in force constants for the bonds to the isotopically labeled atom during the progression from the ground state to the transition state. If no change in bonding occurs at the point of isotopic substitution, the zero-point energy factor is unity producing an isotope effect whose value is very close to one. If, however, the isotopic atom is more strongly bonded at the transition state as compared to the ground state, the zero-point

energy term will be smaller than unity resulting in an inverse (<1) isotope effect. In this case the heavy isotope reacts faster than the light isotope. Conversely, if bonding to the isotopic atom decreases, the zero-point energy term will be greater than unity causing a normal (>1) isotope effect. In this case, the light isotope reacts faster than the heavy (O'Leary, 1976).

Isotope effects can be divided into two separate categories: primary isotope effects and secondary isotope effects. An isotope effect involving isotopic substitution at an atom where the bond is broken or formed during the reaction is a primary isotope effect. A secondary isotope effect, on the other hand, occurs when the isotopic label is located at a position where bond breakage or formation does not occur. However, the atom does experiences a change in bonding environment during the reaction. Secondary isotope effects are further categorized into alpha and beta effects. When the isotopically substituted atom is bonded to the atom where bond breakage or formation is occurring a secondary alpha isotope effect is produced. If the isotopic label is on an atom that is one atom away from where bond cleavage or formation is occurring, a secondary beta isotope effect is produced (Lowry, 1987). In enzyme catalyzed reactions, isotope effects can also arise from binding interactions (Rakowski, 1996).

Primary Carbon Isotope Effects

Primary carbon isotope effects are measured in systems where bond breakage occurs at the isotopically substituted carbon atom. The carbon can be labeled with either ^{14}C or ^{13}C. For an

S_N1 reaction, the primary ^{14}C kinetic isotope effect values range from 1.02-1.05, while for an S_N2 reaction, the primary ^{14}C kinetic isotope effect values range from 1.08-1.15 (Melander, 1980). The work presented in this dissertation involves measurement of a primary ^{13}C kinetic isotope effect. Equation 4-1 can be used to convert ^{14}C isotope effects to ^{13}C isotope effects (Melander, 1980-p.52). By using equation 4-4, it can be determined that ^{13}C

$$k_{12}/k_{14} = (k_{12}/k_{13})^{1.9} \qquad \text{eq. 4-4}$$

kinetic isotope values for an S_N1 range from 1.01-1.03, while values for an S_N2 reaction the primary ^{13}C kinetic isotope effect range from 1.04-1.08.

Isotope effects occur when there is a change in force constants in going from the ground state to the transition state. In the case of primary kinetic isotope effects, transition state symmetry dictates the magnitude of the effect. Consider the simple proton transfer reaction shown in figure 4-2a. For the 3 center symmetric transition state shown in figure 4-2b, the A----H(D) and H(D)----B force constants are equal and there is no motion of H(D) with respect to A and B. As a result, a maximum loss of a vibrational mode occurs leading to relatively large isotope effects. These effects are characteristic of S_N2 reactions.

For an unsymmetric transition state, the H(D) is positioned closer to either A or B (see figure 4-2c). In this case, the mass of the isotopically substituted atoms does contribute to the

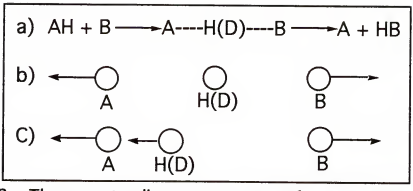

Figure 4-2: Three center linear proton transfer reaction where: a) simple proton transfer reaction, b) symmetric transition state, c) unsymmetric transition state (from Lowry, 1987).

transition state vibrational frequency. A portion of the zero-point energy ground state vibrational frequency contributed by the reactant will be canceled out and the isotope effect will be reduced (Lowry, 1987). In dissociative reactions of glycosides,

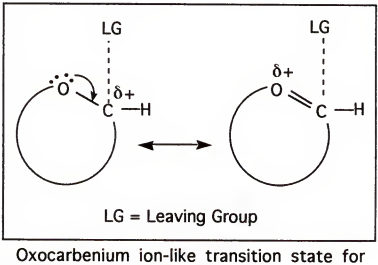

Figure 4-3: Oxocarbenium ion-like transition state for dissociative reactions of glycosides.

primary carbon isotope effects are often reduced by additional bonding in oxocarbenium ion-like transition states as in figure 4-3.

Secondary Kinetic Isotope Effects

Secondary isotope effects are measured by isotopic substitution at a bond that is not broken during the reaction. They arise due to changes in zero-point energy in going from the ground state to the transition state. The vibrational energy levels in a "looser" well are closer together than those in a "tighter" well, and

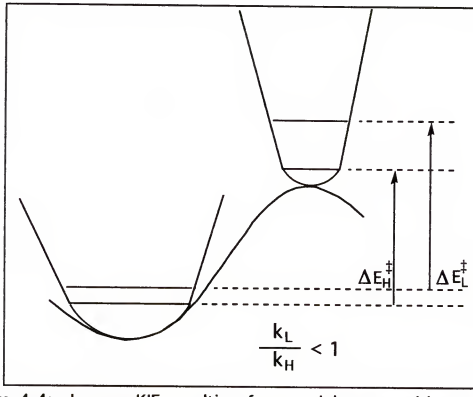

Figure 4-4: Inverse KIE resulting from a tighter transition state. (from Melander, 1980).

the isotope effect is the ratio of k_L/k_H (L = light, H = heavy). If the isotopically labeled atom goes from a looser bonding environment in the ground state to a tighter one in the transition state, an inverse isotope effect will occur (see figure 4-4). The energy of activation for the heavy atom is larger than that of the light

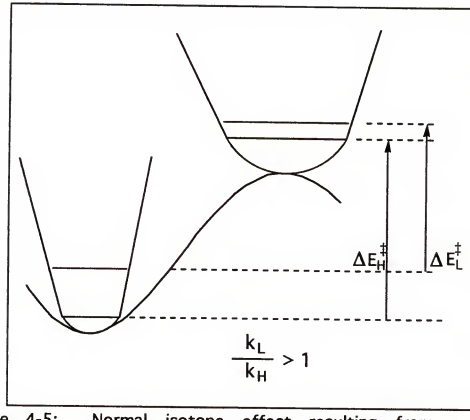

Figure 4-5: Normal isotope effect resulting from a looser transition state (from Melander, 1980).

atom and therefore $K_L/K_H < 1$. If, on the other hand, the isotopically labeled atom is in a looser bonding environment in the transition state as compared to the ground state, a normal isotope effect will occur (see figure 4-5). In this case, the energy of activation for the heavy atom is smaller than that of the light atom and therefore $K_L/K_H > 1$ (Melander, 1980; Lowry, 1987). To convert values of secondary ^3H isotope effects to secondary ^2H isotope effects the Swain relationship (Swain, 1958) can be used (see equation 4-5). It is important to note

$$k_H/k_T = (K_H/K_D)^{1.442} \qquad \text{eq. 4-5}$$

that for small isotope effects this conversion has some uncertainty associated with it (Northrop, 1982).

Secondary α KIEs report on the change in hybridization at the α carbon (the site where bond breakage occurs) in going from the ground state to the transition state (Melander, 1980, p. 172). A normal effect is observed for the transition from sp^3 to sp^2, while an inverse effect results from the transition from sp^2 to sp^3 (see figures 4-4 and 4-5). The magnitude of the effect is indicative of the transition state structure, but firm correlations between the size of a secondary α ^2H or ^3H KIE and a mechanism cannot be made. This is because secondary α effects are very complex and depend not just on the degree of bond tightness or looseness, but on bond angle and the nature of the leaving group .

Secondary β KIEs arise due to the extent of hyperconjugation between the C-H(D) bond and the electron deficient p orbital (Melanders, 1980) (see figure 4-6). The values

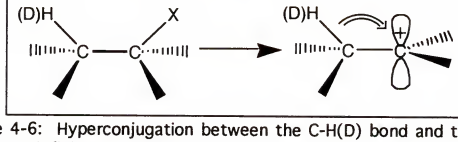

Figure 4-6: Hyperconjugation between the C-H(D) bond and the electron deficient p orbital.

for secondary β deuterium effects often range from 1.05 - 1.15 for an S_N1 system and 1.00 - 1.02 for an S_N2 system (Melander, 1980). The magnitude of these effects depends on the extent of positive charge buildup in the transition state in addition to the dihedral

angle between the C-H(D) bond and the electron-deficient p orbital (Melander, 1980). Therefore, secondary β deuterium KIEs can also enable structural determination because k_L/k_H depends on the orientation of the C-H(D) bond with respect to the carbocation center. Delocalization of the bonding electrons necessitates overlap of the orbital in which they are contained and the electron deficient p orbital of the carbocation (Melander, 1980). The maximum amount of hyperconjugation occurs when the value of the dihedral angle is 0° or 180°. Measurement of secondary α and β deuterium isotope effects is a very powerful tool that was utilized in this project.

Commitment to Catalysis

In order to observe isotopic discrimination and therefore to measure a KIE, the chemical step on which the KIE is reporting must be rate determining or partially rate limiting (Northrop, 1975). If the chemical step is entirely rate limiting, the intrinsic KIE is directly measurable by experiment. If, however, it is only partially rate limiting, the intrinsic KIE is masked by the other steps. Enzymatic reactions comprise at least two more steps in addition to chemistry. These steps are formation of the enzyme-substrate complex and release of product. For enzymatic reactions, chemistry is not always the rate limiting step (Cleland, 1982). For the theoretical enzymatic scheme in figure 4-7, the commitment to catalysis (C_f) is the tendency of the enzyme-substrate complex to

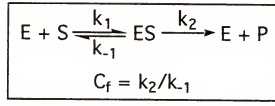

Figure 4-7: Commitment to catalysis factor for a simple enzyme catalyzed reaction.

go forward along the reaction coordinate toward catalysis as compared to its tendency to dissociate to free enzyme and substrate (Northrop, 1977). If a large commitment to catalysis exists, the intrinsic isotope effect is masked which causes a decrease in the observed isotope effect. Substrates that possess a large commitment to catalysis are referred to as "sticky" (Cleland, 1982). The observed V/K isotope effect can be corrected to account for commitment to catalysis through use of equation 4-6 which is for reactions that are not reversible.

$$KIE_{intrinsic} = KIE_{observed} + (KIE_{observed} * C_f) - C_f \qquad \text{eq. 4-6}$$

Knowledge of intrinsic isotope effects are required to reach conclusions about transition-state structure. An estimate of the intrinsic KIE for an enzymatic reaction can be obtained from the KIE for an analogous chemical reaction. This value serves as an upper limit for the enzymatic reaction because most chemical reactions do not have chemical complexity and therefore lack commitment to catalysis. In order to obtain an accurate value of the intrinsic KIE, however, the commitment factor must be determined or commitment to catalysis completely eliminated.

Directly determining the value of the commitment factor (C_f) might require measuring microscopic rate constants and can be very difficult. Simply manipulating pH, temperature, or solvent polarity, however, can rid or minimize a reaction's commitment to catalysis. Another technique used to eliminate commitment to catalysis is design and use of a "slow" substrate which has a slower rate of catalysis (Cleland, 1982). This latter technique was employed in the current study through the use of both pd(UTT) and pdUp.

Techniques for Measuring Isotope Effects

Isotope effects on enzymatic reactions can be measured using the competitive or noncompetitive method. There are advantages and disadvantages associated with each technique. The small kinetic isotope effects measured in this project (all were less than 1.10), necessitate great care and thought given to the experimental design in order to keep errors small.

The Direct Method

The direct method (not performed in this project) involves individual and separate measurement of the rates of reaction for labeled and unlabeled substrates. In this method, the concentration of unlabeled substrate is varied and the enzymatic rate of reaction is measured. The procedure is then repeated for the labeled substrate. Double reciprocal plots for the experiments with the labeled and unlabeled substrates allow for determination and comparison of V_{max} and V/K. The advantage to this method is that

it allows for determination of the KIE for all steps leading to and including the first irreversible step (V/K) or for the overall reaction (V_{max}) (Parkin, 1991). In comparison, the competitive method allows for V/K isotope effect measurements only (see proceeding section).

There are also disadvantages to the direct method. One is that total or near total isotopic substitution of substrates is required. Since only trace labeling can be achieved with tritium, the direct method usually involves deuterium (Northrop, 1977). Another shortcoming to the noncompetitive method is that errors for this method range from 2-10% which limits the use of this method to KIEs larger than 1.25 unless great care is taken (Rosenberg, 1981; Burgner, 1987). Additionally, concentration errors and purity differences between the substrates can alter the double reciprocal plots and give false results (Northrop, 1977).

The Competitive Method

The competitive method was utilized in this project. In this method the two labeled substrates (often labeled with ^{3}H and ^{14}C) are reacted with the enzyme simultaneously in the same reaction mixture. The isotope effect is generated as a result of isotopic discrimination (Northrop, 1977). Generally, one substrate is radiolabeled at the isotopically sensitive position while the other is radiolabeled at a remote position. The latter molecule serves as a reporter for the naturally occurring isotope at the isotopically sensitive site. The substrate pair can also contain a combination of stable and radioactive isotopes. The stable isotope appears at

the isotopically sensitive position and the radiolabel is located at a remote position. The experimental procedure involves running the reaction then separating the reactant from the product. Ratios are determined at time 0 when only substrate is present (or at 100% completion when only product is present) and at some time when the reaction is 40 - 60 % complete. The observed KIE is the ratio of these two ratios.

There are advantages and disadvantages to this method as well. One advantage is that experimental errors as low as 0.3 to 0.5 % can be achieved because it is easier to measure a ratio than an absolute rate. In addition, the isotope effects are independent of substrate and enzyme concentration and competitive inhibitors because the labeled and unlabeled substrate are equally affected (Northrop, 1977). A disadvantage is that the competitive method offers only V/K effects (Simon, 1966) because saturation with both substrate isotopomers is not possible since they are both competing for the same pool of enzyme. Another disadvantage to the competitive method is that radiolabeled substrates are required. In spite of the disadvantages, the advantages to the competitive method, specifically the low experimental error which is essential when measuring small isotope effects, made it the method of choice for our work.

Methodology for the Competitive Method

Before measuring KIEs it is important to determine if the method produces any artifacts which would lead to false results. Chromatography is one way that an artifact can be introduced.

Often the labeled substrates have slightly different chromatographic mobility. In order to avoid introduction of an isotope effect caused by isotopic fractionation, greater than 98% recovery of the product must be obtained (Parkin, 1991).

Another source for introduction of artifacts is if there is an unanticipated isotope effect at any remote isotopic labels. A control experiment must be completed in which a KIE is measured using substrates that both have labels only at the remote positions. If a unity KIE is measured then the remote positions do not have an associated KIE. If the KIE is not unity, however, the observed isotope effects on other positions can be corrected to account for this KIE (Parkin, 1991).

Once the control experiments have been performed, it is important to investigate the method for measuring the KIEs of interest. The method utilized in this project detects either the change in isotopic ratio at 0 % conversion compared to 40 - 60 % conversion or the ratio at 100% conversion to the ratio at 40 - 60 % conversion. The range 40 - 60 % conversion is used because reactions reaching 50% conversion are the most accurate (Duggleby, 1989). In this study, two different methods were used. It is important to note that isotope effects are reported as the rate of the light isotope over that of the heavy isotope. The KIEs for pd(UTT) were based on $^{3}H/^{14}C$ (^{3}H reported on the light isotope and ^{14}C reported on the heavy isotope) ratios of product at near 50 % conversion and the equation for the observed KIE is shown in equation 4-7 (Northrop, 1982). The KIEs for pdUp were based on $^{14}C/^{3}H$ (^{14}C reported on the light isotope and ^{3}H reported on the

heavy isotope) ratios for residual substrate at near 50 % conversion and the equation for the observed KIE is shown in equation 4-8. The ratio of the light isotope over the heavy isotope at 0 % conversion should be the same as that at 100% conversion as long as 100% conversion is achieved.

$$KIE_{obs} = (^{3}H/^{14}C)t_{1/2}/(^{3}H/^{14}C)t_{0} \qquad \text{eq. 4-7}$$

$$KIE_{obs} = (^{14}C/^{3}H)t_{1/2}/(^{14}C/^{3}H)t_{100} \qquad \text{eq. 4-8}$$

The observed KIEs must be corrected for the fraction of conversion (f) of substrate to product because the isotopic composition continually changes as the reaction proceeds. The equations used to correct for these changes are different when product is analyzed and when residual substrate is analyzed and are shown in equations 4-9 and 4-10, respectively, where f = fractional conversion (Bigeleisen, 1958).

$$KIE_{corr} = \ln(1-f)/\ln(1-f*KIE_{obs}) \qquad \text{eq. 4-9}$$

$$KIE_{corr} = \ln(1-f)/\ln[(1-f)*KIE_{obs}) \qquad \text{eq. 4-10}$$

In order to keep experimental errors low, the reaction is run in triplicate to allow for three t_0 points and three $t_{1/2}$ points. Each tube (containing at least 100,000 cpm) is counted for 10 minutes in a repetitive fashion for at least 6 cycles. Finally, the buffer composition and volume in addition to the volume of

scintillation fluid in each vial must be identical, or else the amount of quenching and the channel A/B ratio might vary from tube to tube (Parkin, 1991).

A final issue to be considered concerning methodology for the competitive method is liquid scintillation counting. A multi-channel liquid scintillation counter is used in which ^{3}H is detected in channel A only, whereas ^{14}C is detected in both channels A and B. To determine the $^{3}H/^{14}C$ ratio in each individual tube, the ratio of ^{14}C counts in channels A and B ($A:B_{14}$) must first be determined by measuring the CPM in both channels A and B for a ^{14}C standard. The standard is preferably prepared from one of the ^{14}C isotopic substrates (or products) and the composition of this vial is identical to those used in KIE experiments. Once this value is known, equation 4-11 can be used to determined the $^{3}H/^{14}C$ ratio in each tube (Parkin, 1991):

$$^{3}H/^{14}C = \text{CPM A} - (\text{CPM B} \times A:B_{14})/\text{CPM B} + (\text{CPM B} \times A:B_{14}) \qquad \text{eq. 4-11}$$

KIEs on Similar Systems

When performing KIEs it is desirable to have KIE information from similar systems. In addition, as mentioned above, it is nice to have KIE information for the non-enzymatic reaction as well to use as a comparison. KIEs for a similar chemical reaction can serve as an upper limit value to help determine if a commitment to catalysis is present (Parkin, 1987). The system studied in this project is C-N glycosidic cleavage of pdUp (a 3',5'-deoxynucleoside

diphosphate). The most similar KIE studies have been the acid catalyzed hydrolysis of uridine (Prior, 1984) and the acid catalyzed hydrolysis of AMP and dAMP (Parkin, 1984). An extensive KIE analysis of AMP nucleosidase was also performed (Mentch, 1987; Parkin, 1984; Parkin, 1987; Schramm, 1991). It is important to note that these are not ideal comparisons because the substrates are different. Uridine possesses a 2' hydroxyl group and lacks phosphates. AMP also possesses a 2' hydroxyl group and contains a purine base, not a pyrimidine. A KIE was measured for the acid catalyzed hydrolysis of dAMP as well (Parkin, 1984), but this substrate contains a purine base and not a pyrimidine base.

The KIE studies of the acid catalyzed hydrolysis of uridine have been discussed in Chapter 1. In brief, a secondary tritium isotope effect of 0.87 was measured for the hydroylsis of [6-^{3}H] uridine and an α-secondary deuterium isotope effect of 1.11 were measured. These KIEs indicate a change in hybridization at C6 from sp^2 to sp^3 and an oxocarbenium ion-like transition state, respectively (Prior, 1984).

A comprehensive KIE study of AMP nucleosidase was performed. KIEs were obtained for both the acid catalyzed reaction and the enzyme catalyzed reaction. The following KIEs were determined for the acid catalyzed hydrolysis of AMP: a primary ^{14}C KIE of 1.049 ± 0.009, an α ^{3}H KIE of 1.236 (Parkin, 1984), and a β deuterio KIE of 1.077 ± 0.002 (Mentch, 1987). An α ^{3}H KIE of 1.259 was determined for the acid catalyzed hydrolysis of dATP (Parkin, 1984). The α ^{3}H KIE for the acid catalyzed hydrolysis of dAMP is only slightly greater than that for the acid catalyzed

hydrolysis of AMP which suggests that the nature of the transition states is similar and oxocarbenium-like. This suggests that the absence of the 2' hydroxyl group in dAMP does not cause dramatic differences in the transition state.

AMP nucleosidase performs a similar reaction to UDG in that it cleaves a C-N glycosidic bond. The KIEs for the reaction of AMP nucleosidase with AMP are as follows: a primary ^{14}C KIE of 1.035, an α secondary KIE of 1.069 ± 0.009, and a β secondary KIE of 1.061. These KIEs suggest that an S_N2 reaction is not occurring in the transition state, but rather, an oxocarbenium-like transition state is operative (Parkin, 1987; Mentch, 1987).

KIEs have proven to be valuable tools for determining glycosylase and solvolysis transition states (Schramm, 1991). Models of enzyme transition state interactions based on KIE data have been affirmed by X-ray crystallography with bound transition state analogs (Schramm, 1994; Degano, 1996), thus providing strong support for the accuracy of transition state geometries obtained through KIE studies.

Results

All of the KIEs in this chapter were determined under V/K conditions using the competitive method. The isotope effects are reported in this section while a detailed discussion of the methods used to measure the effects and the interpretations appears in the following section.

Two different chromatographic methods were used to measure kinetic isotope effects for the reaction of UDG with pdUp.

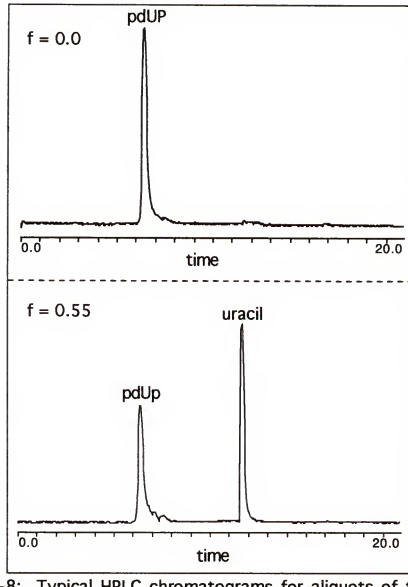

Figure 4-8: Typical HPLC chromatograms for aliquots of the UDG catalyzed hydrolysis of pdUp. Entire uracil and pdUp peaks were collected for KIE experiments.

A comparison of the values from both methods will demonstrate if they are valid. One method utilized Dowex anion exchange mini columns while the other method used C18 reverse phase HPLC (see figure 4-8). The measured values are listed in table 4-1.

Three different methods were use to calculate the KIEs. The values in table 4-1, column A, are from KIE experiments in which

product was analyzed and C18 HPLC was utilized, while the results in table 4-1, column B, are from KIE experiments in which residual substrate was analyzed and C18 HPLC was utilized. The results in table 4-1, column C, are from KIE experiments in which product was analyzed and Dowex anion exchange mini-columns were utilized. The three different methods yielded values which are in good agreement with one another.

Table 4-1: KIE values for UDG vs. pdUp

Isotopomeric pair	Type of KIE	Values: A	B	C
[5-^{3}H; 1'-^{13}C]; [2-^{14}C] pdUp	1° ^{13}C	1.012 ± 0.007	1.013 ± 0.005	1.021 ± 0.004
[5-^{3}H; 1'-^{2}H]; [2-^{14}C] pdUp	2° α ^{2}H	1.064 ± 0.006	1.069 ± 0.007	1.069 ± 0.006
[5-^{3}H; 2'R-2'-^{2}H]; [2-^{14}C] pdUp	2° β ^{2}H	1.067 ± 0.008	1.082 ± 0.008	1.067 ± 0.007
[5-^{3}H]; [2-^{14}C] pdUp	control	1.001 ± 0.006	1.005 ± 0.005	1.021 ± 0.007

The KIE values were obtained by: A) analysis of product by C18 HPLC, B) analysis of residual substrate by C18 HPLC, and C) analysis of product by Dowex mini-columns.

For the C18 HPLC KIE experiments in which product was analyzed, a primary ^{13}C KIE of 1.012 ± 0.007 with the label positioned at the anomeric carbon was measured. The secondary α deuterium isotope effect with the deuterium bound to the anomeric carbon had a value of 1.064 ± 0.006. The secondary β deuterium effect in which the deuterium was positioned beta to the anomeric carbon was 1.067 ± 0.008, respectively. Additionally, the value of the control KIE in which both molecules contained radiolabels at

remote positions was 1.001 ± 0.008. This result confirms that an additional isotope effect is not introduced by the remote labels.

Values were also calculated for the C18 HPLC KIE experiments in which residual substrate was analyzed. A value of 1.013 ± 0.005 was measured for the primary ^{13}C KIE. A secondary α deuterium effect of 1.069 ± 0.006 and a secondary β deuterium effect of 1.082 ± 0.008 were determined. In addition, a value of 1.005 ± 0.005 was measured for the control experiment in which both molecules were labeled at remote positions only.

The third method utilized Dowex anion exchange mini columns and analyzed product. A primary ^{13}C KIE of 1.021 ± 0.004 was observed. The secondary α and β deuterium isotope effects were 1.069 ± 0.006 and 1.067 ± 0.007, respectively. Finally, the value for the control experiment was 1.021 ± 0.007.

In addition to measurement of KIEs for the reaction of UDG with pdUp, a KIE was also measured for the reaction of UDG with [uracil-6-^{3}H] pd(UTT). A secondary α ^{3}H KIE was measured using C18 reverse phase HPLC chromatography (see figure 4-9) and analysis of residual substrate. As seen in figure 4-9, both the pd(UTT) and uracil elute as 2 peaks. This was confirmed by collecting one of the 2 peaks as it eluted from the column, reinjecting the material onto the column, and observing the same 2 peaks. The value for this KIE was 1.009 ± 0.012.

Discussion

The goal of this project was to synthesize new substrates with isotopic labels, and develop a KIE method for UDG. The long

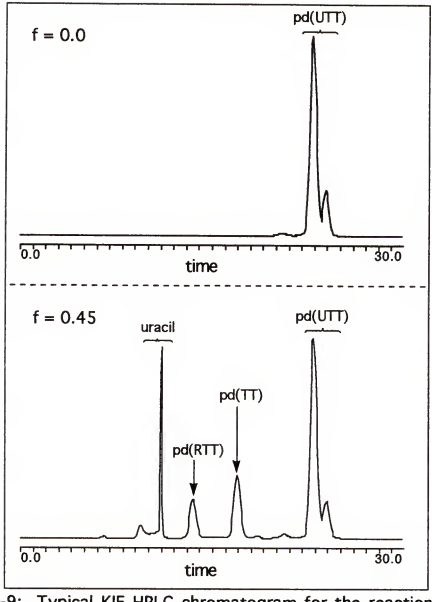

Figure 4-9: Typical KIE HPLC chromatogram for the reaction of UDG with pd(UTT). The entire pd(UTT) peak was collected.

term goal is to obtain information about UDG catalysis in order to determine its mechanism of action. Analysis of multiple KIE experiments allows for modeling of transition state structure (Rodgers, 1982).

KIEs for the Reaction of UDG with pdUp

As kinetic isotope effects for UDG have not been measured in our lab before this study, a detailed investigation of the method was necessary. As will be discussed below, the preferred method for measuring KIEs is one that employs Dowex mini columns. Dowex mini-columns are much easier to use than HPLC. because KIE experiments involving Dowex mini columns require less time and expense.

Method Development for KIEs with pdUp

The first method that was used to measure KIEs for the reaction of UDG with pdUp employed Dowex anion exchange mini columns. Negatively charged materials selectively bind to the resin. Therefore, pdUp and 3',5'-deoxyribosediphosphate bind to the resin and uracil does not when the buffer is water. The observed KIE was the ratio of the $^{14}C/^{3}H$ ratio of product at 50 % conversion and the $^{14}C/^{3}H$ ratio of product at 100 % conversion.

When measuring a KIE it is important that the composition in each liquid scintillation vial be identical to avoid quenching variations in scintillation counting (Parkin, 1991). The f = 0.0 samples and f = 0.4 - 0.6 samples must be treated identically during preparation. For the Dowex method, this means that at both time points, the reaction must be passed through the Dowex mini-column. Since negatively charged molecules (like pdUp) bind to the resin and neutral molecules (like uracil) do not, in place of the $^{14}C/^{3}H$ ratio at f = 0.0 to determine the KIE, the $^{14}C/^{3}H$ ratio at f = 1.0 can be used. Provided that 100 % conversion is obtained, the

$^{14}C/^{3}H$ ratio at f = 0.0 and at f = 1.0 will be identical. Several attempts to obtain 100 % conversion of pdUp were made including using up to ten times more enzyme, increasing reaction times to up to 10 times longer, and adding enzyme in aliquots every 4-6 hours during the reaction. One hundred percent conversion of pdUp with UDG was never obtained. The highest percent conversion obtained was 97 %. Consequently, calf intestinal alkaline phosphatase (CIAP) was used to produce 100 % conversion of pdUp to (2'-deoxyuridine (dU). Since dU is a neutral molecule it does not bind to the resin. This modification allowed for the 100 % conversion samples and the 40 -60 % conversion samples to be treated identically with a very modest difference in the composition of the samples. All columns were eluted with 2 mL of a mixture of 1 mM uracil/1 mM dU which amounts to 2 μmoles of each component in each vial. The maximum amount of radiolabeled uracil in the f = 0.0 vials and dU in the f = 1.0 vials was 0.75 nmoles, which is negligible compared to the amount of cold uracil and dU present in the vials. As a result, quenching variations between tubes should not occur due to differences in composition of the material in the vials.

For the pdUp KIE experiments using Dowex mini columns, a master stock of the desired isotopomeric pair was prepared. A portion of this material was treated with CIAP to obtain 100 % conversion to dU while another portion of the master stock was treated with UDG to obtain 40 - 60 % conversion to uracil. The reaction mixtures were applied to Dowex anion exchange mini columns which were subsequently washed with a mixture of 1 mM

uracil/1mM dU directly into LSC vials until all of the radioactivity was eluted.

The second KIE method utilized C18 reverse phase chromatography. The chromatographic properties of the Dowex anion exchange resin and the C18 reverse phase resin are dramatically different. Negatively charged materials bind well to the Dowex resin. They do not bind well to the C18 resin where binding favors hydrophobic interactions. Therefore, if the KIEs for the reaction of UDG with pdUp are the same using either the Dowex or C18 HPLC method, it suggests that both methods are valid.

For the pdUp KIE experiments utilizing C18 HPLC, a master stock of the desired isotopomeric pair was prepared. A portion was treated with UDG to afford 40 - 60 % conversion. To obtain the $^{14}C/^{3}H$ ratio at t_0 (this ratio will be the same for t_0 and t_{100}) an aliquot of the master stock was applied to the C18 column and the entire pdUp peak was collected. To obtain the $^{14}C/^{3}H$ ratio at f = 0.4 - 0.6, an aliquot of the master stock which had been treated with UDG was applied to the C18 column and the entire uracil and pdUp peaks were collected.

Comparison of the KIEs measured using the two different chromatographic methods demonstrates that either method is viable. For the special case of pdUp where 100 % conversion with UDG was not obtained, the C18 method is slightly better because the composition of each vial is completely identical. In the future, however, when KIEs for larger oligonucleotide substrates are measured, the Dowex method is the method of choice because it is easier and more cost efficient than the C18 HPLC method.

Additionally, the calf intestinal alkaline phosphatase step will be avoided for these KIEs because it is very likely that 100 % conversion by UDG will be obtained. Consequently, the composition of each vial will be identical. Although the experiments have not been performed yet, it will be much easier to obtain 100 % conversion with UDG for substrates including and larger than pd(UCC). This is because the V_{max} for pd(UTT) is 170 times larger than the V_{max} for pdUp and therefore much less enzyme will be required.

A final check of the KIE methodology involved synthesizing new substrate and repeating the C18 HPLC KIE experiment. This involved synthesis of new pdUp [5-^{3}H] and measuring the effect for the isotopomer pair [5-^{3}H] and [2-^{14}C] pdUp. The value for this effect was 1.001 ± 0.008. Since the value is identical to the original value (1.001 ± 0.006) these results suggest systematic errors are not introduced due to use of different batches of substrate.

Interpretation of KIEs for the Reaction of UDG with pdUp

The KIEs measured for the reaction of UDG with pdUp yielded information about the mechanism of UDG. Since for the special case of pdUp the C18 method was slightly better than the Dowex method (see above), this discussion will focus on the results from the KIEs measured by the C18 HPLC method in which product was analyzed (table 4-1, column A). The unity control KIE in which both labels were remote demonstrates that the positions of the ^{14}C and ^{3}H in all of the pdUp molecules are isotopically insensitive. This

is an important KIE because it eliminates the possibility that the remote labels are introducing an additional KIE. In addition, it suggests that changes to the environment of the uracil ring do not occur at the transition state.

The value of the primary ^{13}C KIE that was measured for the isotopomer pair of [5-^{3}H; 1'-^{13}C] and [2-^{14}C] pdUp was 1.012 ± 0.007. This number is below the range of 1.04-1.08 which would be indicative of an associative S_N2 mechanism. Therefore, mechanistic schemes in which the incoming nucleophile and departing leaving group have significant bond order can be ruled out (Melander, 1980). The value is in the range of 1.01-1.03 which is expected for an S_N1-like reaction. This value by itself does not confirm that an S_N1-like mechanism is in effect. It is necessary to confirm that the values of the secondary α and β KIEs also indicate a dissociative S_N1 mechanism.

Both secondary α and β deuterium isotope effects were measured. A secondary β deuterium effect of 1.067 ± 0.008 was measured for the isotopomer pair [5-^{3}H; 2'R-2'-^{2}H] and [2-^{14}C] pdUp. Since values ranging from 1.00 - 1.02 would suggest an S_N2-type displacement at C1' (Parkin, 1987), this type of mechanism can be ruled out. This value falls in the range of 1.05 - 1.15 which is indicative of hyperconjugative interaction between H2' and C1' indicative of a S_N1 transition state (Melander, 1980). A secondary α deuterium effect of 1.064 ± 0.006 was measured for the isotopomer pair [5-^{3}H; 1'-^{2}H] and [2-^{14}C] pdUp. Although this value cannot be firmly correlated to a specific mechanism (Matsson, 1998), it does indicate that the α-H is in a looser

environment, consistent with the expected planarization for an oxocarbenium ion-like transition state. In order to determine the amount of charge and estimate the conformation of the ribose ring, the secondary β pro-S and dideuterio effects for the respective isotopomeric pairs [2-^{14}C] and [5-^{3}H; 2'S-2'-^{2}H] pdUp, and [2-^{14}C] and [5-^{3}H; 2',2'-^{2}H] pdUp must be measured. Before these KIEs can be measured, a synthetic method for making the synthetic precursors [5-^{3}H; 2'S-2'-^{2}H] dUTP, and [5-^{3}H; 2',2'-^{2}H] dUTP must be devised. Once it is known how to synthesize [5-^{3}H; 2'S-2'-^{2}H] dUTP, the synthesis of [5-^{3}H; 2',2'-^{2}H] dUTP will be facile. Thus far, however, the synthesis of [5-^{3}H; 2'S-2'-^{2}H] dUTP has been extremely difficult (see chapter 2). Since the KIE for the reaction of UDG with [uracil-6-^{3}H] was unity, an easy solution to the synthetic problem would be to carry out the entire [2',2'-^{2}H] UMP synthesis in D_2O.

The family of KIEs measured for the reaction of UDG with pdUp indicates that a S_N1-like mechanism is operative. Similar KIE values were determined for the reaction of AMP nucleosidase with AMP and the same conclusion about the transition state was reached (see above "Introduction"). The proposed mechanistic schemes for UDG do not directly address the important question of whether an S_N1 or S_N2 mechanism is operative for UDG. Information can be obtained, however, from the published schematic diagrams of proposed mechanisms as shown in figures 1-11, 1-12, and 1-13 (Mol, 1995; Savva, 1995; Shroyer, 1999). None of these diagrams depicted formation of an oxocarbenium ion. Rather, they illustrated simultaneous attack of water and

departure of the leaving group. The issue of whether UDG utilizes an S_N1-like or an S_N2-like mechanism was left ambiguous. The results of the KIE experiments performed in this study suggest that if concerted nucleophilic attack and departure of uracil is part of the transition state, then loss of uracil is much more advanced, leading to an oxocarbenium ion-like transition state. The very low value for the primary ^{13}C KIE argues that the UDG transition state does not feature much nucleophilic participation.

KIE for the Reaction of UDG with pd(UTT)

The KIE experiment for the reaction of UDG with pd(UTT) involved using the isotopomer pair [uracil-6-^3H] and [uracil-2-^{14}C] pd(UTT). The mixture was treated with UDG to afford 45 % conversion and then residual substrate was isolated by C18 reverse phase HPLC chromatography. The observed KIE was calculated by the ratio of the $^3H/^{14}C$ ratio for residual substrate after 45 % conversion and the $^3H/^{14}C$ ratio for unreacted starting material treated in the same fashion. The corrected KIE was determined by using equation 4-10.

A near unity secondary α KIE was measured for the reaction of UDG with pd(UTT). A unity secondary α KIE means there is no significant covalency change at C6 which argues against nucleophilic attack at this position. If this value represents an intrinsic KIE then the result suggests that the Michael addition mechanism for UDG proposed by Prior and Santi is not valid.

Another possibility is that a commitment to catalysis causes a unity KIE by masking the intrinsic KIE. It is unlikely that

there is a commitment to catalysis for pd(UTT), however, because pd(UTT) is a catalytically challenged substrate. Compared to the oligonucleotide pd(T_5UT_5), the K_m for pd(UTT) is increased by a factor of 11 and the V_{max} for pd(UTT) is reduced by a factor of 100. Therefore, the measured value of unity for the 2°-α KIE is most likely accurate. The most straightforward way to test this will be with β deuterio isotope effects, which might be ~ 1.06 based on our results with pdUp. If the β deuterio KIEs with trinucleotide substrates were smaller, this would suggest that a commitment to catalysis was present.

A future goal of this project is to measure KIEs for uracil containing oligonucleotides of increasing size. As the size increases, the sugar phosphate backbone increases and base-flipping is more likely to occur. In addition, larger oligonucleotides better resemble UDGs natural substrate. A delicate balance will need to be struck. Longer substrates which provide KIEs more informative of the natural reaction will tend to suffer higher commitments to catalysis. The first molecule to follow pdUp will be pd(UCC). The secondary α KIE measured for the reaction of UDG with pd(UTT) and the control KIE measured for pdUp demonstrates that a ^{14}C label at position 2 of uracil, a ^{3}H label at position 5 or uracil, and a ^{3}H label at position 6 of uracil should all be suitable remote labels.

Conclusions

A family of kinetic isotope effects were measured for the reaction of UDG with pdUp. Three possible mechanistic pathways

are illustrated in the diagram in figure 4-10 (Thornton, 1967; More O'Ferrall, 1970; Jencks, 1972) where line a represents an associative S_N2 mechanism, line b represents a highly dissociative S_N2-like mechanism, and line c represents a dissociative S_N1

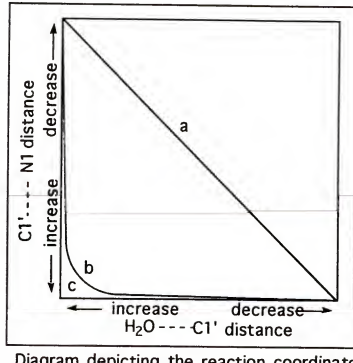

Figure 4-10: Diagram depicting the reaction coordinate for a) an associative S_N2 reaction, b) a highly dissociative S_N2-like mechansim, c) a dissociative S_N1 mechanism (from Thornton, 1967; More O'Ferrall, 1970; Jencks, 1972).

mechanism. All of the KIEs ruled out an associative S_N2-like mechanism (see figure 4-10, line a). The KIEs indicated that positive charge build-up occurs at the anomeric carbon of ribose to yield an oxocarbenium ion-like transition state suggesting an S_N1-like mechanism as seen in figure 4-11 (either line b or c in figure 4-10). The C-N glycosidic bond is partially cleaved and the bond between water and the anomeric carbon of ribose is either not yet formed or very slightly so. Additionally, the unity secondary α KIE

measured for the reaction of [uracil-6-^{3}H] and [uracil-2-^{14}C] pd(UTT) suggests that the proposed Michael addition mechanism for UDG is not valid.

A future goal is to measure a secondary β pro-S and dideuterio effect for the isotopomer pair of [5-^{3}H; 2',2'-^{2}H] and

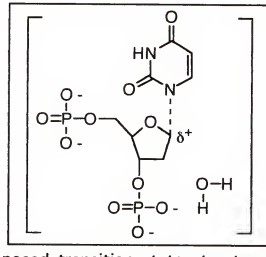

Figure 4-11: Proposed transition state structure for cleavage of uracil from pdUp by UDG. The C-N glycosidic bond is partially cleaved and the bond between the incoming water and the anomeric carbon of ribose is either not yet formed or very slightly so. The protonation state of the departing uracil is not yet known.

[2-^{14}C] pdUp. These effects will yield structural information about the ribose ring because information about the dihedral angle between the C-H(D) bond and the electron deficient p orbital at C1 can be gained. Troubleshooting the synthetic route for synthesis of [5-^{3}H; 2'S-2'-^{2}H] dUTP must occur before this effect can be measured (see chapter 2).

Experimental

Instrumental

HPLC was performed on a Rainin HPXL gradient unit interfaced to a Macintosh personal computer. Separations were completed on a C18 reverse phase column. A Rainin Dynamax UV-1 detector was utilized to monitor separations at 260 nm. A Rainin -Dynamax fraction collector (Model FC-1) was used to collect eluent samples from the HPLC. Liquid scintillation counting was performed using a Packard 1600 TR instrument which dumped data to a floppy disk for subsequent analysis on a personal computer. Dual channel liquid scintillation counting (channel A, 0-15 keV; channel B 15-80 keV) was utilized to determine the $^{3}H/^{14}C$ ratios. Each tube was counted for 10 minutes and cycled through the counter 6-10 times.

General Methodology for Measuring Kinetic Isotope Effects with pd(UTT)

The KIE experiment for UDG vs. pd(UTT) utilized mixtures of radiolabeled isotopomeric substrates, and therefore were competitive (Parkin, 1991). A master stock (300 μL) was prepared which comprised 150,000 CPM each of [uracil-6-^{3}H] pd(UTT) and [uracil-2-^{14}C] pd(UTT) (0.745 mM pd(UTT)), 25 mM Tris-HCl, pH 8.0, and 1 mg/ml BSA. To determine the reference $^{3}H/^{14}C$ ratio at time 0, duplicate aliquots were withdrawn from the master stock and substrate was isolated on a C18 column (100 mM NH_4HCO_3, 3% - 7.8% CH_3CN, 0 - 30 min, absorbance at 260 nm was monitored) and collected directly into scintillation vials (2 mL fractions). Fisher

Scintisafe 30% liquid scintillation fluid (10 mL) was added to each vial. Reaction mixtures (100 ul; 50,000 cpm each isotopomer; 0.232 mM) were initiated by the addition of 62 ng UDG and incubated at 37 °C for the appropriate amount of time (45 - 55 minutes) to afford 40 - 60% conversion. To determine $^{3}H/^{14}C$ ratio for unreacted pd(UTT) (duplicate measurements) after 40 - 60% conversion, all reaction components were isolated on a C18 column (100 mM NH_4HCO_3, 3% - 7.8% CH_3CN, 0 - 30 min, absorbance at 260 nm was monitored) and collected directly into scintillation vials (2 mL fractions). Fisher Scintisafe 30% liquid scintillation fluid (10 mL) was added to each vial. The percent conversion was determined by the ratio of CPM eluted under the pd(UTT) peak and the total radioactivity that eluted from the column.

Triplicate samples of [^{14}C] 2'-deoxyuridine were used to determine the ratio of ^{14}C counts in channels A and B ($A:B_{14}$) and equation 4-11 was used to determine the $^{3}H/^{14}C$ ratio in each individual LSC vial. The reported value and error of a KIE represents the mean and standard deviation of 2 individual KIE experiments taken over 10 cycles of liquid scintillation counting. Equation 4-7 was used to calculate the observed KIEs, while equation 4-9 was used to determine the corrected KIE.

A control experiment was also conducted to ensure that close to 100% of the radiolabeled material applied to the C18 column actually eluted from the column. A mixture (47 μL) containing approximately 170,000 CPM of radiolabeled pd(UTT) was made. An aliquot (23 μL) was removed and applied to a C18 HPLC column. Radiolabeled pd(UTT) was isolated (100 mM NH_4HCO_3, 3% -

7.8% CH_3CN, 0 - 30 min, absorbance at 260 nm was monitored) and collected directly into scintillation vials (2 mL fractions). Another aliquot (23 μL) was added directly to a liquid scintillation vial containing 2 mL 100 mM NH_4HCO_3, 6.5 % CH_3CN. LSC fluid (10 mL) was added to each vial which were counted for 20 minutes each. The total CPM in each tube was calculated. The result was that 99.5 % of the CPM applied to the C18 column eluted from the column.

General Methodology for Measuring Kinetic Isotope Effects with pdUp (Dowex Method)

Kinetic isotope effect (KIE) experiments for UDG vs. pdUp used mixtures of isotopomeric substrates, and therefore were competitive (Parkin, 1991). A master stock (~ 100 μL) of a given $^3H/^{14}C$-labeled isotopomeric pair of pdUp was prepared which comprised 500,000 cpm of each isotopomer (approximately 0.127 mM). In order to determine the reference $^3H/^{14}C$ ratio at f = 1.0, a calf intestinal alkaline phosphatase reaction (CIAP reaction) was made. In order to determine the $^3H/^{14}C$ ratio at f = 0.4 - 0.6, a uracil DNA glycosylase reaction (UDG reaction) was made.

For the CIAP reaction, an aliquot of the master was removed (approximately 340,000 cpm) and added to the CIAP reaction mixture whose final composition was 50 mM Tris-HCl, pH 9.3, 1 mM $MgCl_2$, 0.1 mM $ZnCl_2$, and 0.031 mM pdUp. To the mixture was added 9 units calf intestinal alkaline phosphatase (final volume = 150 μl). The mixture was incubated at 37° C for an appropriate amount of time to obtain 100% conversion of pdUp to dU (4 - 6 hours). To

determine the reference $^{3}H/^{14}C$ ratio, triplicate aliquots were withdrawn from the CIAP reaction mixture after 100% conversion was obtained. The aliquot was applied to a 2.5 cm Dowex mini column (acetate form) and eluted with a 1 mM uracil/1mM deoxyuridine mixture directly into scintillation vials (2 mL fractions). Care was taken to elute all of the radioactivity from the column.

To make the UDG reaction an aliquot of the master was removed (approximately 630000 cpm) and added to a UDG stock mixture whose final composition comprised 1 mg/ml BSA, 25 mM Tris-HCl, pH 8.0, and 0.056 mM pdUp. Three aliquots were removed from the UDG stock mixture and added to three separate UDG reactions whose final composition was 25 mM Tris-HCl, pH 8.0, 1 mg/ml BSA, 0.018 mM pdUp (approximately 200,000 cpm). To initiate the reaction, approximately 200 ug of UDG were added and the reaction was incubated at 37 °C for an appropriate amount of time to obtain 40 - 60% conversion. To determine the $^{3}H/^{14}C$ after 40 - 60% completion was achieved, the entire reaction mixture was applied to a 2.5 cm Dowex mini column (acetate form) and eluted with a 1 mM uracil/1mM deoxyuridine mixture directly into scintillation vials (2 mL fractions). Care was taken to elute all of the radiolabeled uracil from the column.

Triplicate measurements of aliquots from the CIAP reaction allowed for back calculation of the total amount of radioactivity applied to the Dowex columns in the UDG reactions. The percent conversion of pdUp to uracil was determined from a ratio of the radioactivity eluted from the Dowex columns in the UDG reactions

and the total amount of radioactivity applied to the column in the UDG reactions. Triplicate samples of [^{14}C] pdUp were used to determine the ratio of ^{14}C counts in channels A and B (A:B$_{14}$). To determine the ^{3}H/^{14}C ratio in each individual tube, equation 4-11 was utilized (Parkin, 1991). The reported value and error of a KIE represents the mean and standard deviation of 3 individual KIE experiments taken over 10 cycles of liquid scintillation counting. Equation 4-8 was used to calculate the observed KIEs while equation 4-9 was used to calculate the corrected KIEs.

A control experiment was conducted to ensure that nearly 100% of the radiolabeled material applied to the Dowex mini columns actually eluted from the columns. A CIAP reaction mixture (total volume = 50 μL) was prepared containing approximately 116,000 CPM of radiolabeled pdUp, 3 units CIAP enzyme, 50 mM Tris-HCl, pH 9.3, 1 mM $MgCl_2$, and 0.1 mM $ZnCl_2$. The reaction was incubated for 3.5 hours then 950 μL 1 mM uracil/1mM 2'-deoxyuridine was added. An aliquot (240 μL) was added directly to a vial containing 1.76 mL 1 mM uracil/1mM 2'-deoxyuridine. Three more aliquots (240 μL) were applied to three separate 2.5 cm Dowex mini columns (acetate form) and eluted with a 1 mM uracil/1mM deoxyuridine mixture directly into scintillation vials (2 mL fractions). Care was taken to elute all of the radioactivity from the column. Twelve mL LSC fluid were added to each tube and each tube was counted by liquid scintillation counting for 10 minutes. The results were that 99.4 % of the CPM applied to the columns were eluted from the columns.

General Methodology for Measuring Kinetic Isotope Effects with pdUp (C18 HPLC Method)

KIE experiments for UDG vs. pdUp used mixtures of isotopomeric substrates, and therefore were competitive (Parkin, 1991). A master stock (205 - 465 μL) of a given $^{3}H/^{14}C$-labeled isotopomeric pair of pdUp was prepared which comprised 500,000 cpm of each isotopomer (approximately 0.127 mM), ~55 mM Tris-HCl, pH 8.0, and ~2.3 mg/ml BSA. To determine the reference $^{3}H/^{14}C$ ratio at t_0 triplicate aliquots were removed from the master stock (~100,000 cpm each) and the pdUp was isolated on a C18 column (100 mM NH_4HCO_3, 1.5% CH_3CN, absorbance at 260 nm was monitored) and collected directly into scintillation vials (2 mL fractions). Fisher Scintisafe 30% liquid scintillation fluid (10 mL) was added to each vial. Three reaction mixtures were made by mixing aliquots of the master stock with water to afford the final composition of 1 mg/ml BSA, 25 mM Tris-HCl, pH 8.0, 200,000 cpm. The reactions were initiated by the addition of approximately 200 ug UDG and incubated at 37 °C for the appropriate amount of time (4.5 - 5.5 hours) to afford 40 - 60% conversion. To determine $^{3}H/^{14}C$ ratio for uracil after 40 - 60% conversion (triplicate measurements), all reaction components were isolated on a C18 column (100 mM NH_4HCO_3, 1.5% CH_3CN, absorbance at 260 nm was detected) and collected directly into scintillation vials (2 mL fractions). Fisher Scintisafe 30% liquid scintillation fluid (10 mL) was added to each vial. The percent conversion was determined by the ratio of CPM eluted under the uracil peak and the total radioactivity that eluted from the column.

Triplicate samples of [^{14}C] pdUp were used to determine the ratio of ^{14}C counts in channels A and B (A:B$_{14}$). To determine the ^{3}H/^{14}C ratio in each individual tube equation 4.7 was utilized (Parkin, 1991). The reported value and error of a KIE represents the mean and standard deviation of three individual KIE experiments taken over 6 -10 cycles of liquid scintillation counting. These KIEs were determined by both analysis of product (using equations 4-8 and 4-10) and residual substrate (using equations 4-8 and 4-9).

A control experiment was conducted to ensure that close to 100% of the radiolabeled material applied to the C18 column actually eluted from the column. A mixture (44 μL) containing 100,000 CPM radiolabeled pdUp was made. An aliquot (20 μL) was added directly to a vial containing 2 mL 100 mM NH_4HCO_3, 1.5% CH_3CN. Another aliquot (20 μL) was isolated on a C18 column (100 mM NH_4HCO_3, 1.5% CH_3CN) and collected directly into scintillation vials (2 mL fractions). LSC fluid (10 mL) was added to each vial and the vials were counted for 10 minutes each. Thus, 99.1 % of the radioactivity applied to the column eluted from the column.

CHAPTER 5
CONCLUSIONS AND FUTURE WORK

Conclusions

The work described in this dissertation has laid the ground work for future study of the mechanistic pathway of UDG. Synthetic routes were devised for the syntheses of uracil-containing UDG substrates. The kinetic behavior of UDG with some of these substrates is presented in this dissertation. The kinetic studies of a C200S UDG mutant suggested that the lone cysteine residue of *E. coli* UDG is not required for catalysis. Additionally, methods for measuring KIEs were developed and applied to determine kinetic isotope effects for *E. coli* UDG.

Radiolabeled UDG substrates were synthesized through the use of multi-enzyme synthetic routes. A three step procedure involving 13 different enzymes allowed for the synthesis of labeled dUTP from glucose or ribose and orotic acid. The molecule dUTP is the precursor to pdUp, pd(UCC), and future oligonucleotides whose syntheses also involve multi-enzyme synthetic procedures. The synthetic method provided dUTPs in yields ranging from 13 - 53 %. That dUTP serves as a convenient intermediate was shown by its facile conversion to pdUp, the substrate featured in the UDG KIE experiments.

Determination of kinetic constants for the reactions of UDG with a 781 base pair uracil-containing DNA substrate (HCAII-U) and the catalytically challenged nucleoside diphosphate, pdUp, led to interesting discoveries about the enzyme. The role of the lone cysteine residue in *E. coli* UDG was investigated through the use of a C200S mutant. By comparing kinetic constants for the reaction of wild type UDG and C200S UDG with HCAII-U, it was determined that cysteine 200 was not an essential residue for catalysis. In addition, the kinetic study of the hydrolysis of pdUp by UDG demonstrated that UDG does not require binding of an oligonucleotide for activity. This result updates the previous belief that pd(UT)p is the smallest UDG substrate. However, pdUp is a very slow substrate, indicating that an oligonucleotide phosphate backbone is important for optimal catalysis.

The alternate substrates pd(UTT) and pdUp serve as excellent molecules for KIE analysis. The reduced rate of UDG catalysis with these substrates reduces the possibility of commitment factors. Two methods were developed to measure isotope effects for the hydrolysis of pdUp by UDG. One involved C18 reverse phase HPLC chromatography and yielded KIE values with errors ranging from ± 0.005 - 0.008. The other method involved Dowex anion exchange chromatography and yielded KIE values with errors ranging from ± 0.004 - 0.007. C18 reverse phase HPLC chromatography was utilized to measure a KIE for the hydrolysis of pd(UTT) by UDG. The error for this KIE was ± 0.012.

The unity 2° α tritium KIE measured for the reaction of UDG with the isotopomer pair [uracil-6-^{3}H] and [uracil-2-^{14}C] pd(UTT)

illustrated that there was no change in covalency at C6 of uracil during catalysis. This result along with the results from X-ray crystallography data which do not identify a properly disposed nucleophile at the active site, help to rule out the proposed Michael addition mechanism for UDG. Kinetic isotope effects were also determined for the hydrolysis of pdUp by UDG. The respective values for a primary ^{13}C KIE for the isotopomer pair of [5-^{3}H; 1'-^{13}C] and [2-^{14}C] pdUp and a β secondary deuterium KIE for the isotopomer pair [5-^{3}H; 2'R-2'-^{2}H] and [2-^{14}C] pdUp were 1.012 ± 0.007 and 1.064 ± 0.006. These values suggest a dissociative SN1-like transition state with very little nucleophilic participation.

Future Work

The findings from this project have opened the door to many new investigations into the mechanism of UDG. One experiment that will yield important transition state information is the measurement of a β secondary dideuterium effect with the deoxyribose ring dual labeled at C2'. This will allow for estimation of the degree of charge built up at the anomeric carbon in the transition state. The dihedral angles between the C-H(D) bonds and the electron deficient p orbital at the anomeric carbon can be estimated from the β deuterium isotope effects for the pro S and pro R deuterium isotopomers. As a result, the geometry of the ribose ring can be determined. Note that a pre-requisite is that the problem of the $^{2}H/^{1}H$ exchange at position two of ribose-5-phosphate must first be corrected so the required deuterated compounds can be synthesized. In the longer term, one might

synthesize an N-15 isotopomer with the labeled nitrogen being at the glycosidic position. This compound would allow for refinement of the C-N distance at the transition state. ^{18}O might be incorporated into the uracil 2- and 4-keto groups to report on interactions at those positions.

A long term goal of the project is to measure KIEs for oligonucleotides of increasing size. Since DNA is a "sticky" substrate there will likely be a commitment to catalysis making measurement of intrinsic KIEs difficult. By studying the KIEs for oligonucleotide substrates of increasing size, a better understanding of the onset of commitment to catalysis for UDG will be obtained. In addition, the study of the kinetic behavior of oligonucleotides of increasing length will enable the investigation of interactions between the enzyme and the DNA sugar-phosphate backbone. It is believed that these interactions are very important for base-flipping to occur (Slupphaug, 1996). KIE information may allow for probing of the role of base flipping in UDGs mechanistic pathway.

REFERENCES

Ames, B.N., and Shigenaga, M.K., Ann. NY Acad. Sci. 663, 85-96 (1992).

Ames, B.N., Shigneaga, M.K., and Hagen, T.M., Proc. Natl. Acad. Sci. USA 90, 7915-7922 (1993).

Anderson, A., and Cooper, R.A., Biochim. Biophys. Acta 177, 163-165 (1969).

Aruoma, O.I., Halliwell, B., and Dizdaroglu, M., J. Biol. Chem. 264, 13024-13028 (1989).

Barnes, D., Lindahl, T., and Sedgwick, B., Curr. Opin. Cell Biol. 5, 424-433 (1993).

Barrio, J.R., Barrio, M.C.G., Leonard, N.J., England, T., and Uhlenbeck, O.C. Biochemistry 17, 2077-2081 (1978).

Batterham, T.J., Ghambeer, R.K., Blakley, R.L., and Brownson, C., Biochemistry 6, 1203-1208 (1967).

Baykov, A.A., Eutushenko, O.A., and Avaeva, S.M., Anal. Biochem. 171, 266-270 (1988).

Bennett, S.E., Sanderson, R.J., and Mosbaugh, D.W., J. Biol. Chem. 269, 21870-21879 (1994).

Bennet, S.E., Sanderson, R.J., and Mosbaugh, D.W., Biochemistry 34, 6109-6119 (1995).

Berg, O.G., Winter, R.B., and von Hippel, P.H., Biochemistry 20, 6926-6948 (1981).

Bigeleisen, J., and Mayer, M.G., J. Chem. Phys. 15, 261-267 (1947).

Bigeleisen, J., and Wolfsberg, M., Adv. Chem. Phys. 1, 15 (1958).

Blackburn, G.M., and Gait, M.J., in Nucleic Acids in Chemistry and Biology. Oxford University Press, Oxford, 286 (1990).

Blakley, R.L., Ghambeer, R.K., Batterham, T.J., and Brownson, C., Biochem. Biophys. Res. Commun. 24, 418-426 (1966).

Booker, S., and Stubbe, J., Proc. Natl. Acad. Sci. USA 90, 8352-8356 (1993).

Booker, S., Licht, S., Broderick, J., and Stubbe, J., Biochemistry 33, 12676-12685 (1994).

Borowy-Borowski, H., Lipman, R., and Tomasz, M., Biochemistry 29, 2999-3004 (1990).

Buddenbaum, W.E., and Shiner, V.J., Jr., in Isotope Effects on Enzyme-Catalyzed Reactions (Cleland, W.W., O'Leary, M.H., and Northrop, D.B., Eds.). University Park Press, New York, 1-9 (1977).

Burgner, J.W., II, Oppenheimer, N.J., and Ray, W.J., Jr., Biochemistry 26, 91-96 (1987).

Burland,V., Plunkett,G. III., Daniels,D.L. and Blattner,F.R., Genomics 16, 551-561 (1993).

Chan, G., Doetsch, P., Haseltine, W., Biochemistry 24, 5723-5728 (1985).

Chu, G. J. Biol. Chem. 269, 787-790 (1994).

Chun, E., Gonzales, L., Lewis, F., Jones, J., and Rutman, R. Cancer Res. 29,1184-1194 (1969).

Cleland, W.W., in Isotopes in Organic Chemistry (Buncel, E., and Lee, C.C., Eds.). Elsevier, New York, Chap. 2 (1987).

Crofts, D.C., Downie, I.M., and Heslop, R.B., J. Chem. Soc. 3, 3673-3675 (1960).

Crosby, B., Prakash, L., Davis, H., and Hinkle, D.C., Nuc. Acids Res. 9, 5797-5809 (1981).

David, S., and Williams, S., Chem. Rev. 98, 1221-1261 (1998).

Dawson, R.M.C., Elliott, D.C., Elliott, W.H., and Jones, K.M., Data for Biochemical Research Oxford University Press, New York. 112-114 (1987).

Degano, M., Gopaul, D.N., Scapin, G., Schramm, V.L., and Sacchettini, J.C., Biochemistry 35, 5971-1981 (1996).

Dianov, G., Price, A., Lindahl, T. Mol. Cell. Biol. 12 1605-1612 (1992).

Dianov, G., Lindahl, T., Curr. Biol. 4, 1069-1076 (1994).

Dizdaroglu, M., Karakaya, A., Jaruga, P., Slupphaug, G., and Krokan, H., Nuc. Acids Res. 24, 418-422 (1996).

Domena, J. D., and Mosbaugh, D.W., Biochemistry 24, 7320-7328 (1985).

Domena, J.D., Timmer, R.T., Dicharry, S.A., and Mosbaugh, D.W., Biochemistry 27, 6742-6751 (1988).

Dudley, B., Hammond, A., and Deutsch, W.A., J. Biol. Chem. 17, 11964-11967 (1992).

Duggelby, R.G., and Northrop, D.B., Bioorg. Chem. 17,177-193 (1989).

Duncan, B.K., Rockstroh, P.A., and Warner, H.R., J. Bacteriol. 134, 1039-1045 (1978).

Eastman, A., Pharmacol. Ther. 34, 155-166 (1987).

Erlich, M., Zhang, X-Y., and Inamdar, N.M., Mut. Res. 238, 277-286 (1990).

Feather, M.S., and Lybyer, M.J., Biochemical and Biophysical Res. Commun. 4, 538-541 (1969).

Fox, M., and Scott, D., Mutat. Res. 75, 131-168 (1980).

Fram, R., Curr. Opin. Oncol. 4, 1073-1079 (1992).

Frederico, L.A., Kunkel, T.A. and Shaw, B.R. Biochemistry 29, 2532-2537 (1990).

Frederico, L., Kunkel, T., and Shaw, B., Biochemistry 32, 6523-6530 (1993).

Friedberg, E., Walker, G., and Siede, W., in DNA Repair and Mutagenesis. ASM Press, Washington D. C. (1995).

Frosina, G., Fortini, P., Rossini, O., Carrozzino, F., Raspaglio, G., Cox, L.S., Lane, D.P., Abbondandol, A., and Dogliotti, E., J. Biol. Chem. 271, 9573-9578 (1996).

Garrett, C.E., Doctoral Dissertation, University of California, San Francisco, CA, (1979).

Gentil, A., Caral Neto, J., Mariage Samson, R., Margot, A., Imbach, J., Rayner, B., Sarasin, A., J. Mol. Biol. 227, 981-984 (1992).

Gottesman, M.M., and Beck, W.S., Biochem. Biophys. Res. Commun. 24, 353-359 (1966).

Griffin, C.E., Hamilton, F.L.D., Hopper, P., and Abrams, R., Arch. Biochem. Biophys. 126, 905-911 (1966).

Grossman, L., Caron, P., Mazur, S., and Oh, E., FASEB J. 2, 2696-2701 (1988).

Grossman, L., Lin, C., and Ahn, L., in DNA Damage and Repair (Nickoloff, J., and Hoekstra, M., Eds.). Humana Press, Totowa, NJ, (1998).

Hatahet, Z., Kow, Y., Purmal, A., Cunningham, R., and Wallace, S., J. Biol. Chem. 269, 18814-18820 (1994).

Hayes, F., Williams, D., Ratliff, R., Varghese, A., and Rupert, C., J. Am. Chem. Soc. 93, 4940-4942 (1971).

Higley, M., and Lloyd, R.S., Mutat. Res. 294, 109-116 (1993).

Hornton, R.M., Hunt, H.D., Ho, S.N., Pullen, J.K., and Pease, L.R., Gene 77, 61-68 (1989).

Ivanetich, K.M., and Santi, D.V. Progress in Nucleic Acids Research and Molecular Biology 42, 127-156 (1992)

Iyer, V., and Szybalski, W., Proc. Natl. Acad. Sci. USA 50, 355-362 (1963).

Jackson, R.C., J. Biol. Chem. 253, 7440-7446 (1978).

Jencks, W.P, Chem. Rev. 72, 705 (1972)

Joyce, C.M., and Derbyshire, V., Methods in Enzymology 262, 3-13 (1995).

Kavli, B., Slupphaug, G., Mol, C.D., Arvai, A.S., Petersen, S.B., Tainer, J.A., and Krokan, H.E., EMBO 15, 3442-3447 (1996).

Klimasauskas, S., Kumar, S., and Roberts, R.J., Cell 76, 357-369 (1994).

Kohn, K., Spears, C., and Doty, P., J. Mol. Biol. 19, 266-288 (1987).

Krokan, H., Standal, R., and Slupphaug, G., Biochem J. 325, 1-16 (1997).

Kumar, N.V., and Varshney, U., Nucl. Acids. Res. 25, 2336-2343 (1997).

Kunkel, T.A., and Wilson, S.H., Nature 384, 25-26 (1996).

Lehninger, A., Nelson, D., and Cox, M., in Principles of Biochemistry. Worth Publishers, New York. Chapters 14 and 24, (1993).

Lindahl, T., Proc. Natl. Acad. Sci. USA 71, 3649-3653 (1974).

Lindahl, T., Prog. Nucleic Acid Res. Mol. Biol. 22, 135-192 (1979).

Lindahl, T., Ann. Rev. Biochem. 51, 61-87 (1982).

Lindahl, T., Nature 362, 709-715 (1993).

Lindahl, T., and Karlstrom, O., Biochemistry 12, 5151-5154 (1973).

Lindahl, T., Ljungquist, S., Siegert, W., Nyberg, B., and Sperens, B., J. Biol. Chem. 252, 3286-3294 (1977).

Lindahl, T., and Nyberg, B., Biochemistry 11, 3610-3618 (1972).

Lindahl, T., and Nyberg, B., Biochemistry 13, 3405-3410 (1974).

Lober, G., and Kittler, L., Photochem. Photobiol. 25, 215-233 (1977).

Loeb, L.A. and Preston, B.D., A. Rev. Genet. 20, 201-230 (1986).

Lowry, T.H., and Richardson, K.S., in Mechanism and Theory in Organic Chemistry. HarperCollins, New York. Chapters 2 and 3, (1987).

Lutz, W.K., Mut. Res. 238, 287-295 (1990).

Matsson, O., and Westaway, K.C., Advances in Physical Organic Chemistry 31, 143-248 (1998).

Mauro, D.J., De Riel, J.K., Tallarida, R.J., and Sirover, M.J., Chromasoma 102, S67-S71 (1993).

McGeoch, D.J., Dalrymple, M.A., Davison, A.J., Dolan,A., Fram, M.C., McNab, D., Perry, L.J., Scott, J.E., and Taylor, P., J. Gen. Virol. 69, 1531-1574 (1988).

McLaren, A.D., and Shugar, D., in Photochemistry of Proteins and Nucleic Acids. Permagon Press, Oxford, 184-191 (1964).

Melander, L., and Saunders, W.H., in Reaction Rates of Isotopic Molecules. John Wiley, New York, Chapter 8 (1980).

Mentch, F., Parkin, D.W., and Schramm, V.L., Biochemistry 26, 921-930 (1987).

Mol, C.D., Arvai, A.S., Slupphaug, G., Kavli, B., Alseth, I., Krokan, H.E., and Tainer, J.A., Cell 80, 869-878 (1995).

Montgomery, J.C., Venta, P.J., Taxhian, R.E., and Hewett-Emmett, D., Nuc. Acids Res. 15 4687 (1987).

More O'Ferrall, R.A., J. Chem. Soc. B. 274 (1970).

Mosbaugh, D.W., Rev. Biochem. Tox. 9, 69-130 (1988).

Mosbaugh, D.W., and Bennet, S.E., Prog. Nucleic Acid Res. 48, 315-370 (1994).

Mosbaugh, D.W., and Tainer, J.A., J. Mol. Biol. 287, 331-346 (1999).

Myers, C.E., Young, R.C., and Chabner, B.A., J. Clin. Invest. 56, 1231-1238 (1975).

Nealon, K., Nicholl, I.D., and Kenny, M.K., Nucleic Acids Res. 24 3763-3770 (1996).

Newcomb, T.G., and Loeb, L.A., in DNA Damage and Repair (Nickoloff, J.A., and Hoekstra, M.F., Eds.). Humana Press, Inc. Totowa, NJ, (1998).

Northrup, D.B., Biochemistry 14, 2644-2651 (1975).

Northrop, D.B., in Isotopic Effects on Enzyme-Catalyzed Reactions (Cleland, W.W., O'Leary, M.H., Northrop, D.B., Eds.). University Park Press, New York, 122-152 (1976).

Northrup, D.B., Methods Enzymol. 87, 607 (1982).

O'Leary, M.H., in Isotope Effects on Enzyme Catalyzed Reactions (Cleland, W.W., O'Leary, M.H., Northrop, D.B., Eds.). University Park Press, New York, 233-251 (1976).

Olsen, L. C., Aasland, R., Wittwer, C.U., Krokan, H.E., and Helland, D.E., EMBO 8, 3121-3125 (1989).

Panayotou, G., Brown, T., Barlow, T., Pearl, L.H., and Savva, R., J. Biol. Chem. 273, 45-50 (1998).

Parikh, S.S., Maol, C.D., Slupphaug, G., Bharti, S., Krokan, H.E., and Tainer, J.A., EMBO J. 17, 5214-5226 (1998).

Parkin, D.W., Leung, H.B., and Schramm, V.L.. J. Biol. Chem. 259, 9411-9417 (1984).

Parkin, D.W., and Schramm, V.L., J. Biol. Chem. 259, 9418-9425 (1984).

Parkin, D.W., and Schramm, V.L., Biochemistry 26, 913-920 (1987).

Parkin, D.W., in Enzyme Mechanisms from Isotope Effects (Cook, P.F., Ed.). CRC Press, Boca Raton, FL. 269-290 (1991).

Pogolotti, A.L. Jr., Nolan, P.A., and Santi, D.V., Biochemistry 18, 2794-2798 (1979).

Prior, J.J., Maley, J., and Santi, D.V., J. Biol. Chem. 259, 2422-2428 (1984).

Prior, J.J., and Santi, D.V., J. Biol. Chem. 259, 2429-2434 (1984).

Purmal, A.A., Wallace, S.S., and Kow, Y.W., Biochemistry 35, 16630-16637 (1996).

Putnam, C.D., Shroyer, M.N., Lundquist, A.J., Mol, C.D., Arvai, A.S., Mosbaugh, D.W., and Tainer, J.A., J. Mol. Biol. 287, 331-346 (1999).

Rakowski, K., and Paneth, P., J. Mol. Struct. 378, 35-43 (1996).

Reinsch, K.M., Chen, L., Verdine, G.L., and Lipscomb, W.N., Cell 82, 143-153 (1995).

Rising, K., A., and Schramm, V.L., J. Am. Chem. Soc. 116, 6531-6536 (1994).

Roberts, J.J., and Pascoe, J., Nature 235, 282-284 (1972).

Roberts, J.J., Adv. Radiat. Biol. 7, 211-435 (1978).

Roberts, J.R., and Cheng, X., Annu. Rev. Biochem. 67, 181-198 (1998).

Rodgers, J., Femec, D.A., and Schowen, R.L., J. Biol. Chem. 104 3263-3268 (1982).

Rosenberg, S., and Kirsch, J.F. Biochemistry 20, 3189-3196 (1981).

Rydberg, B., and Lindahl, T., EMBO J. 1, 211-216 (1982).

Saiki, R.K., Scharf,S., Faloona, F., Mullis, K.B., Horn, G.T., Erlich, H.A., and Arnheim, N., Science 230, 1350-1354 (1985).

Sancar, A., and Rupp, W., Cell 33, 249-260 (1983).

Sancar, G., and Tang, M., Photochem. Photobiol. 57, 905-921 (1993).

Savva, R., McAuley-Hecht, K., Brown, T., and Pearl, L., Nature 373, 487-493 (1995).

Schmidt, M., Frey, B., Kaluza, K., and Sobek, H., Biochimica 2, 13-15 (1996).

Schramm, V.L., in Enzyme Mechanisms from Isotope Effects (Cook, P.F., Ed.). CRC Press, Boca RAton, FL. 367-388 (1991).

Schramm, V.L., Horenstein, B.A., and Kline, P.C., J. Biol. Chem. 269, 18259-18262 (1994).

Segel, I.H., in Enzyme Kinetics. John Wiley, New York. 398-401 (1975).

Setlow, J.K., Curr. Top. Radiat. Res. 2, 195-248 (1966).

Setlow, R.B., Science 153, 379-386 (1966).

Setlow, R.B., Prog. Nucleic Acids Res. Mol. Biol. 8, 257-295 (1969).

Simon, H., and Palm, D., in Angew. Chem. Int. Ed. Engl. 5, 920-933 (1966).

Shroyer, M.N., Bennett, S.E., Putnam, C.D., Tainer, J.A., and Mosbaugh, D.W., Biochemistry 38, 4834-4845 (1999).

Sigrell, J.A., Cameron, A.D., Jones, T.A., and Mowbray, S.L., Protein Science 6, 2474-2476 (1997).

Singer, B., and Kusmierek, J., Annu. Rev. Biochem. 51, 655-693 (1982).

Singer, B., and Grunberger, D., in Molecular Biology of Mutagens and Carcinogens. Plenum, New York. 55-78 (1983).

Singer, B., Cancer Res. 46, 4879-4885 (1986).

Singhal, R., Prasad, R., and Wilson, S. J. Biol. Chem. 270, 949-957 (1995).

Slupphaug, G., Mol, C., Kavli, B., Arvai, A.S., Krokan, H.E., and Tainer, J.A., Nature 384, 87-92 (1996).

Starzyk, R.M., Koontz, S.W., and Schimmel, P., Nature 298, 136-140 (1982).

Stivers, J.T., Pankiewicz, K.W., and Watanabe, K.A., Biochemistry 38, 952-963 (1999).

Swain, C.G., Stivers, E.C., Reuwer, J.F., and Schaad, L.J., J. Am. Chem. Soc. 80, 5885-5893 (1958).

Takahashi, I., and Marmur, J., Nature 197, 794-795 (1963).

Tao, W., Grubmeyer, C., and Blanchard, J.S., Biochemistry 35, 14-21 (1996).

Taylor, J., Garrett, D.S., Brockie, I. Svoboda, D., and Telser, J., Biochemistry 29, 8858-8866 (1990).

Thornton, E.R., J. Am. Chem. Soc. 89, 2915 (1967)

Tomilin, N.V., and Aprelikova, O., Int. Rev. Cytol. 114, 125-178 (1989).

Van Houten, B., Microbiol. Rev. 54, 18-51 (1990).

Varghese, A.J., Photophysiology 7, 207-274 (1972).

Varshney, U., Hutcheon, T., and van de Sande, J.H., J. Biol. Chem. 263, 7776-7784 (1988).

Varshney, U., and van de Sande, J.H., Biochemistry 30, 4055-4061 (1991).

Vassylyev, D.G., Kashiwagi, T., Mikami, Y., Arihoshi, M., Iwai, S., Ohtsuka, E., and Morikawa, K., Protein Engineering 8, 64 (1995).

von Hippel, P.H., and Berg, O.H., J. Biol. Chem. 264, 675-678 (1989).

Wacker, A., Dellweg, H., Träger, L., Kornhauser, A., Lodermann, E., Türk, G., Selzer, R., Chandra, P., and Ishimoto, M., Photochem. Photobiol. 3, 369-394 (1964).

Wang, S. Y., Fed. Proc. 24, 71 (1965).

Wang, S.Y., in Photochemistry and Photobiology of Nucleic Acids. Academic Press, New York. 54-55 (1976).

Weibauer, K., and Jiricny, J., Proc. Natl. Acad. Sci. USA 87, 5842-5945 (1990).

Weis, B., and Grossman, L., Adv. Enzymol. Biol. 60, 1-34 (1987).

Witkin, E., Escherichia coli. Bacteriaol. Rev. 40, 869-907 (1976).

Wolfsberg, M., Stern, M., Pure Appl. Chem. 8, 225-242 (1964).

Wood, R.D., and Shviji, M.K.K., Carcinogenesis 18, 605-610 (1997).

Xiao, G., Tordova, M., Jagadeesh, J., Drohat, A., Stivers, J.T., and Glilliland, G.L., Proteins: Structure, Function, and Genetics 35, 13-24 (1999).

Yeung, A., Mattes, W., Oh, and E., Grossman, L., Proc. Natl. Acad. Sci. USA 80, 6157-6161 (1983).

Zimmer, D.P., and Crothers, D.M., Proc. Natl. Acad. Sci., USA 92, 3091-3095 (1995).

Zoltewicz, J.A., Clark, F.O., Sharpless, T.W., and Grahe, G., J. Am. Chem. Soc. 92, 1741-1750 (1970).

BIOGRAPHICAL SKETCH

Eve Lynn Hunovice, daughter of Leslie T. and Judith E. Hunovice, was born in Baltimore, Maryland, on May 1, 1972. She grew up in Owings Mills, Maryland, with her sister Rachel A. Epstein. After graduating from Pikesville High School in 1990, she attended Northwestern University. In 1994 she graduated from Northwestern University and received a bachelor of science degree in chemistry. She earned her doctor of philosophy degree in chemistry from the University of Florida in 1999 under the guidance of Dr. Benjamin A. Horenstein. She plans to attend the Washington College of Law at The American University beginning in late August 1999.

I certify that I have read this study and that in my opinion it conforms to acceptable standards of scholarly presentation and is fully adequate, in scope and quality, as a dissertation for the degree of Doctor of Philosophy.

Benjamin A. Horenstein, Chair
Associate Professor of Chemistry

I certify that I have read this study and that in my opinion it conforms to acceptable standards of scholarly presentation and is fully adequate, in scope and quality, as a dissertation for the degree of Doctor of Philosophy.

Nigel G. Richards
Associate Professor of Chemistry

I certify that I have read this study and that in my opinion it conforms to acceptable standards of scholarly presentation and is fully adequate, in scope and quality, as a dissertation for the degree of Doctor of Philosophy.

David E. Richardson
Professor of Chemistry

I certify that I have read this study and that in my opinion it conforms to acceptable standards of scholarly presentation and is fully adequate, in scope and quality, as a dissertation for the degree of Doctor of Philosophy.

Jon D. Stewart
Assistant Professor of Chemistry

I certify that I have read this study and that in my opinion it conforms to acceptable standards of scholarly presentation and is fully adequate, in scope and quality, as a dissertation for the degree of Doctor of Philosophy.

Nancy D. Denslow
Associate Scientist of
Biochemistry and Molecular
Biology

This dissertation was submitted to the Graduate Faculty of the Department of Chemistry in the College of Liberal Arts and Sciences and to the Graduate School and was accepted as partial fulfillment of the requirements for the degree of Doctor of Philosophy.

December 1999

Dean, Graduate School